CRANFIELD UNIVERSITY

Nithya Subramanian

Fault diagnosis in Aircraft Fuel System components with Machine learning algorithms

SCHOOL OF AEROSPACE, TRANSPORT AND MANUFACTURING

PhD Thesis
Academic Year: 2018 - 2022

Supervisor: Prof Andrew Starr
Associate Supervisor: Dr Suresh Perinpanayagam
01 2022

CRANFIELD UNIVERSITY

SCHOOL OF AEROSPACE, TRANSPORT AND MANUFACTURING

PhD Thesis

Academic Year 2018 - 2022

Nithya Subramanian

Fault diagnosis in Aircraft Fuel System components with Machine learning algorithms

Supervisor: Prof Andrew Starr
Associate Supervisor: Dr Suresh Perinpanayagam
01 2022

This thesis is submitted in partial fulfilment of the requirements for the degree of Doctor of Philosophy

ABSTRACT

There is a high demand and interest in considering the social and environmental effects of the component's lifespan. Aircraft are one of the most high-priced businesses that require the highest reliability and safety constraints. The complexity of aircraft systems designs also has advanced rapidly in the last decade. Consequently, fault detection, diagnosis and modification/ repair procedures are becoming more challenging. The presence of a fault within an aircraft system can result in changes to system performances and cause operational downtime or accidents in a worst-case scenario.

The CBM method that predicts the state of the equipment based on data collected is widely used in aircraft MROs. CBM uses diagnostics and prognostics models to make decisions on appropriate maintenance actions based on the Remaining Useful Life (RUL) of the components

The aircraft fuel system is a crucial system of aircraft, even a minor failure in the fuel system can affect the aircraft's safety greatly. A failure in the fuel system that impacts the ability to deliver fuel to the engine will have an immediate effect on system performance and safety. There are very few diagnostic systems that monitor the health of the fuel system and even fewer that can contain detected faults. The fuel system is crucial for the operation of the aircraft, in case of failure, the fuel in the aircraft will become unusable/unavailable to reach the destination.

It is necessary to develop fault detection of the aircraft fuel system. The future aircraft fuel system must have the function of fault detection. Through the information of sensors and Machine Learning Techniques, the aircraft fuel system's fault type can be detected in a timely manner.

This thesis discusses the application of a Data-driven technique to analyse the healthy and faulty data collected using the aircraft fuel system model, which is similar to Boeing-777. The data is collected is processed through Machine learning Techniques and the results are compared.

Keywords:

Machine learning, Diagnosis, PHM, CBM, Aircraft Fuel System, Component level

ACKNOWLEDGEMENTS

Undertaking this PhD has been a truly life-changing experience for me, and it would not have been possible to do without the support and guidance that I received from many people.

My sincerest thanks go to my supervisor Prof Andrew Starr and Dr Suresh Perinpanayagam for allowing me to work on this project and for giving so freely of their time, continuous advice, guidance, and support throughout the project.

I am grateful to my Amma (Meerabai) and Appa (Subramanian) for their love, patience, encouragement and support all my life. Thanks for putting me first in all your decisions big and small. I do not have any words to express how thankful and blessed I feel to be your daughter.

Hasani Azamar, you are an intrinsic part of my Cranfield (academic and personal) life. It was a bumpy road, we got there at the end (with a lot of good memories). Thanks for patiently listening and answering all my academic and philosophical questions.

PhD research requires a pleasant environment, I am also grateful to all the IVHM colleagues for the excellent working environment and the support throughout the research.

TABLE OF CONTENTS

LIST OF FIGURES

LIST OF TABLES

LIST OF EQUATIONS

LIST OF ABBREVIATIONS

AE	Auto Encoder
ANN	Artificial neural network
APU	Auxiliary Power Unit
CAA	Civil Aviation Authority
CBM	Condition Based Maintenance
CNN	Convolutional Neural Network
DBN	Deep Belief Neural Network
DPV	Direct Proportional Valve
DL	Deep Learning
ECU	Engine Control Unit
EASA	European Union Aviation Safety Agency
FAA	Federal Aviation Administration
FCU	Fuel Control Unit
FD	Fault Detection
FDD	Fault Detection and Diagnosis
FFT	Fourier Transform
FI	Fault Isolation
FN	False Negative
FP	False Positive
IATA	International Air transport Association
ICAO	International Civil Aviation Organisation
LSTM	Long Short-Term Memory
ML	Machine Learning
MLP	Multi-layer preceptor
MRO	Maintenance, repair, and overhaul
NN	Neural Network
PHM	Prognostics and Health Management

PoF	Physics of Failure
RNN	Recurrent Neural Network
ROI	Return of Investment
RUL	Remaining Useful Life
Std	Standard Deviation
STFT	Short Time Fourier Transform
SVM	Support Vector Machines
TN	True Negative
TP	True Positive

1 Introduction

1.1 Research Background

Aircraft maintenance is an important process to make certain the safety of the passengers and the operation of the aircraft. Maintaining the aircraft consists of numerous complex activities such as inspection, of the modification that is carried to the international standards (CAA, FAA, etc.,) usually referred to as Maintenance, repair, and Overhaul (MRO) [1].

According to research conducted by the International Air transport Association (IATA) in 2017, the commercial aircraft industry has spent about $75 billion on (MRO), and it is anticipated to rise to $118 billion by 2027[2]. The maintenance of the aircraft will concentrate not only on the equipment breakdowns but also on improving performance and availability. The complexity of aircraft systems designs has advanced rapidly in the last decade. Consequently, fault detection, diagnosis and modification/ repair procedures are becoming more challenging.

The presence of a fault within an aircraft system can result in changes to system performances and cause operational downtime or accidents in a worst-case scenario. The CBM method that predicts the state of the equipment based on data collected is widely used in aircraft MROs. CBM uses diagnostics and prognostics models to make decisions on appropriate maintenance actions based on the Remaining Useful Life (RUL) of the components [3].

The term ‘Diagnostics’ refers to subsequent event assessment and deals with fault detection, fault isolation and fault identification [4]. ‘Prognostics’ is the process to predict the RUL, probability of consistent function of equipment based on the data gathered from the sensors or physics-of-failure models (PoF) [5]. The diagnosis of the systems is usually done by obtaining the knowledge from the experience of the engineers with the machine. For instance, an expert engineer can detect the faults of engines just by the change in vibration frequency or detect the bearing faults by utilizing enhanced signal processing methods to analyse the vibration.

For the first principle or PoF, information on the system is readily accessible, which can also be used to identify the parameter causing the fault. The physics-based method and the expert-knowledge methods are more time-consuming and not cost-efficient compared to other diagnostic methods. Due to these reasons industries are moving towards the automated method to reduce the maintenance phase and increase diagnostic accuracy. Moreover, with the help of artificial intelligence, the method of fault detection is expected to be rational and adequate to automatically detect and identify the health conditions of the devices [6,7].

Machine Learning (ML) and Deep Learning (DL) techniques have been used in fault detection and diagnosis methods in terms of decision-making and classification, respectively. The data used in the ML or DL techniques can be directly retrieved from the signals/raw data or it can be the features extracted from the sensor readings of the system/sub-systems [8].

In an aircraft, an on-board diagnostics system may display several fault codes because of a single faulty component, the consequent fault code is produced as dependent systems react to incorrect inputs. With the help of research, the aircraft systems might self-diagnose in future, but in the current situation, the occurrence of unforeseen faults will continue which will require ground-based test equipment to collect and analyse data.

This thesis discusses the application of Machine learning and Deep learning methods to analyse the healthy and faulty data collected using the aircraft fuel system model, which is constructed as a replica of Boeing-777. The aircraft fuel system is constructed to store and supply fuel to the gas turbine engines and the auxiliary power units (APU) securely perform various flight operations, including emergencies. The fuel system is constructed to maintain and ensure the appropriate flow rate and pressure of fuel for the respective engines [9] The fuel system is essential for the operation of the aircraft, in case of failure; the fuel in the aircraft will be unable to reach its destination [10]. Hence, automatic, and improved fault detection and diagnosis for fuel systems are key elements for the aircraft’s operation and flight safety.

1.2 Research Aim and objectives

This thesis aims to apply different data-driven methods - Machine Learning to the experimental data obtained from an Aircraft fuel system to get a better diagnosis and prediction performance to improve the safety, availability, and reliability of the Aircraft fuel system components. This method provides the solution to identify cases of multiple severities of faults at the component level.

	Objectives
1	Identify the research gap through a literature review
2	Collecting data using the aircraft fuel system to provide historical records for the diagnosis model
3	Creating a machine learning fault detection model based on the collected data and comparing it to other methods
4	Creating a machine learning fault isolation model based on the collected data
5	Creating a machine-learning fault identification model based on the collected data
6	Comparing and validating the proposed method with the Machine learning-based and deep learning models.

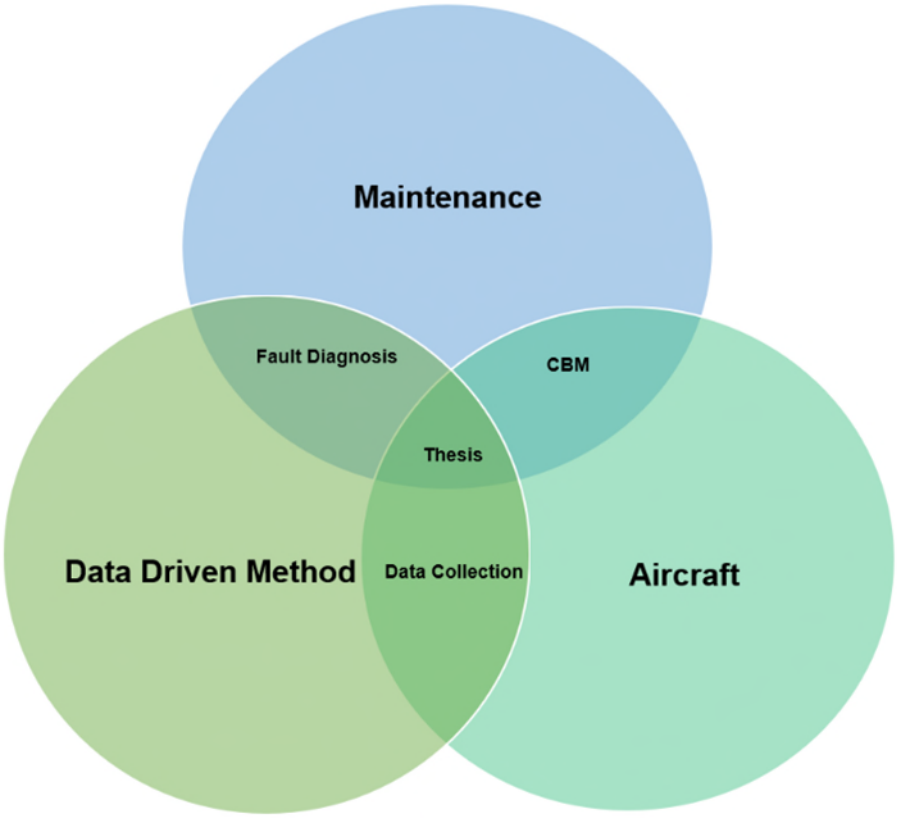

Figure 1 Research Scope

1.2 Thesis Structure

Chapter 1 - informs the background of the research, aim, objective and contribution.

Chapter 2 - reviews current maintenance strategies, diagnostic methods, fuel systems & their faults, and previous work on fault diagnostics. Furthermore, it underlines challenges and gaps in the existing time series fault diagnosis methods. Hence, Section 2.1 Maintenance.

Section 2.2 discusses Maintenance evolution.

Section 2.3 describes condition-based maintenance steps.

Section 2.4 highlights fault diagnosis methods.

Section 2.5 reviews Aircraft fuel systems and their potential faults.

Section 2.6 focuses on the different time series fault diagnosis methods in other industries and the aircraft industry.

Section 2.7 is the conclusion

Chapter 3 – Methodology describes the architecture of the research methodology.

Section 3.1 explains the experimental setup and the procedures to collect data;

Section 3.2 focuses on the Faut diagnosis steps.

Section 3.3 illustrates the problem solving

Section 3.4 considers in detail the methods used for the diagnosis

Section 3.5 is the methods used to compare the different machine learning methods

Chapter 4 – Results – concentrates on the data processing and diagnosis methods.

Section 4.1 focuses on the data visualisation and interpretation

Section 4.2 highlights the results obtained through the methods used to diagnose.

Section 4.3 is the conclusion of the results obtained through the methodology.

Section 4.4 explains the limitations of the research.

Chapter 5 – Discussion – examines the results obtained from the data collected and the methods used to diagnose the faults.

Chapter 6 - Conclusion encapsulates the research and emphasises the research aim and objectives. Moreover, it describes contributions to knowledge and future work.

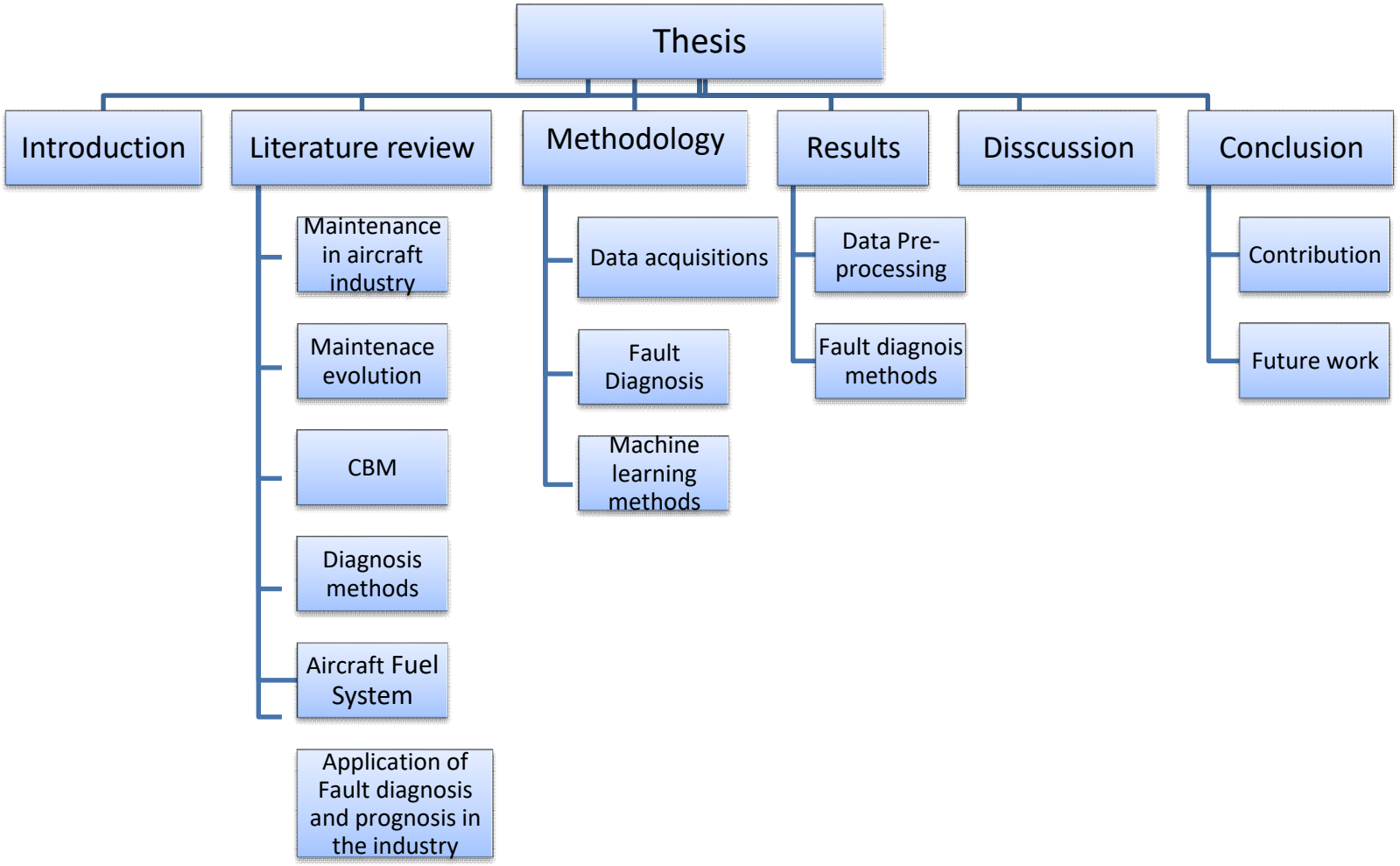

Figure 2 Thesis Structure

2 Literature Review

2.1 Maintenance

The main objectives of the aircraft industry are to provide a fast and reliable form of transportation with high safety standards. Aircraft maintenance is highly regulated by different aeronautical authorities (CAA, EASA, FAA and ICAO) due to its requirement for operational safety, safety for the passengers, complex infrastructure, and competition in the industry.

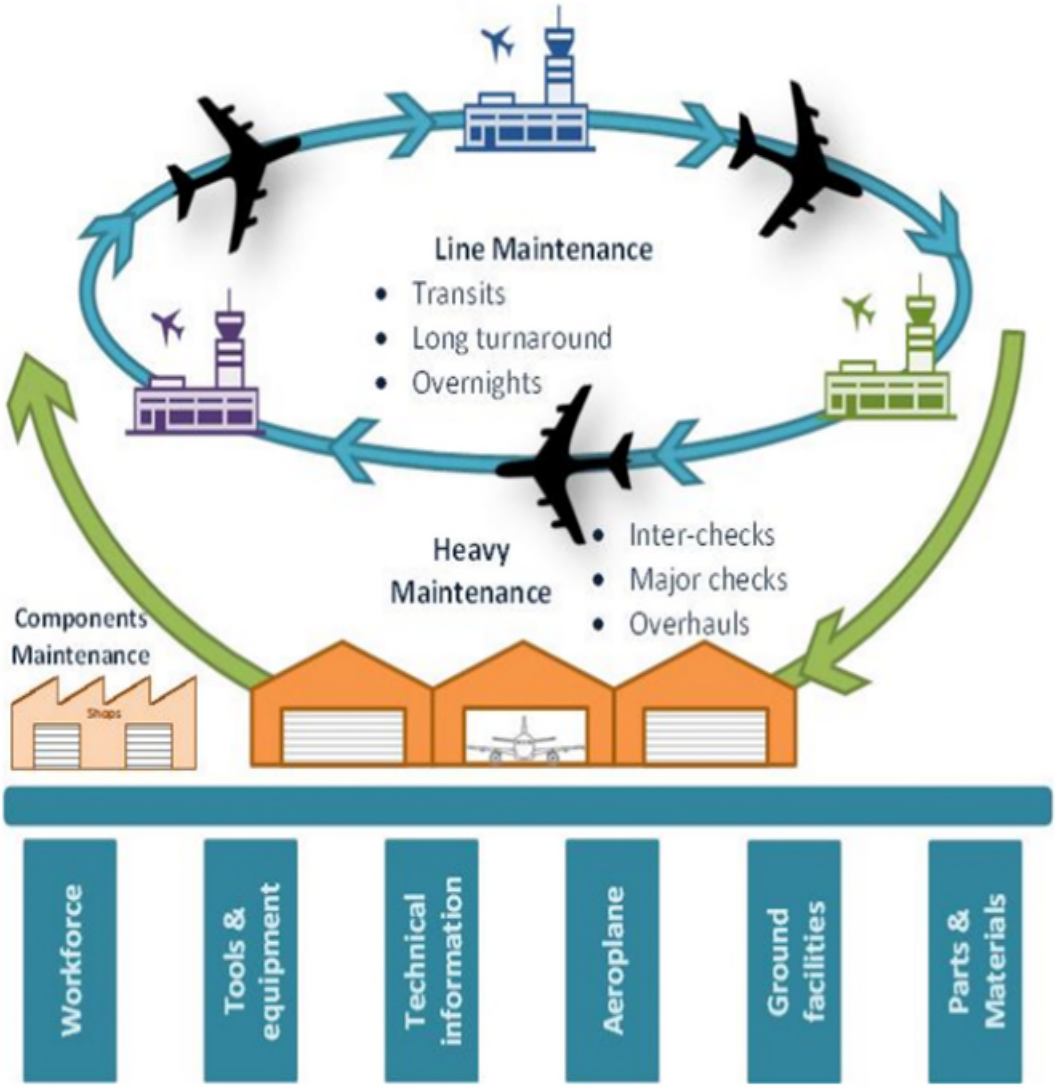

Figure 3 Maintenance and service process[11]

In addition to its significance to the safety of the operations and its governing obligations, aircraft maintenance makes a considerable impact on an airline's operating costs. The maintenance cost of the aircraft typically includes the routine maintenance and services provided between the fight schedules, overnight services (Line Maintenance) and extensive overhauls (Heavy Maintenance).

These maintenance costs comprise 3 main elements –

1) Labour cost
2) The expense of the components required for maintenance or repair.
3) Cost of sub-contracting to other MROs for heavy maintenance.

According to research conducted by the International Air transport Association (IATA) in 2017, the commercial aircraft industry has spent about $75 billion on (MRO), and it is expected to increase up to $118 billion by 2027[2]. Even with a well-planned maintenance operation, the MROs are susceptible to delays or disruption during major checks. Due to this reason, MROs are still exploring better ways to avoid non-scheduled tasks and reduce their negative impacts over the scheduled plan.

2.2 Maintenance Evolution

There are numerous strategies for maintenance, repair, and overhaul (MRO) to attain industrial needs cost-effectively and to reduce maintenance costs without requiring more investments.

These strategies include:

1. Corrective maintenance
2. Preventive maintenance
    - Predetermined maintenance
    - Condition-based maintenance

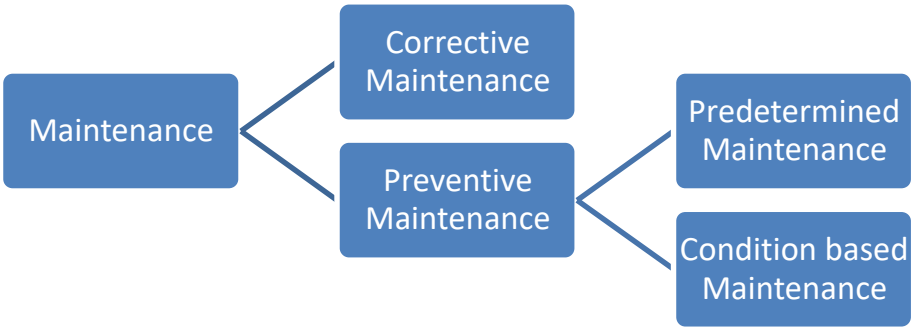

Figure 4 Maintenance Strategies

The corrective maintenance seeks to replace when the components fail or are incapable of performing the assigned tasks effectively. The main disadvantage of this maintenance method is its labour intensive, and can also cause catastrophic failure and downtime [12]

Preventive maintenance is a process of inspecting the components at specified periods to an appropriate standard to determine whether they can continue in service [13] it is of two types predetermined maintenance and condition-based maintenance.

Predetermined maintenance forecasts the failures and replaces the components after predicted cycles or time-period with the help of maintenance plans created by expert options [13]. The advantages of predetermined maintenance compared to corrective maintenance are taking less downtime and longer system life, but the drawback is the upfront cost and the potential for over-maintenance schedules [12].

Condition Based Maintenance (CBM) utilizes diagnostics and prognostics models to make decisions on appropriate maintenance procedures established based on the system's RUL [14].

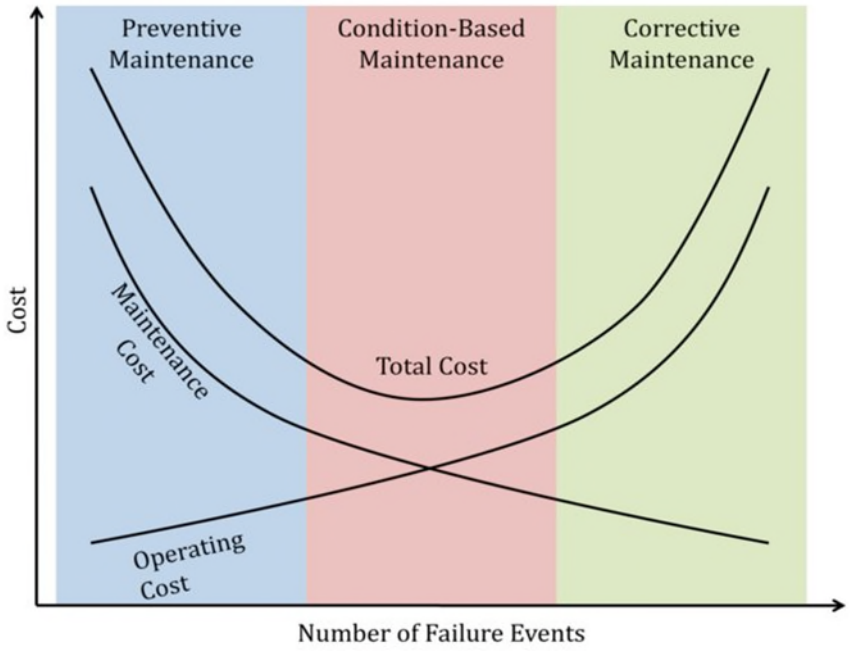

Figure 5 Operating and Maintenance Cost Chart[15]

2.3 Condition Based Maintenance

CBM is considered to be the sophisticated maintenance approach, that is facilitating the reduction of the occurrence of machinery failures by detecting the faults at an early stage [16]. The CBM method is widely applied in industries, that require the interpretation of collected data and is primarily knowledge-based and data-driven[15]. For instance, the vibration analysis methods are usually applied to rotating components (e.g., pumps, compressors, gearboxes, bearings), as vibration is the source of the fault in these components, it can be detected using the change in the frequency or amplitude of the vibration.

The requirement of CBM policy was initiated by the maintenance necessitating condition monitoring of the equipment. The ISO-13374 standard, ‘Condition Monitory and Diagnostics of Machines’ [17], explains the serviceability of a condition monitoring system.

The approach that is used to extrapolate the RUL by observing the trends in the data is called Prognostics and Health Management (PHM). The results obtained from PHM will use in advanced failure warnings and increased availability of the aircraft by indicating timely repair actions.

The main benefit of PHM is that it can decrease the maintenance cost, and idle time of the aircraft, reduce storing up the inventories and can avoid no-fault found issues [18]. PHM investigation concentrates on devising robust and accurate models to forecast the health condition of the system for MROs to help with decision-making. Models that are involved with mathematical interpretations, theories and estimations make PHM easier to interpret and execute in real-world applications, particularly by aircraft MROs [19].

PHM framework's main aim is to extract, process and analyse the data from the sensor (component level or the vehicle as a whole). The analysed data will be used in making informed decision making in the MROs. The data obtained from the sensors follow these required stages of pre-processing, feature extraction and diagnostics/prognostics model before reaching the decision-making stage[20].

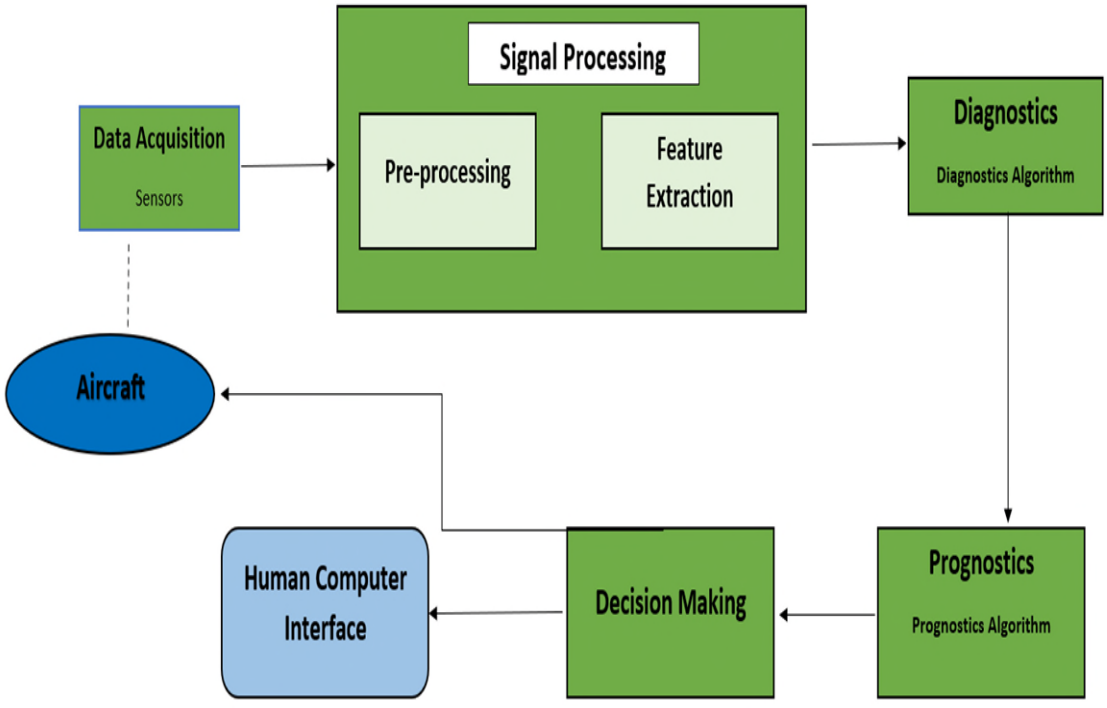

Figure 6 Architecture of PHM

The data from the sensors are usually noisy or have missing elements, due to this the data is cleansed and extracted in the signal processing stage. The accuracy of fault diagnosis or prognosis depends mainly on extracting the feature subset from the data from the sensors/ simulations that can be used to differentiate the types of faults and isolate the fault-initiating part[20].

Over the periods, the dimensionality of the data supplied to the machine learning algorithms has exponentially increased. High dimensionality data is challenging to the current machine learning methods. With the presence of many features, a learning model tends to overfit, subsequently reducing the performance of the algorithm [21].

Features that are extracted are fed to the diagnostic algorithm. The diagnostics can be done in three different methods – data-based, expert-based, and physics-based. Data-driven is the procedure of gathering data from the sensors during the failure progression without considering the physical meaning or knowledge behind it.

The experience of the engineer with the domain can be formulated and represented by an expert in specific feature extraction methods and the classification of faults. Expert knowledge is generally represented in form of rule-based systems. Physics-based features are obtained by physical phenomena occurring during the failure progression. The results for the Physics-based are more accurate compared to other techniques due to their good representative mathematical model [22].

PHM is a study conducted in various industries to improve the system's reliability, availability, and safety and to decrease the maintenance cost of industrial assets. Even though there are considerable research attempts have been made in the field of PHM, there is still a huge gap between academic research and industrial expectations.

2.3.1 Data Acquisition

To achieve further diagnostics and prognostics purposes, acquiring and storing data by monitoring the physical component/system is the initial and crucial stage of the PHM framework. Along with the conventional sensors (e.g., temperature, pressure, and flow rate), sensory devices (e.g., strain gauges, acoustic sensors, ultrasonic sensors) are used to collect the data to analyse the trends of degradation[23].

The aircraft system is constructed with various complex components that are overlapping to make sure the operation and to increase the redundancy of the components. If any of these components' performances reduces because of faults the whole system performance will reduce respectively, due to this reason various sensors are positioned at each subsystem. The Data from sensors are typically processed by the aircraft's computer onboard, which in turn increases the complexity of the systems. If the real-time data processing onboard indicates the pilot with the alters if the case of any unfortunate failures in the system or subsystem.

These data can also be utilized to enhance the operation of aircraft by indicating the pilot's optimal engine throttle settings or altitude corrections. In terms of the collected data from the sensors, a remote analysis can be done from the ground to generate a model to improve the prognostics and diagnosis.

2.3.2 Signal Processing

2.3.2.1 Data Pre-Processing

Raw signals collected from the sensors are extremely prone to noise, missing values, and irregularities, such data affects the quality of the data-driven method. To enhance the quality of the data and, subsequently, increase the quality of prediction from the model, the signals must be pre-processed.

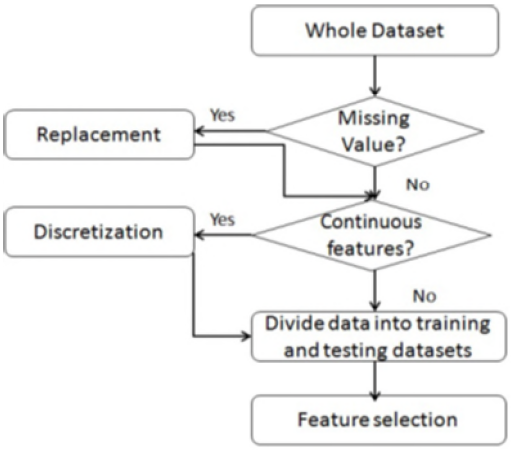

Figure 7 Data Pre-processing Flow Chart

2.3.2.2 Feature Extraction

Over the years, the dimensionality of the data supplied to the machine learning algorithms has exponentially increased. High dimensionality data is challenging to the current machine learning methods. With the presence of many features, a learning model tends to overfit, subsequently reducing the performance of the algorithm [21]. For the processes of machine learning, pattern recognition and image processing, the extracted features from the signals are required for better performance.

The feature extraction is performed before providing the data to the algorithm to reduce the redundancy and help the subsequent learning and simplification steps, and for better human/ expert analyses.

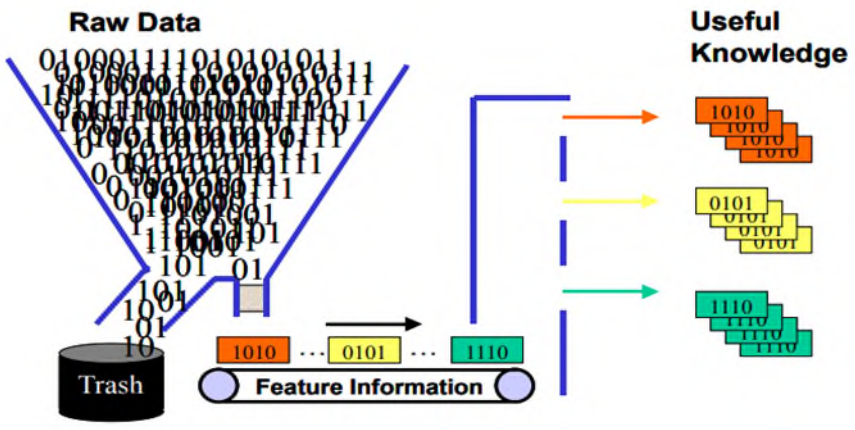

Figure 8 Feature extraction

With a comparison between noised and feature-extracted data used in blind deconvolution and time-synchronous method, there was an increment in fault prognosis accuracy in the helicopter gear system observed[24] The features can be extracted in three different methods: time, frequency, and time-frequency domain.

2.3.2.2.1 Time-domain

A time-domain analysis is an evaluation of physical signals, mathematical functions, or time series of economic or environmental data concerning time. The time-domain evaluation delivers the transient response of components that are to be inspected, this type of analysing obtains a better understanding of both mechanical and electrical signals/data.

The feature is time-domain and performs a significant role in fault detection, diagnosis, and prognostic. Nevertheless, the time-domain features are not feasible for noisy signals, and it will require pre-treatment techniques to improve/clean signals before the diagnostic assessment.

2.3.2.2.2 Frequency domain

The frequency domain is an evaluation of signals or mathematical functions, about frequency, as an alternative to time-based analysis. In the frequency domain, visualisation tools like spectrum analysers are used when visualising signals. The Fourier transform (FFT) and inverse Fourier transform can be used to shift between the time domain and frequency domains.

2.3.2.2.3 Time-frequency domain

To prevent the non-stationary characteristic of signals, the two-dimensional function of time and frequency is required. Short-Time Fourier Transform (STFT) works under the same principle as FFT, which uses smaller sections of the signal (windows), that are centred at zero. SFFT is commonly used to transform the time-domain signal into time-frequency signals.

2.3.3 Fault Diagnosis

The system-level diagnostics methodology is particularly advantageous in applications engineering assets, as downtime or unscheduled maintenance is not cost-efficient. This methodology proposes swiftly and accurately to the MROs when the faulty or degraded part must be replaced or repaired to attain full operational performance. The diagnostic methods usually concentrate on the components and are very rare at the system level. For instance, if the gas turbine engine is the system, the compressor in it will be considered as the component. When a diagnostic analysis at the system level is done on the engine (system), the main concentration is detecting a fault in the system and in case a fault is identified in the compressor (component), replacing this component will restore a healthy condition. When diagnostics are done at the component level then the root cause of the compressor failure is analysed. The compressor could fail due to contamination, tip clearance, corrosion, deterioration, and damage caused by a foreign object, these scenarios are not considered at system-level diagnostics[25]. Diagnosis without any prior knowledge is a complex problem to solve in the PHM field[26]. Fault diagnosis is usually done in three stages – Fault detection, isolation, and identification.

2.3.4 Prognostics

‘Prognostics’ is the process to predict the RUL, probability of consistent function of equipment based on the data gathered from the sensors or physics-of-failure models[5]. The RUL evaluation is a process that initiates the identification of a fault and its impacts. Prognostics is widely used in the medical field and is regarded as a matured technology; it also has an impact on patient management tasks [27]. On the other hand, prognostics is still a developing technology in engineering.

2.3.5 CBM in the Aerospace industry

CBM strategy comprising traditional CBM policies for periodic inspections of stochastically degrading aircraft components was proposed by Si et al [28]. In this study, the component reliability is calculated but not considered in the decision-making process.

In another study, the Kalman filter was used to estimate future degradation and RUL of redundant multi-component systems assuming different wear profiles. Prognostic information from multiple prognostic models is used to specify maintenance intervention dates that minimize maintenance costs. In this work, we considered some operational aspects by integrating costs into maintenance costs[29].

To estimate the crack growth size in aircraft, a fuselage cracks model-based forecasting framework was used by Wang et al [30] In this study the maintenance cost is decreased by the suggested architecture by finding a middle ground between the probabilities of failure occurrence and the maintenance process.

2.4 Methods used to Diagnose

The diagnostics methods taxonomy can be done in various ways based on the preferred reasonings. For instance, the grouping can be done based on the diagnostic algorithms, and the methods can also be grouped depending on different fault severity modes.

The diagnostics methods can be grouped according to the data - qualitative methods that perform the analysis using the factors (e.g., change in pressure or temperature), or terms of quantitative methods that obtain their results by assessing the factors on specified tolerances (e.g., system electrical resistance lower than 50kΩ). In this Literature review, a categorization of diagnostic methods is proposed using an algorithm-based perception.

According to the approach shown in Figure 9, the diagnostic techniques are categorised based on the attributes of the algorithms that are used, irrespective of qualitative or quantitative attributes. Current diagnostic methods in the study can be characterised into three main classifications:

- Model-Based Methods (Physics-based)
- Data-Driven Methods (Artificial intelligence, Statistics)
- Expert System Methods (Rule-based)

2.4.1 Expert-based Diagnosis

The rule-based method has been widely used expert/knowledge-based method. The Rule-based method is based on the principle of IF-THEN statements utilizing the knowledge about the system and trends in their changes. The expert-based method of diagnosis merges both the experience of the engineers and rule sets for interpretation [31].

Parameters changing trends are analysed using domain expertise gathered from the interpretation of the functions of an asset [32]. Expert-based methods evaluate the difference in the interim glitch data and the data of previous failures and imply the life expectancy from prior events using expert and fuzzy systems [33] Transferring domain expertise to rules comes with complexities, as it entails another technique for prognostics of the system.

2.4.2 Model-based Diagnosis

The model-based method typically uses physics-based models to estimate the accurate reliability of systems or machinery. The Physics of Failure (PoF) are the empirical equation based on the physical science of the components[34]. The RULs of the components can be predicted using failure parameters like crack, wear and tear, and corrosion using physics laws and mathematical equations[19,35].

Figure 9 Classification of Fault Diagnostics Methods

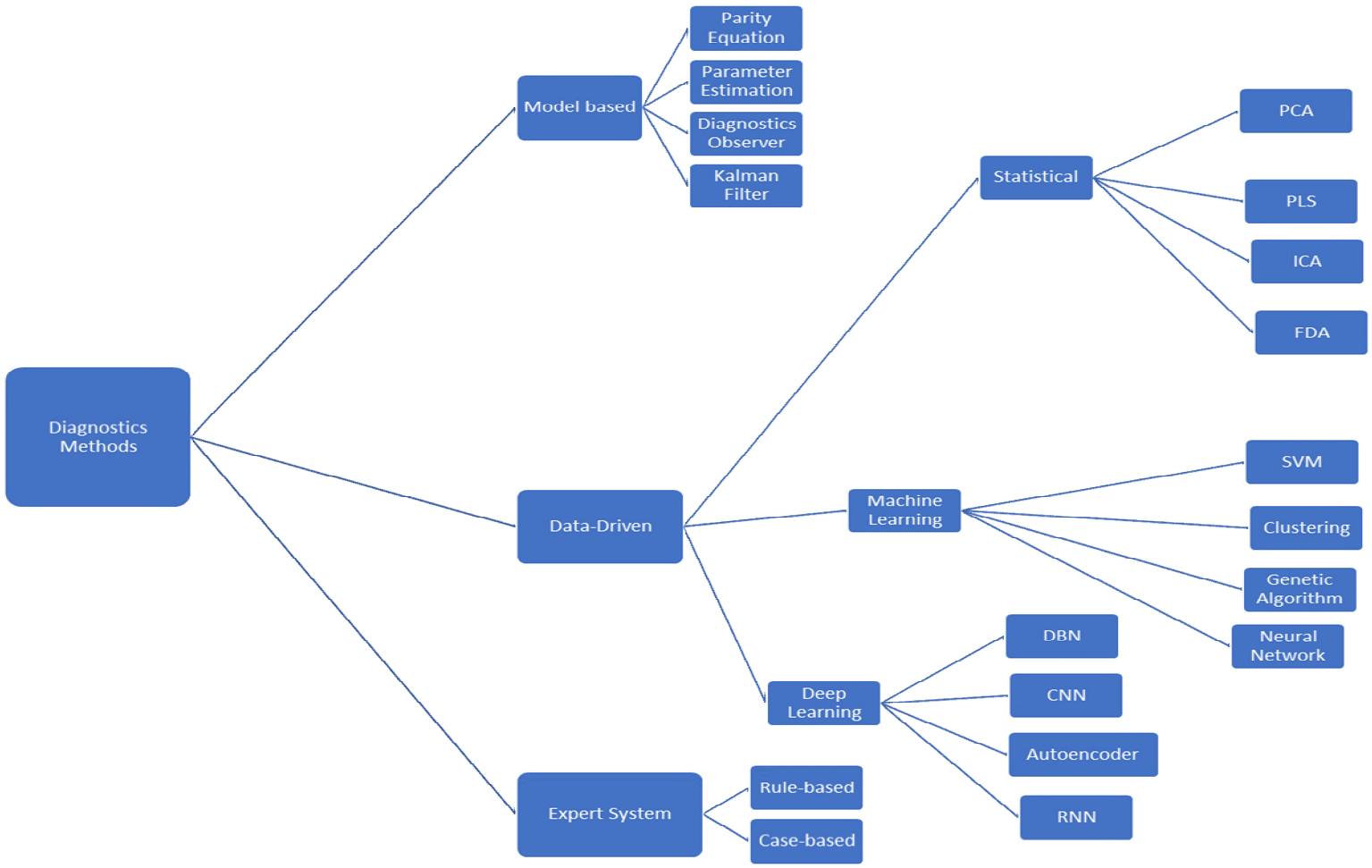

The RUL of the component caused by the fatigue can be predicted using the crack-growth model[36] The model-based method is very accurate in predictions compared to other diagnostic methods, but the main limitation of this method is that the model that is made for specific equipment cannot be transferred or reutilised.

2.4.3 Data-Driven Method

Data-driven methods are developed from the design, usage, and historical (healthy and faulty) data that are appropriate to maintenance decision-making. There are three groupings of Qualitative FDD methods: Statistical methods, Shallow or Machine learning methods and Deep learning methods

2.4.3.1 Statistical Method

Statistical methods contain many models, the most popularly used methods for classification problems are - principal component analysis (PCA), partial least squares (PLS), independent component analysis (ICA), fisher discriminant analysis (FDA) and the derivation of these methods. The statistical methods perform better with the feature that is in time series and dimensionality reduced.

2.4.3.1.1 PCA

Principal Component Analysis (PCA) works on the orthogonal transformation to select the features from the data. PCA maintains the important pieces of information from the data while diminishing their dimensions [37]

2.4.3.1.2 PLS

Partial least squares (PLS) use covariance information to identify the linear structure to transfer the data to a different domain, due to this reason PLS is widely used in fault detection problems [38].

2.4.3.1.3 ICA

Independent Component Analysis (ICA) method is widely used for analysing signals with non-Gaussian variables. Whereas the PCA and PLS can be used to analyse only Gaussian distributions [39].

2.4.3.1.4 FDA

Fisher discriminant analysis (FDA) is widely used for fault classification methods as it detects the right class/label of the data [40].

2.4.3.2 Machine Learning Method

Machine learning algorithms are an efficient tool for the issues caused by redundant data from the sensors and the experts. Widely used methods for fault diagnoses are genetic algorithm [41], support vector machine (SVM) [42], cluster analysis [43] and neural network (NN) [44].

2.4.3.2.1 SVM

For the binary classes, fault classification and no-fault found scenarios Support Vector Machine (SVM) is the most used machine learning method. The SVM method is derived from statistical learning theory, which is a computational method used in separating functions for classification and estimation functions in regression problems[37].

The SVM method has been extensively employed in gas turbine diagnostic problems by using their optimal classification feature. For instance, as SVM trains on engine dimensions, containing both healthy and faulty engine states the algorithm can classify as either healthy or faulty [45]or multiple faults [46]

2.4.3.2.2 Decision Tree

In addition, the fault causes are further classified using the decision tree technique since it gains a prudent accuracy and low-cost computation among other signal processing techniques [47]. Saravanan et al. proposed a decision tree to classify rules to build a repository of faults in a gearbox based on statistical value extracted from wavelet transform [48].

2.4.3.2.3 Neural Network

A Shallow learning neural network (NN) has various yet connected layers called neurons, each neuron produces a sequence of real-valued stimulations. Input neurons become triggered because of sensors depending on the environment, other neurons become stimulated through weighted connections from previously active neurons[49]. ANN (Artificial Neural Network) algorithm used in forecasting the initial wear of high-speed milling cutters with time-domain data, ANN algorithm has produced a more precise remaining useful life [50].

2.4.3.3 Deep learning methods

With the ability to learn features from raw data by deep architectures with many layers of non-linear data processing units, Deep Learning has become a promising tool for intelligent bearing fault diagnosis.[51]

Various deep learning methods have been previously used for fault diagnosis [52,53] including autoencoders [54,55], Deep Belief Networks (DBN) [56–58]], Recurrent Neural networks (RNN) [59–61] and Convolutional Neural Networks (CNN) [44,62–64]. The autoencoders and DBN model approach are employed in actuator fault diagnosis [65,66]. Moreover, the one-layer autoencoder has proven effective in fault classification [67].

2.4.3.3.1 Autoencoder

A simple autoencoder (AE) algorithm can train the model with only healthy data and estimate the multivariate time series data to find unusual defects for anomaly detection[68]. The AE is an unsupervised algorithm that admits the output value is equal to the input value. The Autoencoder extracts the features from a faulty dataset and transfers the non-linearized features to SoftMax classification to identify the fault category [69].

2.4.3.3.2 Convolutional neural network

Convolution Neural Network (CNN) is one of the most well-known fault diagnosis methods as the time domain data can be applied to the one-dimensional CNN algorithm in real-time. However, the study conducted by Zhang et al[70] compared the CNN method with traditional SVM, Multi-layer preceptor (MLP) and DBN; the feature extraction of CNN was lagging compared to other models.

2.4.3.3.3 Recurrent Neural Network

A recurrent Neural Network (RNN) is a sequential learning model that is mostly used in time-series data and predictions, due to its effective learning from the data. But the simple RNN has a gradient vanishing problem during the transfer of nodes from the first node to the last node, the information is dissipated [71]. Long Short-Term Memory (LSTM) Networks[63], are an improved form of RNNs can be used to solve the long-term dependencies and vanishing gradient problem. LSTMs perform better in extracting the features from long temporal sequences due to their architecture of gate neural networks [72].

LSTM network was intended to achieve fault detection and identification using available measurement signals and it performs better than convolutional networks[73]. Moreover, an LSTM model is proposed to achieve forecasting of trends and compared results demonstrated the better performance by neural network-based model [74].

2.4.4 Comparison of the Algorithms

With the ability to learn features from raw data through deep architectures with many layers of non-linear data processing units, Deep Learning has become a promising tool for intelligent bearing fault diagnosis[51].

In the fuel system test rig representing an Unmanned Aerial Vehicle (UAV) fuel system, the performance of the DT classifier is reasonably better and faster compared to the SVM and KNN in dealing with lower sample sizes used for the training phase[75].

A decision tree-based model is an effective supervised ML technique to implement the classification methods in high-dimensional data space. In DT models, the input and the corresponding output in the training data are explained and the data is continuously split based on a specified parameter [76,77]. DTs are used effectively in many diverse areas such as medical diagnosis, remote sensing, and speech recognition. They are also successfully applied for diagnostics and prognostics applications. Their application for diagnostics and prognostics is also wide and they have been applied for many systems such as electric products, rotating machinery[78], and the chemical industry [79]. One of the main features of DT is its capability to break down a complicated decision-making process into a set of simpler decisions, therefore it provides a solution that is often easier to interpret [76].

Artificial neural networks represent one of the most popular and highly effective data-driven approaches for diagnostics [80,81] in engineered systems. Palacios et al. [82] used different classifiers such as Naive Bayes, K-NN, ANN, and SVM fault identification of induction motor. They concluded that K-NN and neural Network gives more accuracy in terms of correctly classified instances for a given dataset. Fault detection analysis conducted on mechanical failures in the electric motors it was found that ANN performs with high accuracy and high fault tolerance when compared with SVM, CNN and RNN[83].

Machine Learning Technique	Advantage	Disadvantage
ANN	• Can model complex, non-linear systems • Can use many types of input data, though particularly normalised numerical values	• Requires a large amount of data for training • Might be time-intensive in

	• Classification accuracy is high • Can work with incomplete information • Can parallel process	determining the appropriate model and data training • High risk of over-fitting
Decision Tree	• Is easy to understand and interpret • Requires less effort for data preparation as there is no need for normalization or scaling of data • Can handle missing values • Has automatic features extraction • Has higher robustness to noise • Has more accurate results • Has a low risk of over-fitting	• Requires a large amount of data • • Consumes more time • Is instable in facing even small changes • Encounters difficulty in dealing with continuous attributes • Has relatively low accuracy for large domains
Auto encoder	• Classification accuracy is high • Fewer Errors due to the replication of input and output layers • Can handle missing values • Has automatic features extraction • Has higher robustness to noise • Has more accurate results	• Requires a large amount of data for training • Might be time-intensive in determining the appropriate model and data training • High risk of over-fitting

2.5 Aircraft Fuel System

Fuel systems design differs between aircraft depending on the comparative size, requirement, and complexity of the aircraft. In a multi-engine aircraft, the fuel system usually comprises numerous fuel tanks, that are mounted in the wing or the fuselage (or both) and in some instances in the empennage. The fuel storage tanks will contain internal fuel pumps that are linked with filters, valves, and pipes to feed the engine and maintain the aircraft's centre of gravity[84]. The fuel system is designed for the essential performances of the aircraft and to guarantee the safety of the flight, compatibility, dependability, and maintainability.

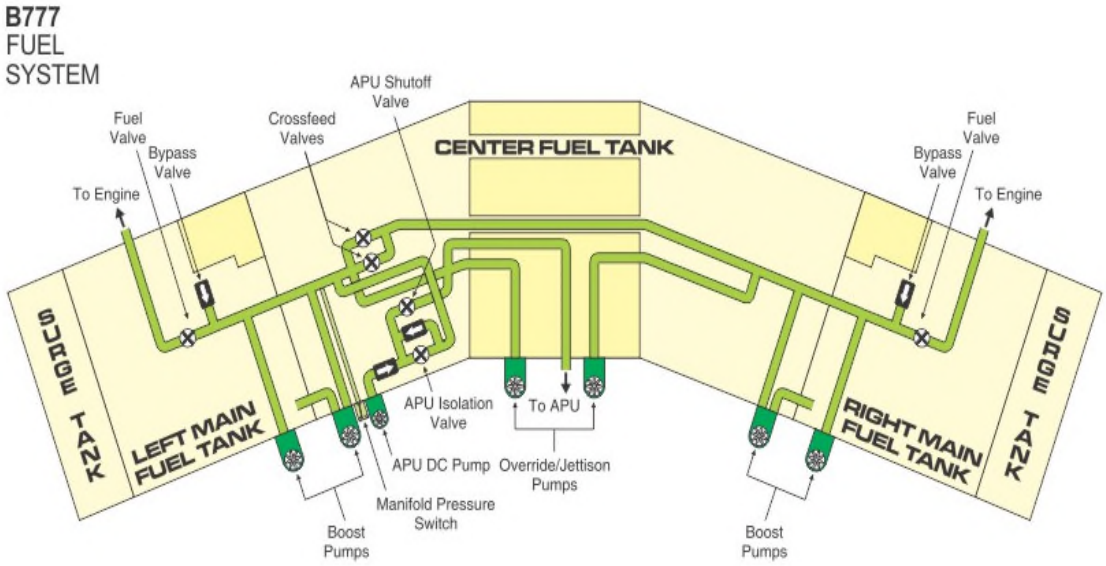

Figure 10 Boeing B777 Fuel System[85]

2.5.1 Aircraft Fuel system – Potential faults

The faults caused in aircraft fuel systems are usually due to degradation of components exposure (particulate contaminants), corrosion (initiated due to dust, dirt, rust, and ash), or erosion (initiated due to the chemical reaction). The conventional faults in the fuel system can be categorized into three [21].

A) Equipment faults (leaking pipes, Cracked joint),

B) Actuator faults (sticking valve, clogged filter, clogged nozzle) – Incapable to open or closing, stuck, or broken

C) Sensor faults (blocked flow meter) – Incapable to measure the reading accurately

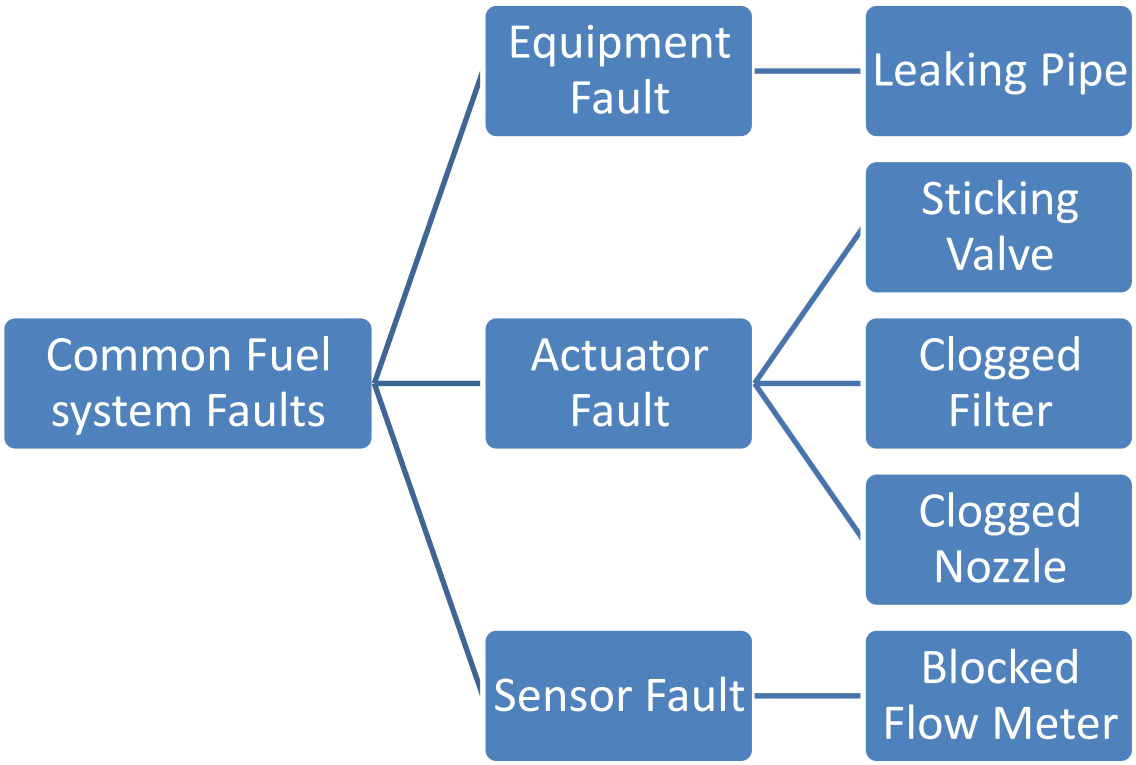

Figure 11 Common Fuel System faults

2.5.1.1 Equipment Fault

Fuel tank/pipe leakage - the aircraft will lose some or all fuel resulting in loss of power due to fuel starvation and potentially resulting in engine failure.

2.5.1.2 Actuator Fault

2.5.1.2.1 Sticking Value

If the valve doesn't operate to the desired extent, then the fuel delivered to the engine will be reduced or stopped, when this occurs the pressure build-up will cause a rupture in the fuel pipe causing the engine to choke [86].

2.5.1.2.2 Clogged Fuel filter

Fuel filters generally are usually fine mesh. The Main application of the fuel filter is to trap fine sediments that can as be small as a thousandth of an inch in diameter. If the fuel filter gets blocked or misfunctions the flow rate of the system reduces leading to a drop in engine performance. Filter clogging is an indication of fuel contamination that might result in flight plan termination to further investigate or replace the fuel filter[87].

2.5.1.2.3 Clogged Nozzle

Nozzle blockage can occur to the accumulation of degraded particles in the fuel system, which in turn will decrease the flow of the fuel and increase the pressure of the fuel[88]

2.5.1.3 Sensor Fault

Blocked Flow Meter- The flow meter measures the amount of fuel that flows through the system this allows the engine to perform at its full potential, making it a vital component. A faulty or clogged sensor can provide incorrect input signals to the Engine Control Unit (ECU) that, in turn, will provide incorrect controls for other components[89].

2.6 Conclusion

There is a requirement in the industry to develop advanced maintenance solutions that concentrate on increasing the efficiency of aircraft performance without compromising the safety and quality of flight.

PHM is a study conducted in various industries to improve system reliability, availability, and safety and to reduce the maintenance cost of engineering assets. Although much research effort has been made in the field of PHM, there is still a large gap between academic research and industry expectations.

There are also research gaps in the study of component-level failures in complex systems such as aircraft fuel systems. There is a connection between the components, and if the failure of one component escalates, it will affect the readings of the other sensors or cause an error.

Fault Diagnosis is crucial to reducing maintenance and operating costs, productivity and increasing competitiveness, as well as improving the passenger experience. However, collecting, transmitting, storing, processing, and visualising data can be challenging. There are a variety of tools that are constantly evolving and are selected according to the type of data collected (labelled or not) and the type of analysis selected (real-time or offline, classification, clustering, regression). In general, the implementation of certain time series tools is inadequate. Standard tools are often used for implementation, but this often results in the loss of the series timeline structure.

Finally, this chapter reviews and compares fault diagnostic methods that apply specifically to the aerospace domain. Failure diagnosis methods can be divided into qualitative methods and quantitative methods. Quantitative methods can further segment into data-driven and model-driven methods.

	Qualitative Methods	Quantitative Methods	
		Model-based Methods	Data-driven Methods
Advantage	Wide application Simplicity	Do not need extensive operating data Able to diagnose unknown failure mode	Adaptable and flexible Do not need system model
Disadvantage	Difficult to perform in complex system Require sufficient domain knowledge and experience Cannot cope with unknown failure mode	Require sufficient system information to build model Limited flexibility Hard to perform in complex system	High dependence on the quantity and quality of system operating data High computational complexity

Table 1Comparing present diagnostic methods

Table 1 summarizes the strengths and weaknesses of the fault diagnosis method. The model-based method requires physical interpretation of the system and its functions to derive the empirical formulas for fault diagnosis, which is time restraints and impossible to derive on a large scale.

Even though their main advantage is that the diagnosis can be done at a material level, system level, or component level. The model-based methods often have a high rate of false positives, resulting in false positives and additional maintenance costs and activities. Moreover, the assumptions used to create the model do not reflect the real operating scenario.

This current research focuses on developing aircraft fuel system data, a time series database method that applies to the working for the pipe, values, and sensors. The machine learning method is chosen because of the availability of data and limited knowledge of the system under investigation.

3 Methodology

In recent years, CBM is incorporated in many fields such as maintenance of machinery, software engineering, electronics, metrology, signal processing, telecommunication and so on. Even though the initial cost of execution of CBM is high, it compensated in a long run with its added advantages of increased safety, system reliability and availability of the system. CBM techniques also reduce maintenance costs by providing better maintenance planning and decision-making during maintenance.

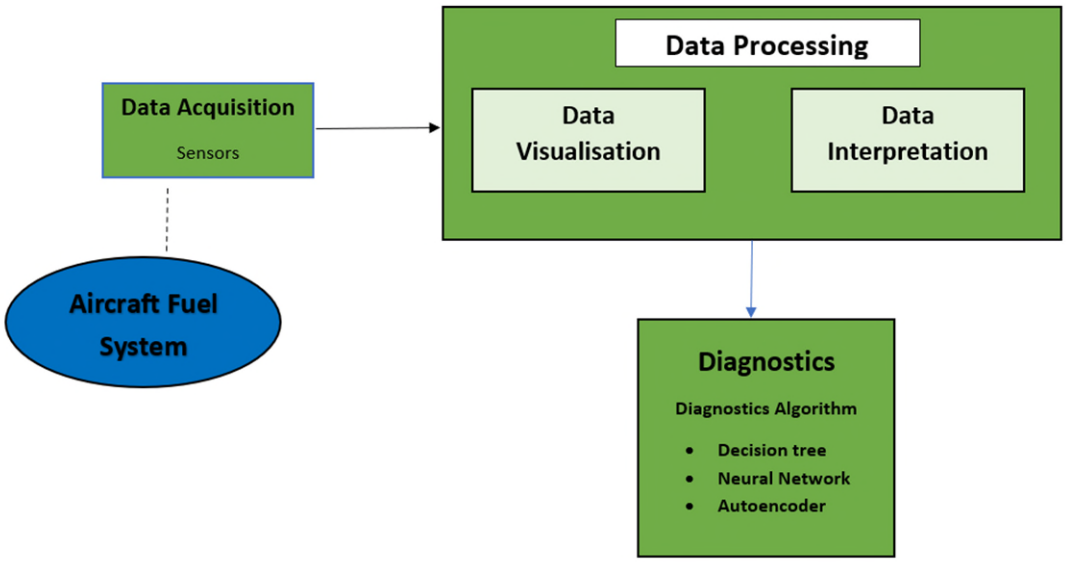

Figure 12 Methodology layout

3.1 Data Acquisition

Degradations are caused due to many reasons, so there is no one appropriate parameter to directly measure the existing faults. So, these parameters are obtained by the function of several measurable parameters that can be used to identify the quantitative extent of degradation, which can be an empirical model prediction of a vital part of degradation. For instance, the thickness of the fuel pipe may be an appropriate parameter but there is no discreet method to directly measure it.

In such cases, measurable parameters like temperature, pressure and flow rate can predict the wall thickness. Several measures of degradation source will give the close remaining useful life approximation. If the degradation is not dealt with in time and if the severity surpasses the threshold value, it may lead to failure.

3.1.1 Experimental setup

In an aircraft fuel system, the typical faults can be categorised into three types – equipment, actuator, and sensor faults. The equipment faults – affect the operating ability of the system (leaking pipe). Actuator faults impact the actuated parts of the system (pump or valve faults), and sensor faults alter the sensor operation. The faults caused in aircraft fuel systems are usually due to degradation of components exposure (contaminants), erosion (initiated due to dust, dirt, rust, and ash), or corrosion (initiated due to the chemical reaction).

It is not possible to simulate different severity of faults in real aircraft fuel systems due to the cost involved and the safety of the aircraft. So, to obtain sensor readings a rig replicating the aircraft fuel system of Boeing-777 is used. In a real fuel rig scenario, the degradation happens after a long period of usage, and the data from it is hard to obtain, time-consuming and expensive. Three modes can be applied were injected into the experimental model to get degradation data[90]

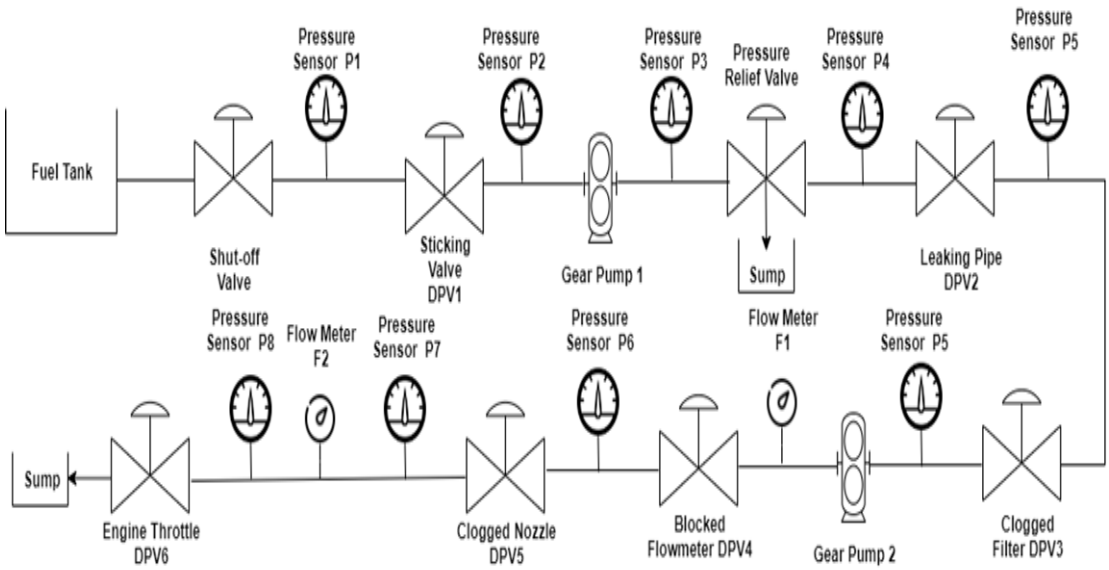

Figure 13 Layout of the fuel rig system

1) Increase speed degradation testing – Running the rig for a longer time period for the degradation to occur is not possible so the tests under particular critical conditions (e.g., very high speed, extreme loads) may aggravate degradation like fatigue, corrosion, creep, etc.
2) Imitating degradation modes – The cause of the degradation can be replicated using the rig. For instance, a leaking pipe can be replaced by a DPV, that can generate an output (flow, pressure) relative to electronic control input so that the leaking pipe fault can be imitated by steadily closing DPV. Using this technique can produce reproducible healthy and faulty signals.
3) From the previous research done on the degradation in aircraft fuel systems, the approximate degraded modes can be simulated.

The fuel system rig (Figure 13& Figure 14) contains an electrical gear pump with an internal relief valve, a shut-off valve, one filter, two tanks (main tank and sump tank, the last one imitating the engine), a non-return valve, variable restrictor to simulate engine injection and backpressure when partially closed. It also contains nine pressure sensors (marked P1-P9), two flow meters (F1-F2) and laser sensors that gauge pumps rotational speed.

Sensor	Description
Absolute Pressure Sensor	Measurement range: 0-5 bar, Output Signal: 0-5V, Quoted accuracy: ±0.25% (full scale), Power Supply: 12.8V DC
Gauge Pressure Sensor	Measurement range: 0-4 bar, Output Signal: 0-5V, Quoted accuracy: ±0.25% (full scale), Power Supply: 12.8V DC
Flow Meter	Measurement range: 0-2L/min, Output Signal: 0-5V, Quoted accuracy: ±3% (full scale), Temperature sensitivity: ±0.2% per ℃, Reference temperature: 23℃, Power Supply: 12.8V DC
Laser Sensor	Sensing range: 0-10 m, Power Supply: 10-30V DC

Table 2 Sensor Description

The Experimental setup in the IVHM lab (Cranfield University) replicates Boeing 777 fuel system [90]. The five faults (with different severity) such as Leaking pipe, clogged filter, clogged nozzle, sticking valve and blocked flow meter are introduced into the Rig (Figure 14). The original rig operation is modified for this experiment purpose and the connection of fuel flow between the left-wing tank and right-wing tank is eliminated.

Figure 14 Aircraft fuel system test rig in Cranfield University IVHM Centre

The data for five different faults with (0% to 100 %) severity can be collected from this rig setup. For example, in any aircraft fuel system if the is the presence of a leaking pipe the fuel flow pressure will decrease. These faults are imitated by replacing the faulty components with a Direct Proportional Valve (DPV). If the DPV is fully closed, then the data obtained from the rig is considered to be healthy data. The severity of the faults can be introduced by opening the DPV valves. By doing so the slow development, spilling, and abrupt and recurrent types of degradation can be simulated on the rig

Fault type	Fault
Equipment fault	Leaking pipe
Actuator Fault	Sticking valve, Clogged filter, Clogged nozzle
Sensor Fault	Blocked flow meter

Table 3 Fault injected into the fuel system

The Volumetric flow rates in the core and pressure rates at nine different locations are determined using flowmeters and pressure sensors. To obtain the healthy data from the fuel system, DPV valves are set in such a way (Table 4) DPV1(Sticking Valve) – 100% open, DPV2 (Leaking pipe) - 100% closed, DPV3 (Clogged Filter) - 100% open, DPV4 (Blocked Flowmeter) - 100% open and DPV5 (Clogged Nozzle)- 100% open. Pressure and flow rates for the healthy condition were recorded for 18 minutes to attain a good estimation and pump rotational speed was set at a variable 500rpm to 700rpm. The feedback loop of the pump control unit was dynamic, so the pump speed was varying for the entire testing session.

3.1.2 Limitations

- This thesis is based on machine learning techniques, which in turn require a large historical data for a more accurate diagnostic result. As the data

was collected in a rig and not in a real-case scenario the historic data on the degradation of the systems are not available.

- This research undertakes that the sensors in the aircraft fuel system rig are adequate for fault diagnosis.
- This research considers only the faults that frequently occur in the aircraft fuel system, it doesn't concentrate on the minor or unknown faults
- The data collected with the operation of all the DPVs (DPV1,3,4, 100% open and DPV2 – 100% closed) is considered to be the baseline healthy data.
- The fuel rig setup doesn't have any disturbances, so the data collected is clean from noise. This does not represent the real case scenario.

3.1.3 Experiment procedure

The original rig operation is modified for this experiment purpose and the connection of fuel flow between the left-wing tank and right-wing tank is eliminated. For consistency reasons the results of the Pump 2 in a variable speed of 500rpm to 700rpm. The tests are run with different scenarios - incidents with a specific fault escalating in time and for five different faults with different severity, as mentioned in Table 4. The fault severity was increased from 0% to 100%. Faulty readings were taken with the constant values of 0%, 25% and 50%.

Table 4 presents the rig alignment of the experiment. For uniformity, all the types of fault data were collected at the same severity. The experiment of the rig was conducted at a steady state condition. For all the data collection for the healthy state, the leaking pipe DPV was at 0% open and, the other DPV valves were open at 100%. For instance, for the clogged nozzle experiment, the DPV 5 was open between 50% and 75%. The other DPVs except for DPV2(leaking pipe) were 100% open.

Gear pump 1 (acts as a low-pressure pump) is controlled to run at a variable speed and gear pump 2 (acts as a high-pressure pump) is regulated to deliver a constant flow rate. The shut-off valve and the engine throttle valve (DPV6) are fully opened throughout the experiment.

Fault Type	Fault Severity (%)	DPV1 open (%)	DPV2 open (%)	DPV3 open (%)	DPV4 open (%)	DPV5 open (%)
Healthy	0	100	0	100	100	100
Sticking valve	25	75	0	100	100	100
Sticking valve	50	50	0	100	100	100
Leaking pipe	25	100	25	100	100	100
Leaking Pipe	50	100	50	100	100	100
Clogged Filter	25	100	0	75	100	100
Clogged Filter	50	100	0	50	100	100
Blocked Flow meter	25	100	0	100	75	100
Blocked Flow meter	50	100	0	100	50	100
Clogged Nozzle	25	100	0	100	100	75
Clogged Nozzle	50	100	0	100	100	50

Table 4 Data Collection with different fault severity

3.2 Data Processing

In an aircraft, an onboard diagnostics system may display several fault codes because of a single faulty component, the consequent fault code is produced as dependent systems react to incorrect inputs. With the help of research, the aircraft systems might self-diagnose in future, but in the current situation, the occurrence of unforeseen faults will continue which will require ground-based test equipment to collect and analyse data.

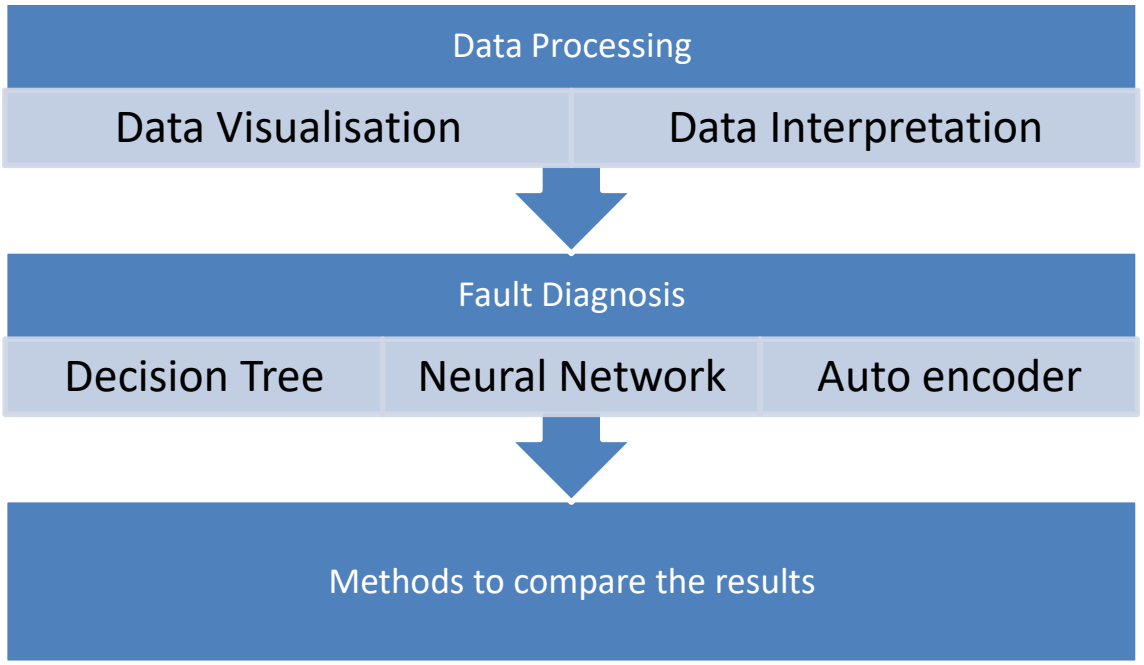

Figure 15 Data Flow chart

3.2.1 Data Visualisation

3.2.1.1 Healthy

The experiment of the rig was conducted at a steady state condition. For all the data collection for the healthy state, the leaking pipe DPV2 was at 0% open and, the other DPV valves (1,3,4,5) including the shut-off value and engine throttle were open at 100%.

3.2.1.1.1 Pressure

Figure 16 represents the pressure reading of all the pressure sensors from P1 to P9. Expect the pressure reading of P3 and P7 which are placed after the gear pump (1&2), all the other pressure sensor readings follow the same pattern. The pressure rate drops at the P5 sensor which is placed before the gear pump 2

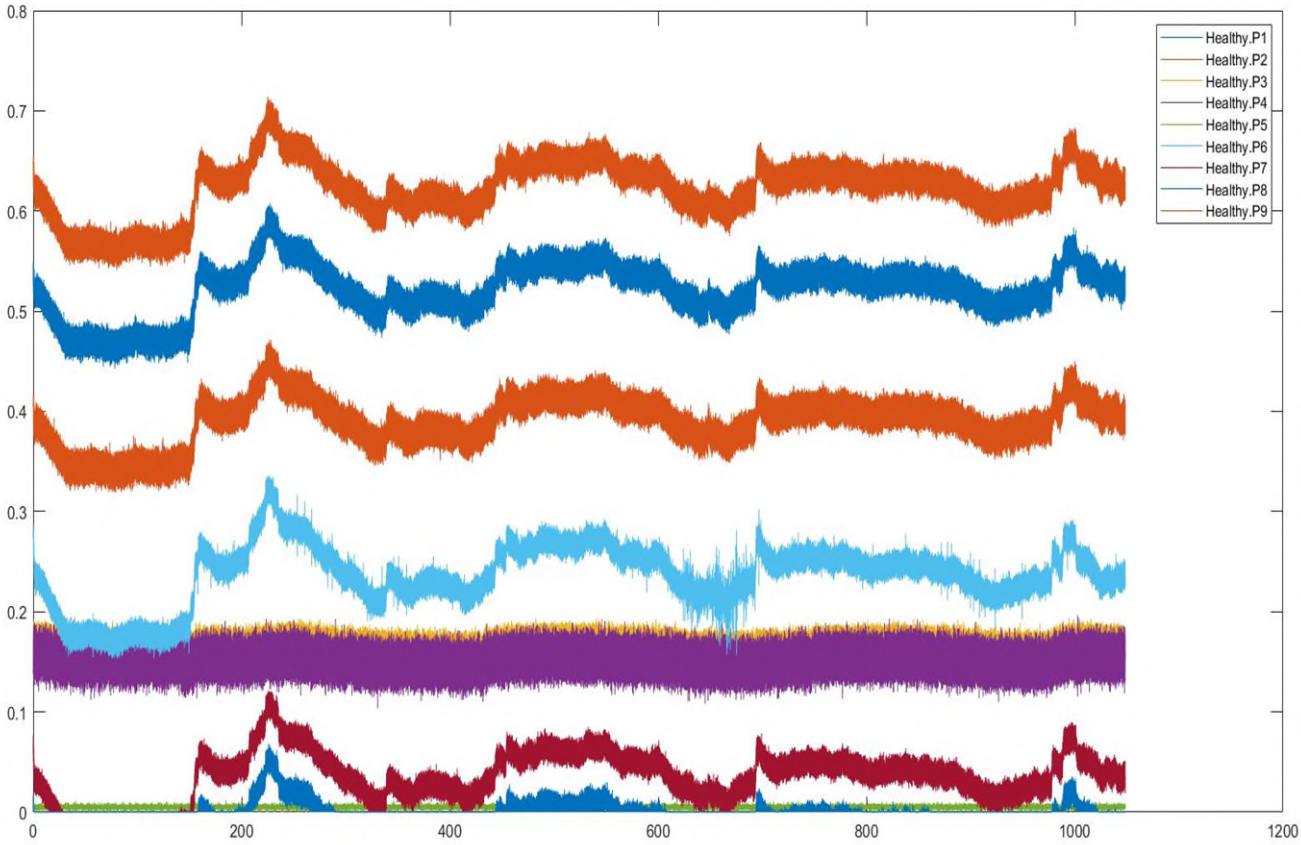

Figure 16 Healthy - Pressure

3.2.1.1.2 Flowrate

The Flowrate for this experiment is kept constant, this is to observe the components that compensate for the failure of others. Figure 17 represents the flow rate data collected by the F1 & F2 sensor. It can be noticed that the average flow rate is around 0.6l/sec throughout the fuel system rig.

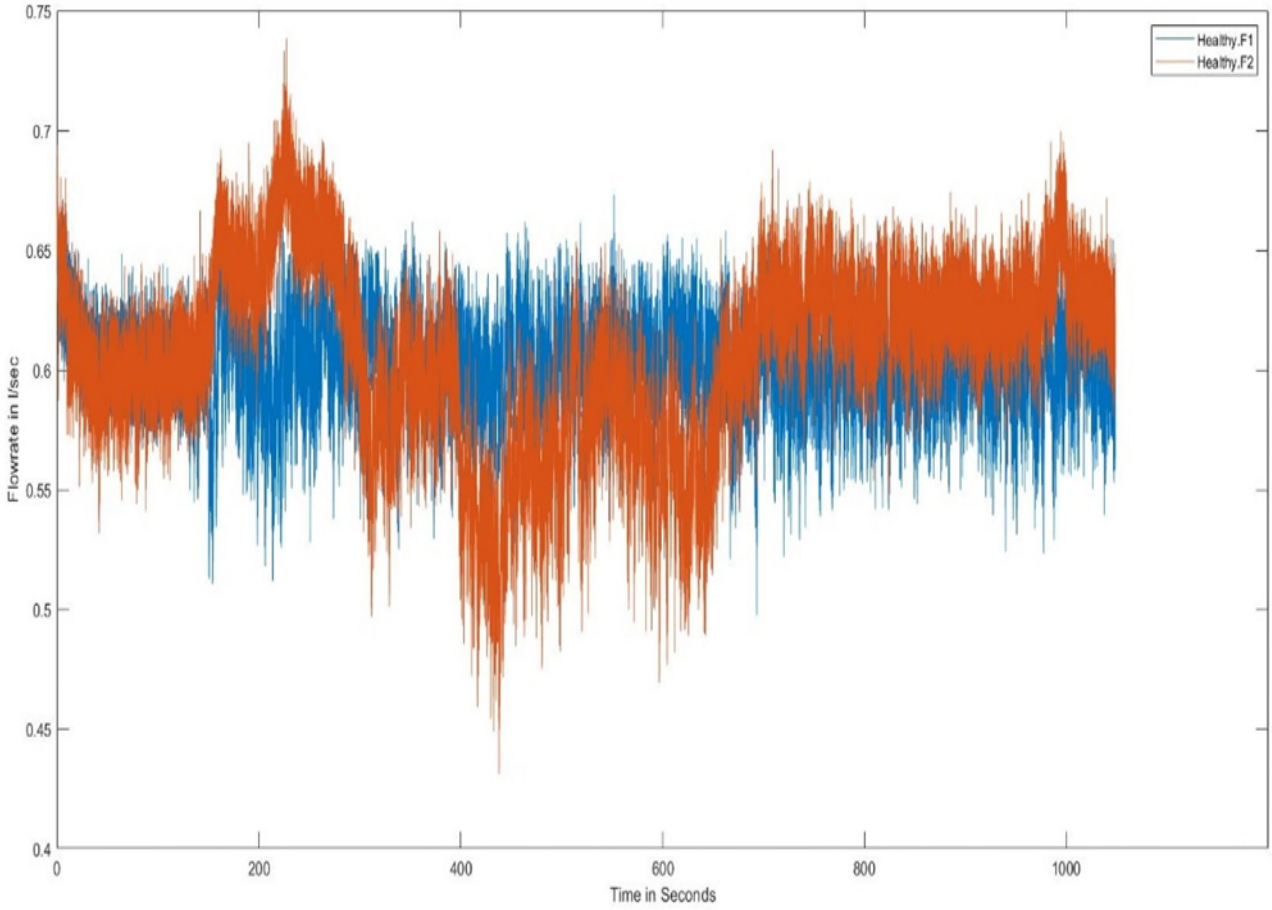

Figure 17 Healthy Flow rate

3.2.1.2 Sticking Valve

For the sticking valve scenario, the DPV 1 valve is open at 75% and 50% to imitate the valve sticking at 25% and 50% and the valve not opening to its maximum has pressure and flow rate difference across the fuel system.

3.2.1.2.1 Pressure

The valve DPV1 is positioned between the pressure P1 and P2, and the reading of the pressure sensor P2 decreases respectively when the sticking fault occurs. As shown in Figure 18 & Figure 19initial pressure differed all the following pressure reading follows the same pattern except for the pressure reading of P3 and P7 which are placed after the gear pump (1&2), all the other pressure sensor reading follow the same pattern. The pressure rate drops at the P5 sensor which is placed before gear pump 2.

Even though the pressure reading follows the same pattern for Figure 18 Sticking Valve (Pressure Sensor) – 25% Severity & Figure 19 Sticking Valve (Pressure Sensor) – 50% Severity. There is a massive difference in the pressure drop at P4, P6 and P8.

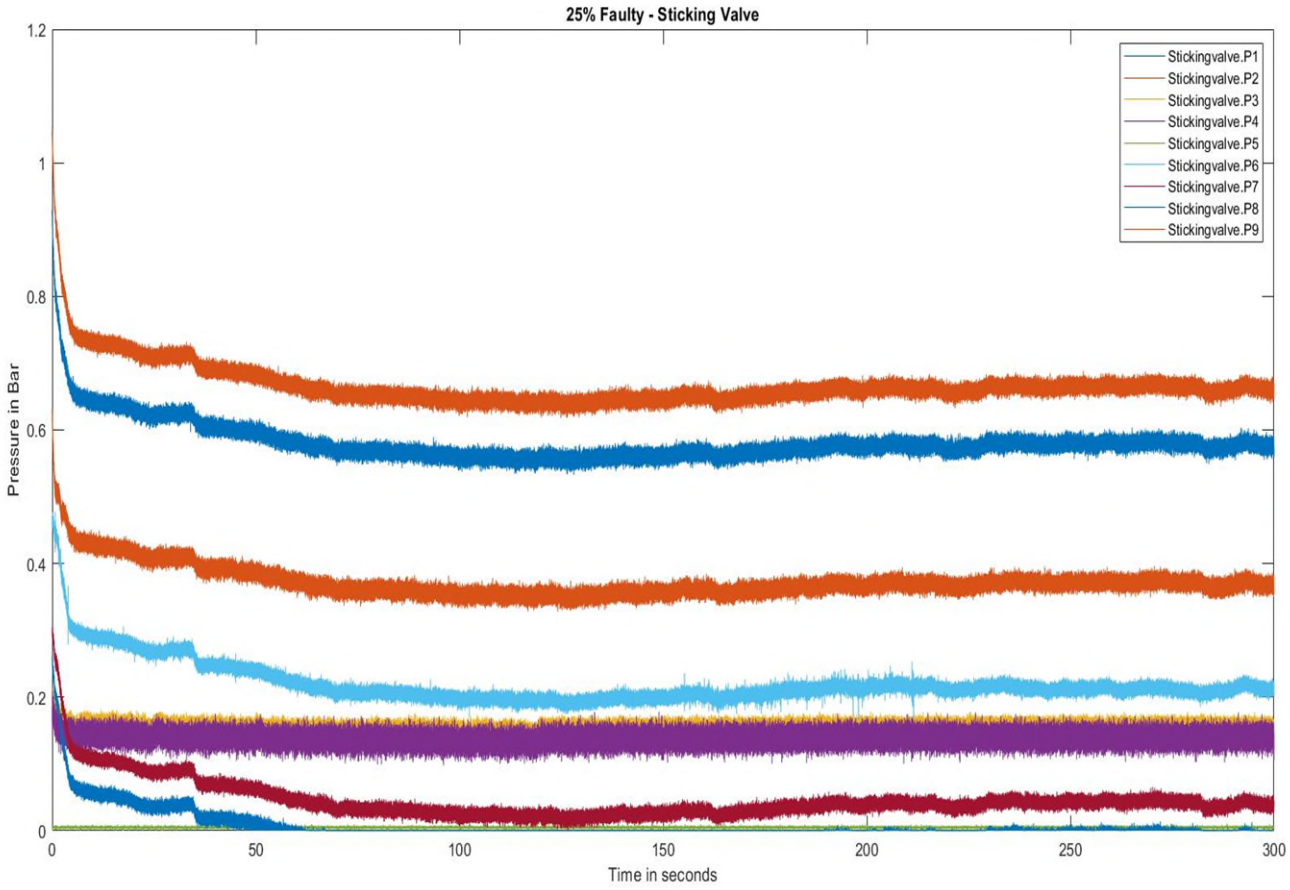

Figure 18 Sticking Valve (Pressure Sensor) – 25% Severity

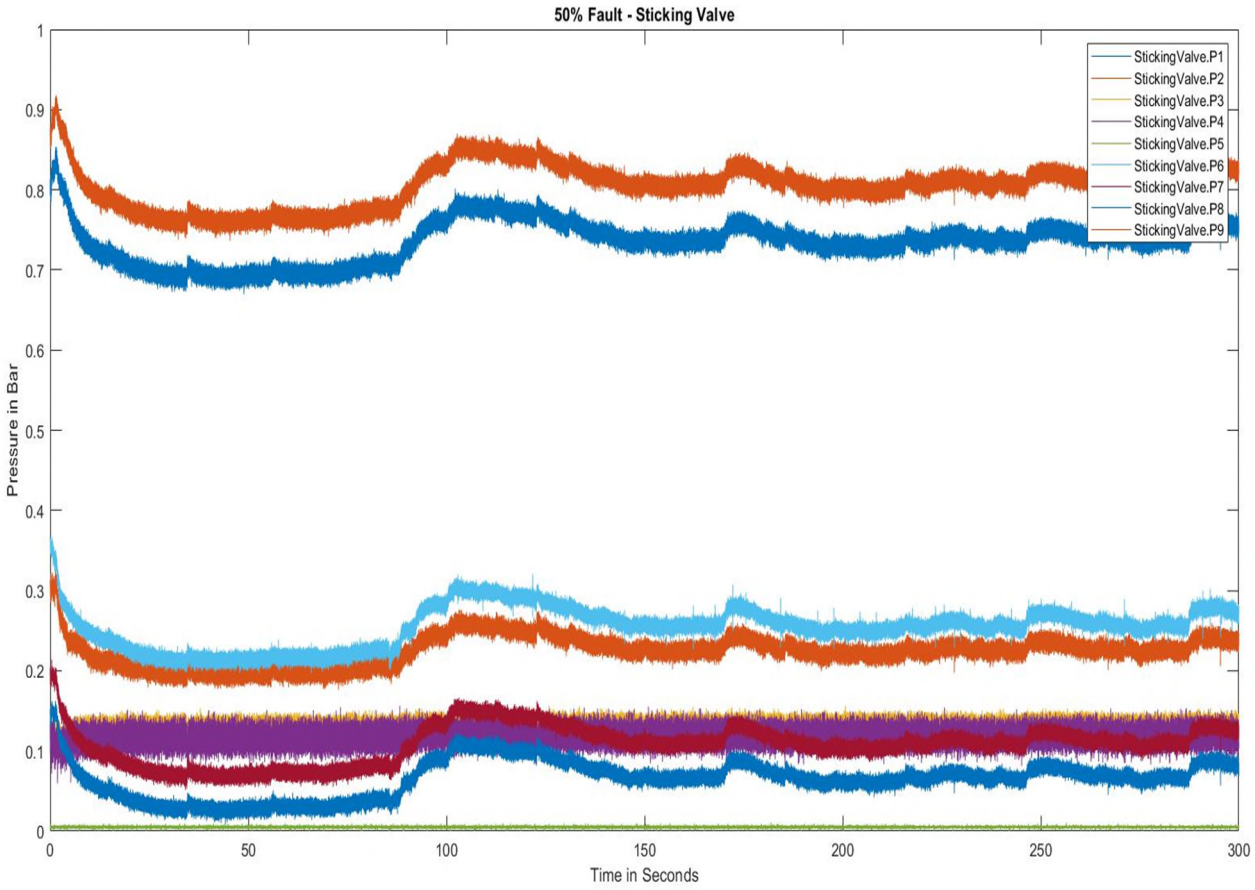

Figure 19 Sticking Valve (Pressure Sensor) – 50% Severity

3.2.1.2.2 Flowrate

The flow rate F1 is almost stable as the healthy case and the flow rate measured at flow meter F2 has a drop-in flow rate comparatively. The Flow rate represented in Figure 20 Sticking Valve (Flow Rate) – 25% Severity has more effect on flow rate compared to the Figure 21 Sticking Valve (Flow Rate) –50% Severity

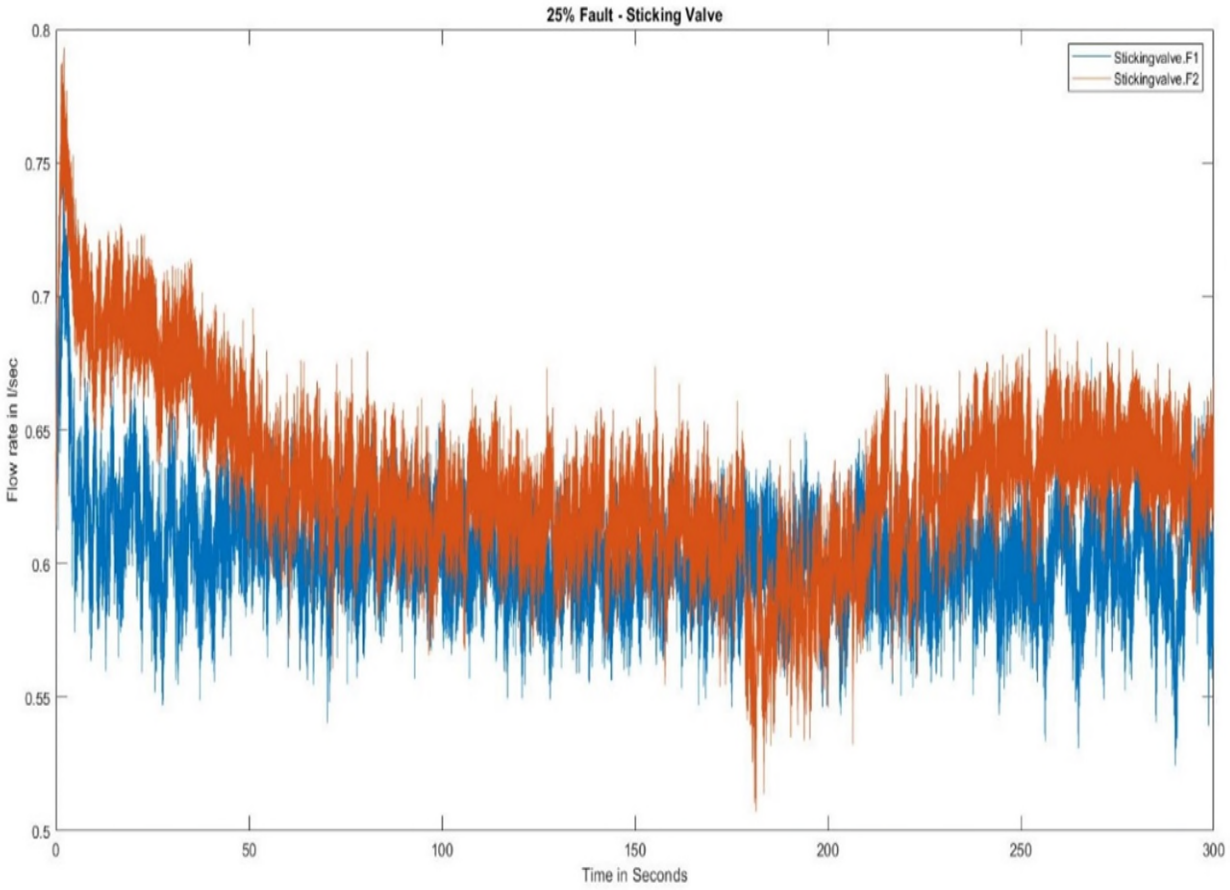

Figure 20 Sticking Valve (Flow Rate) – 25% Severity

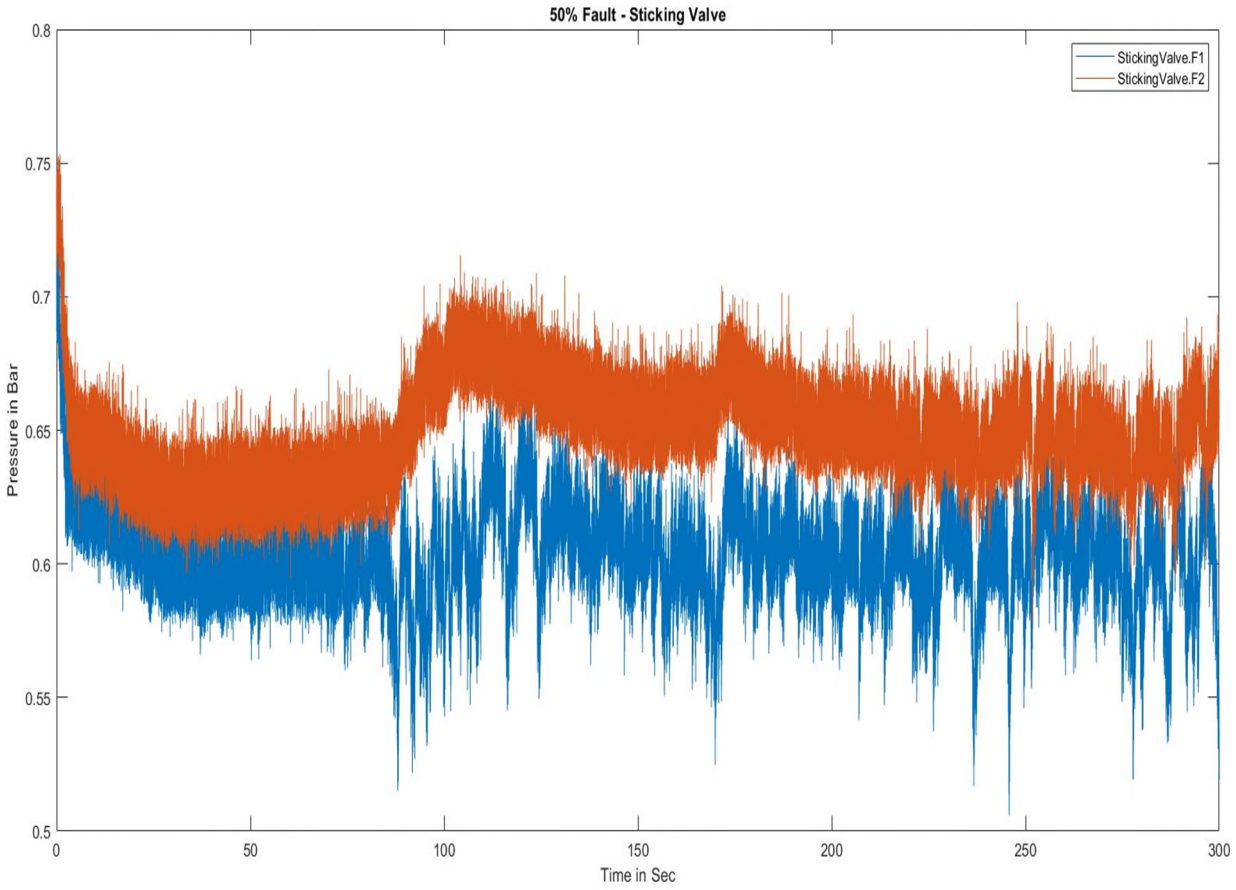

Figure 21 Sticking Valve (Flow Rate) –50% Severity

3.2.1.3 Leaking Pipe

For the Leaking pipe scenario, the DPV 2 valve is open 25% and 50% to imitate the valve sticking 25% and 50% and the valve not opening to its maximum has pressure and flow rate difference across the fuel system.

3.2.1.3.1 Pressure

In the case of a leaking pipe fault, the valve DPV2 is positioned between the two-gear pump which is operating at variable speed. The pressure sensor that is placed before the DPV2 valve is P3 and the one after is P4, the pressure drops at P4 due to the leaking pipe simulation. The pressure sensor reading of P1 & P2 will not change.

As shown in Figure 22 & Figure 23 initial pressure differed all the following pressure reading follows the same pattern except for the pressure reading of P3 and P7 which are placed after the gear pump (1&2), all the other pressure sensor reading follow the same pattern. The pressure rate drops at the P5 sensor which is placed before gear pump 2.

Even though the pressure reading follows the same pattern for Figure 20 Sticking Valve (Flow Rate) – 25% Severity & Figure 23 Leaking Pipe (Pressure Sensor) – 50% Severity. There is a massive drop in the pressure drop at P4.

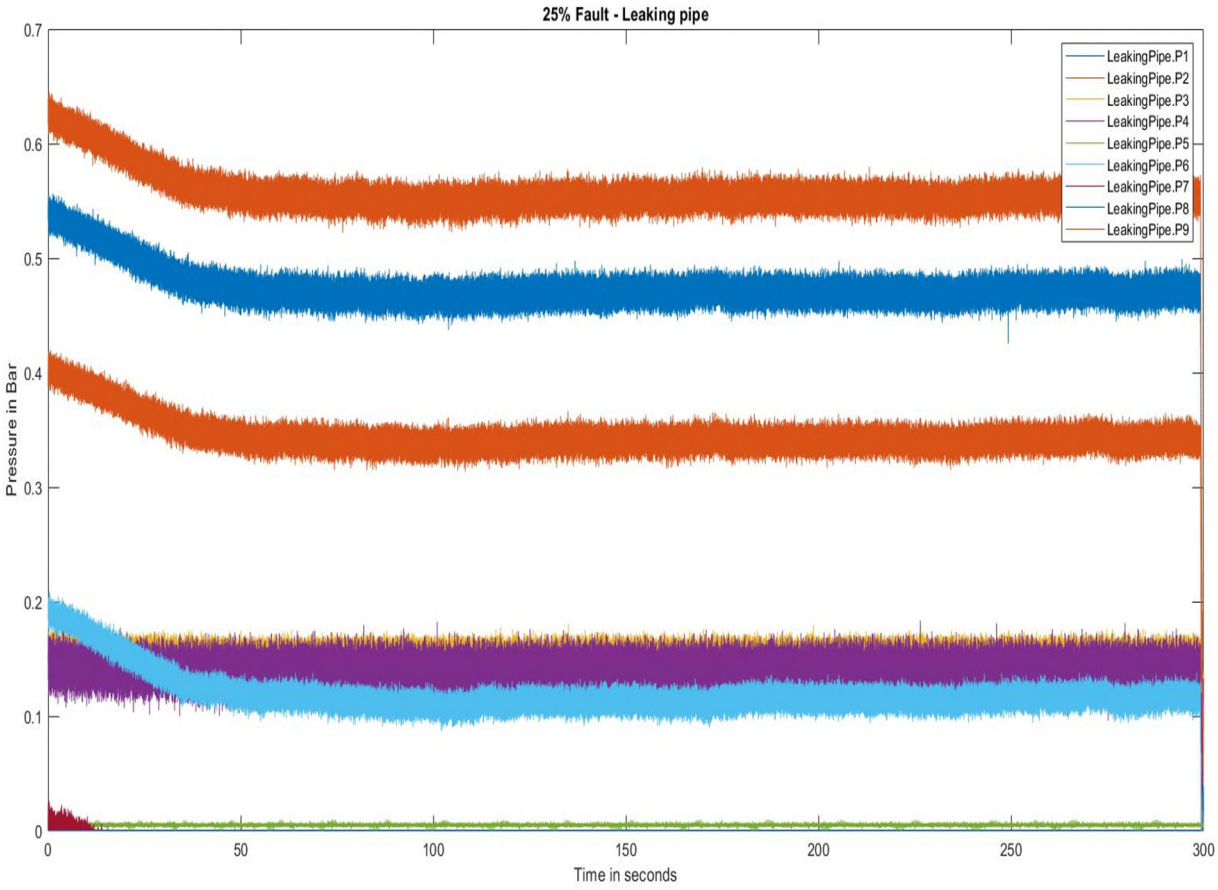

Figure 22 Leaking Pipe (Pressure Sensor) – 25% Severity

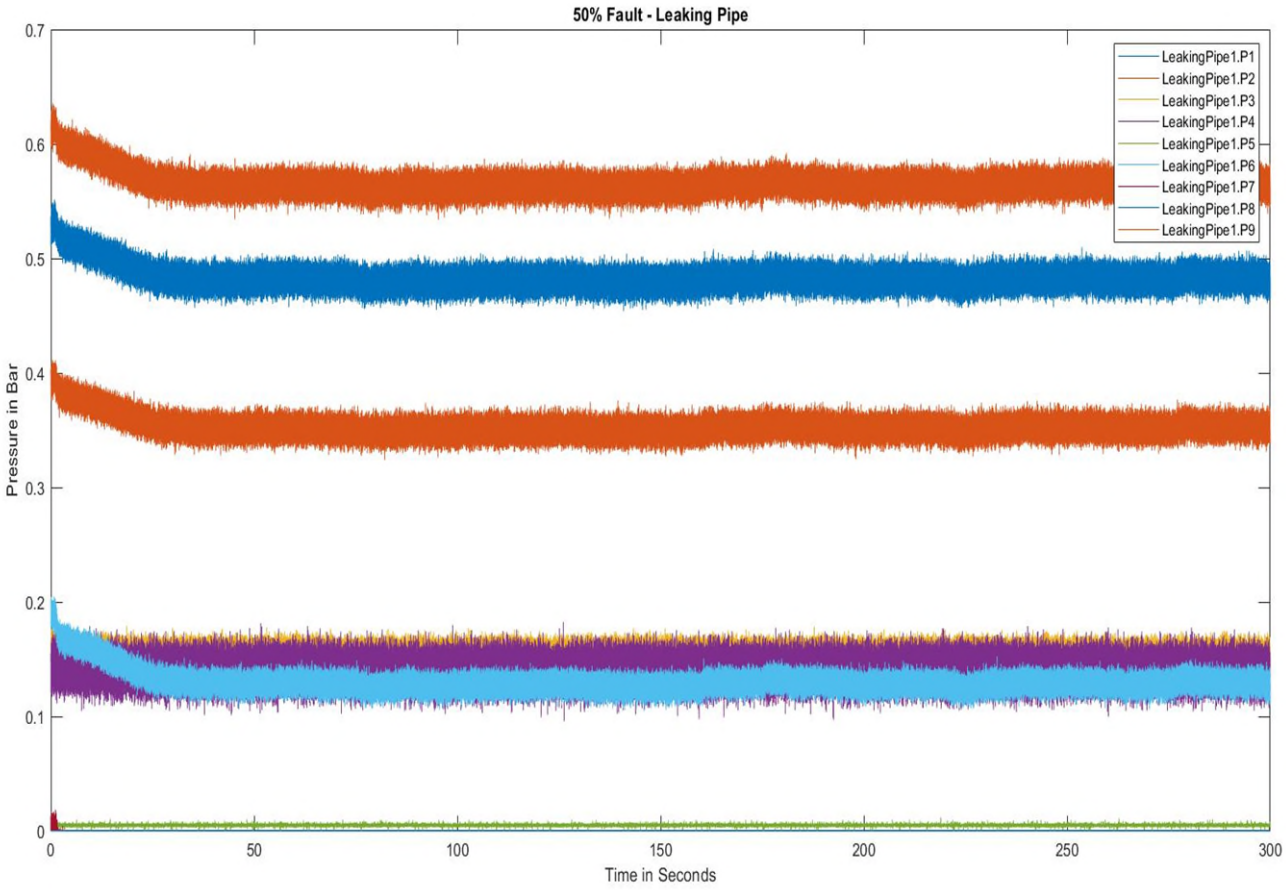

Figure 23 Leaking Pipe (Pressure Sensor) – 50% Severity

3.2.1.3.2 Flowrate

The flow rate F1 is almost stable as the healthy case and the flow rate measured at flow meter F2 has a drop-in flow rate comparatively. The Flow rate represented in Figure 24 Leaking Pipe (Flowrate) – 25% Severity is less impacted compared to Figure 25 Leaking Pipe (Flowrate) –50% Severity.

Figure 25

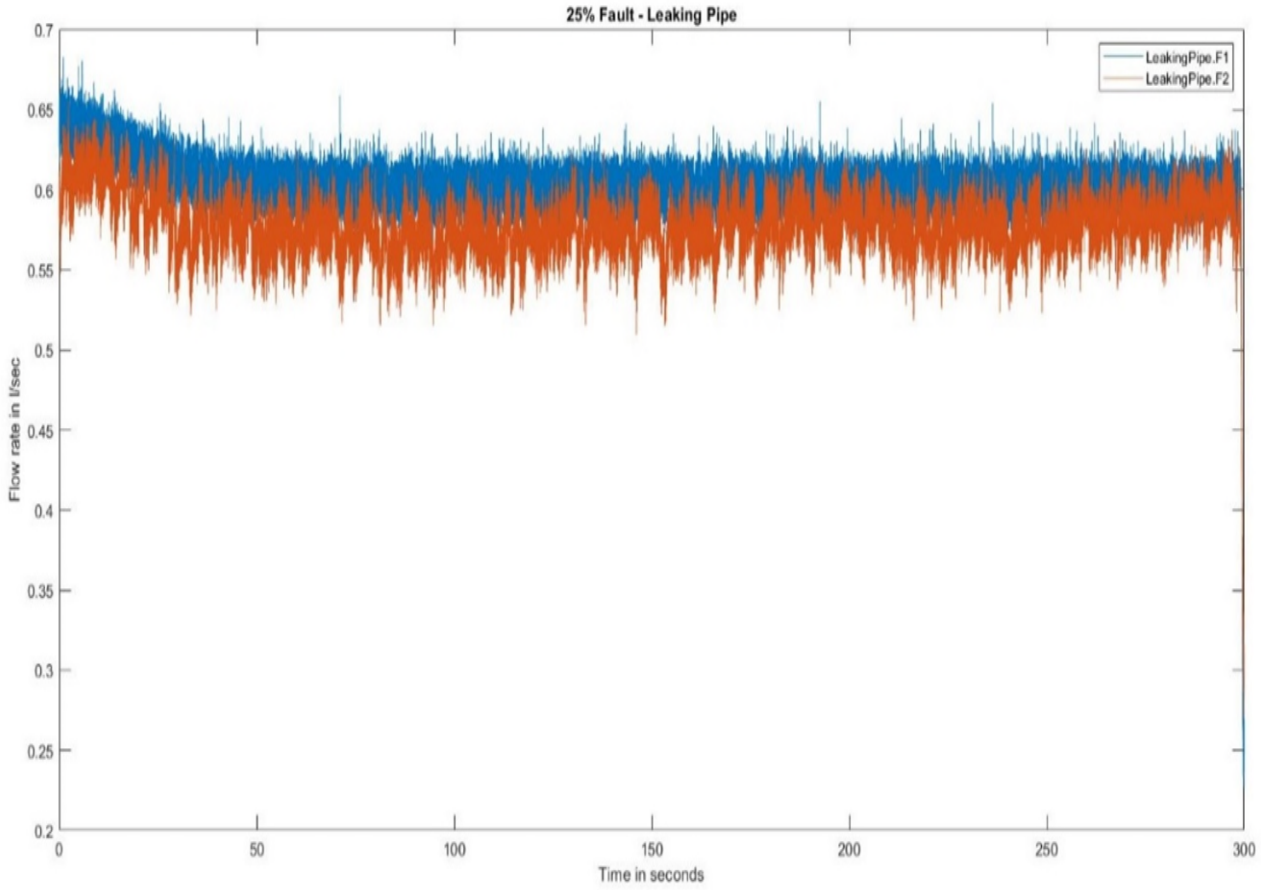

Figure 24 Leaking Pipe (Flowrate) – 25% Severity

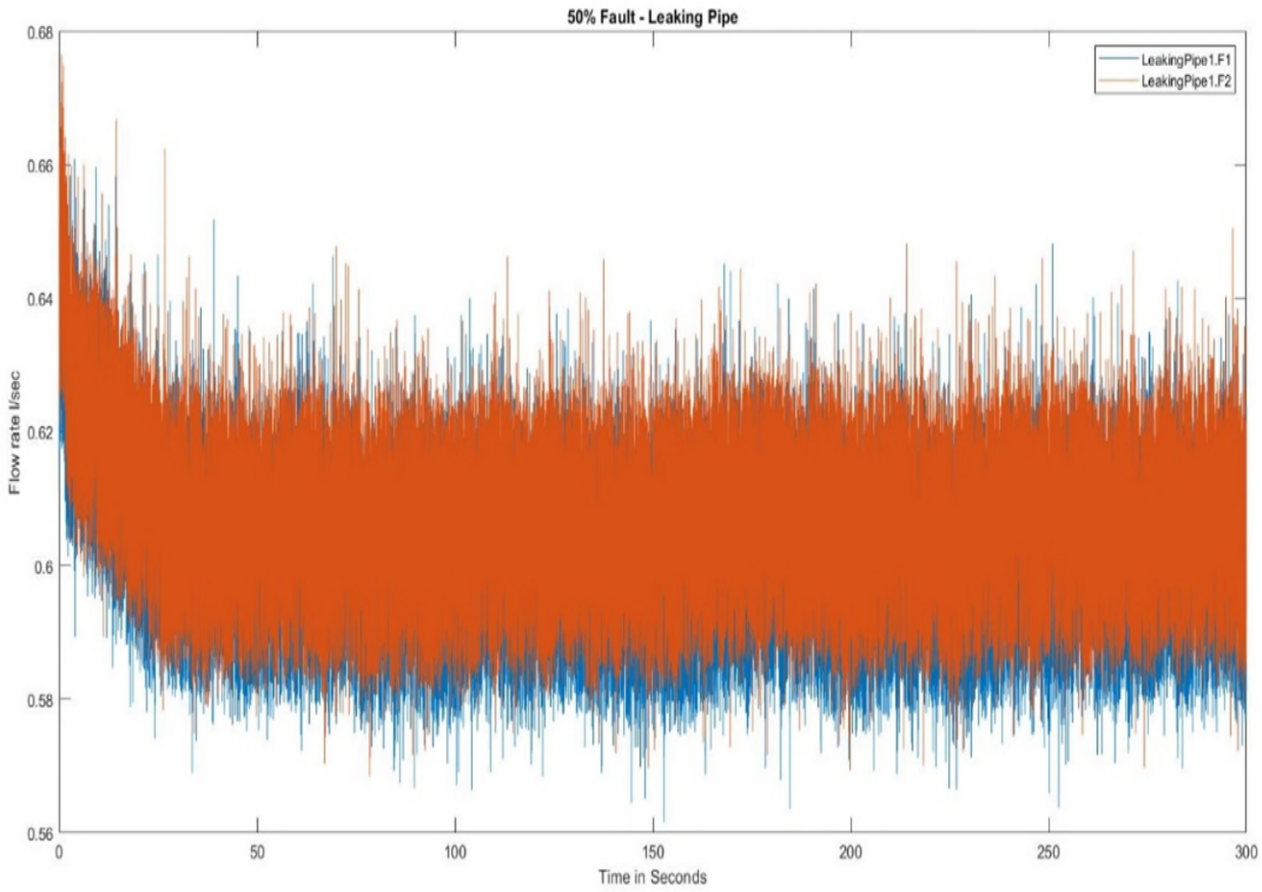

Figure 25 Leaking Pipe (Flowrate) –50% Severity

3.2.1.4 Clogged Filter

For the Clogged filter scenario, the DPV 3 valve is open at 75% and 50% to imitate the clogged filter at 25% and 50% and the valve not opening to its maximum has pressure and flow rate difference across the fuel system.

3.2.1.4.1 Pressure

In the case of a Clogged filter fault, the valve DPV3 is positioned between the two-gear pump which is operating at variable speed to provide a constant flow of 0.6l/min. The pressure sensor that is placed before the DPV3 valve is P4 and the one after is P5, the pressure drops at P5 due to the clogged filter simulation. The pressure sensor reading of P1 & P2 shouldn't change similar to other scenarios but for the clogged filter case there is a pressure drop even in P1 & P2 for Figure 26 Clogged Filter (Pressure Sensor) – 25% Severity.

But in Figure 27 Clogged Filter (Pressure Sensor) – 50% Severity the pressure P1 and P2 react similarly to previous failures. Even P3 and P7 which was almost constant in previous scenarios have increased by more than 0.2 bar for Figure 26 Clogged Filter (Pressure Sensor) – 25% Severity and 0.7 for Figure 27 Clogged Filter (Pressure Sensor) – 50% Severity. The pressure sensor reading at P4 has dropped as low as the leaking pipe for Figure 26 Clogged Filter (Pressure Sensor) – 25% Severity but for Clogged Filter (Pressure Sensor) – 50% Severity P4 has returned to normal. As there is no previous data for given severities the data obtained is assumed to be normal for the clogged filter fault.

The pressure P7 which are placed after gear pump 2 stayed constant even though other pressure sensor varied massively.

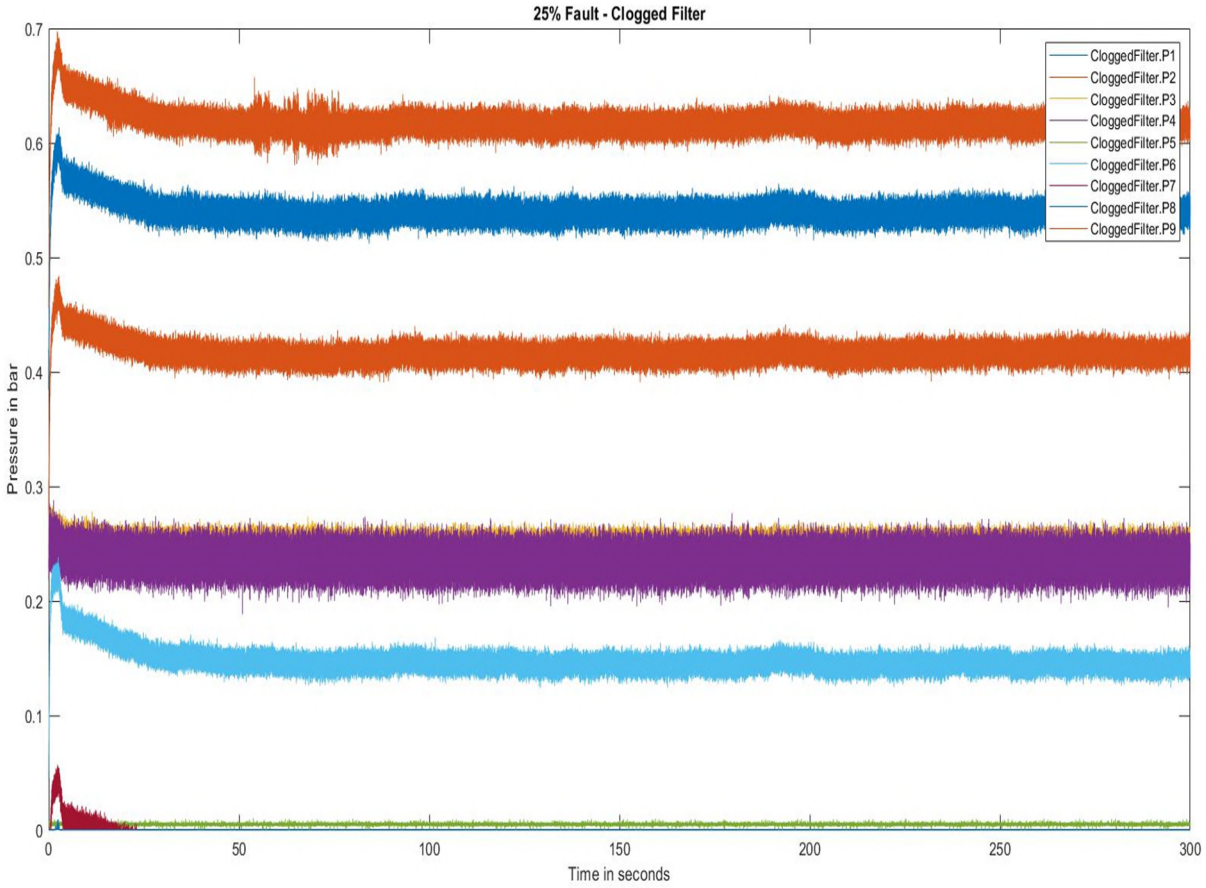

Figure 26 Clogged Filter (Pressure Sensor) – 25% Severity

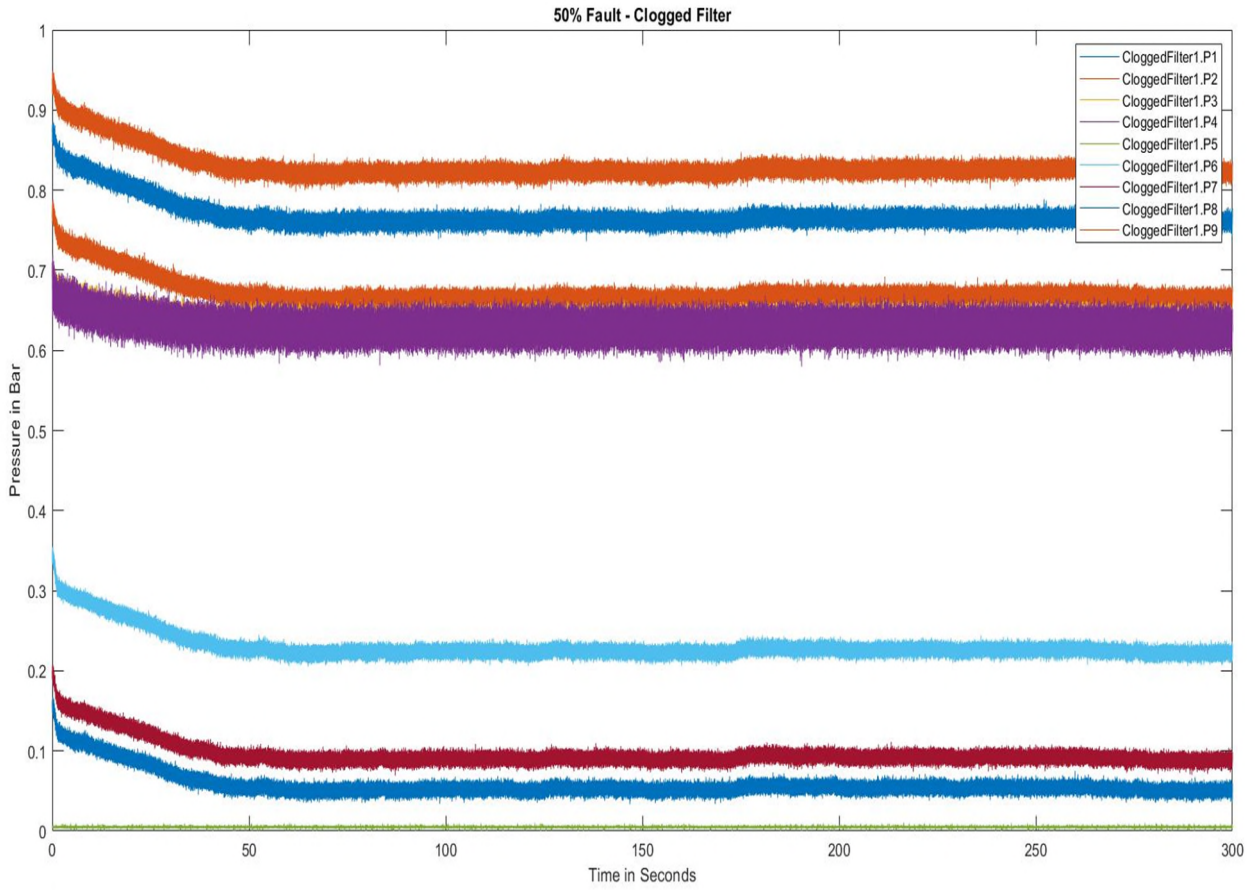

Figure 27 Clogged Filter (Pressure Sensor) – 50% Severity

3.2.1.4.2 Flowrate

The flow rate F1 is almost stable as the healthy case and the flow rate measured at flow meter F2 has a drop-in flow rate comparatively. The Flow rate represented in Figure 28 Clogged Filter (Flowrate) – 25% Severity is less impacted compared to Figure 29 Clogged Filter (Flowrate) – 50% Severity

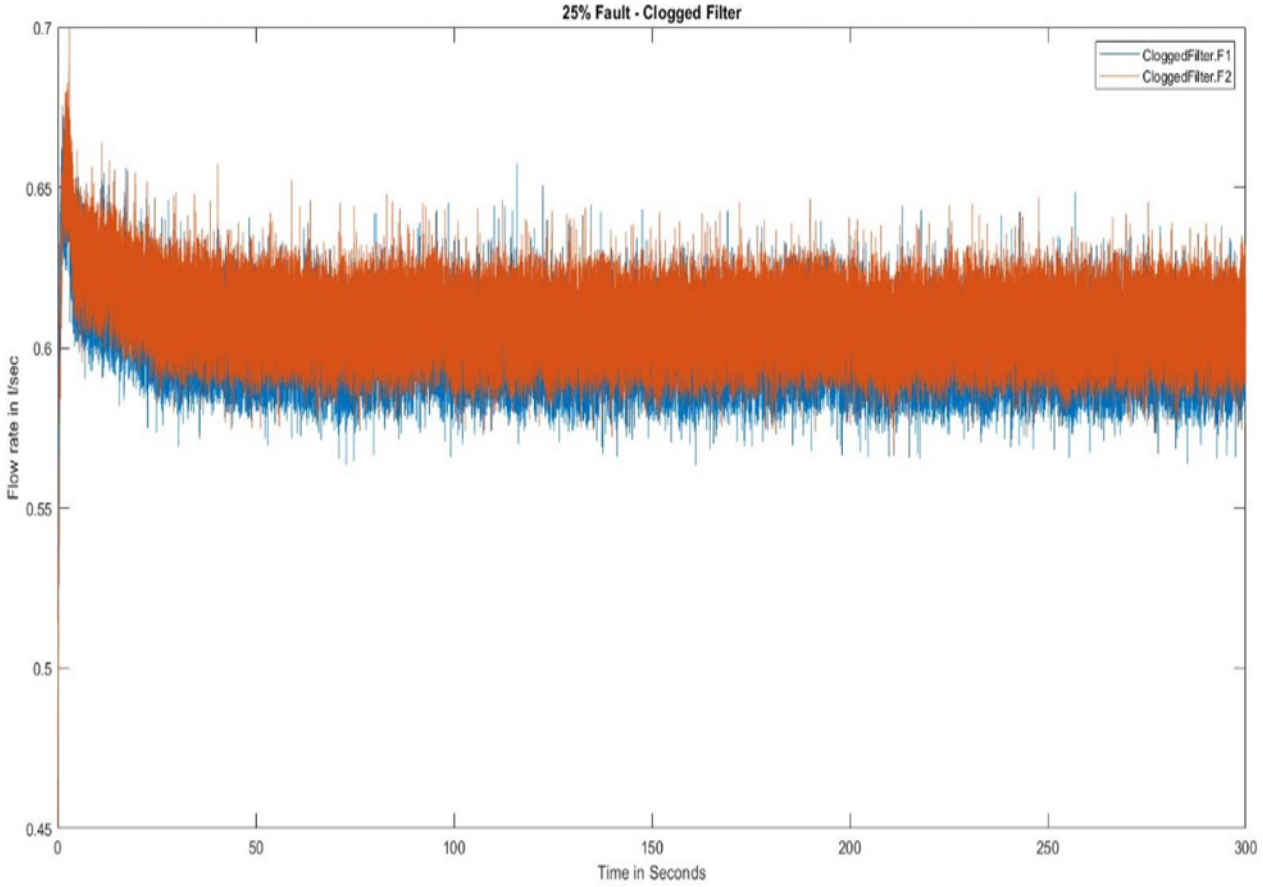

Figure 28 Clogged Filter (Flowrate) – 25% Severity

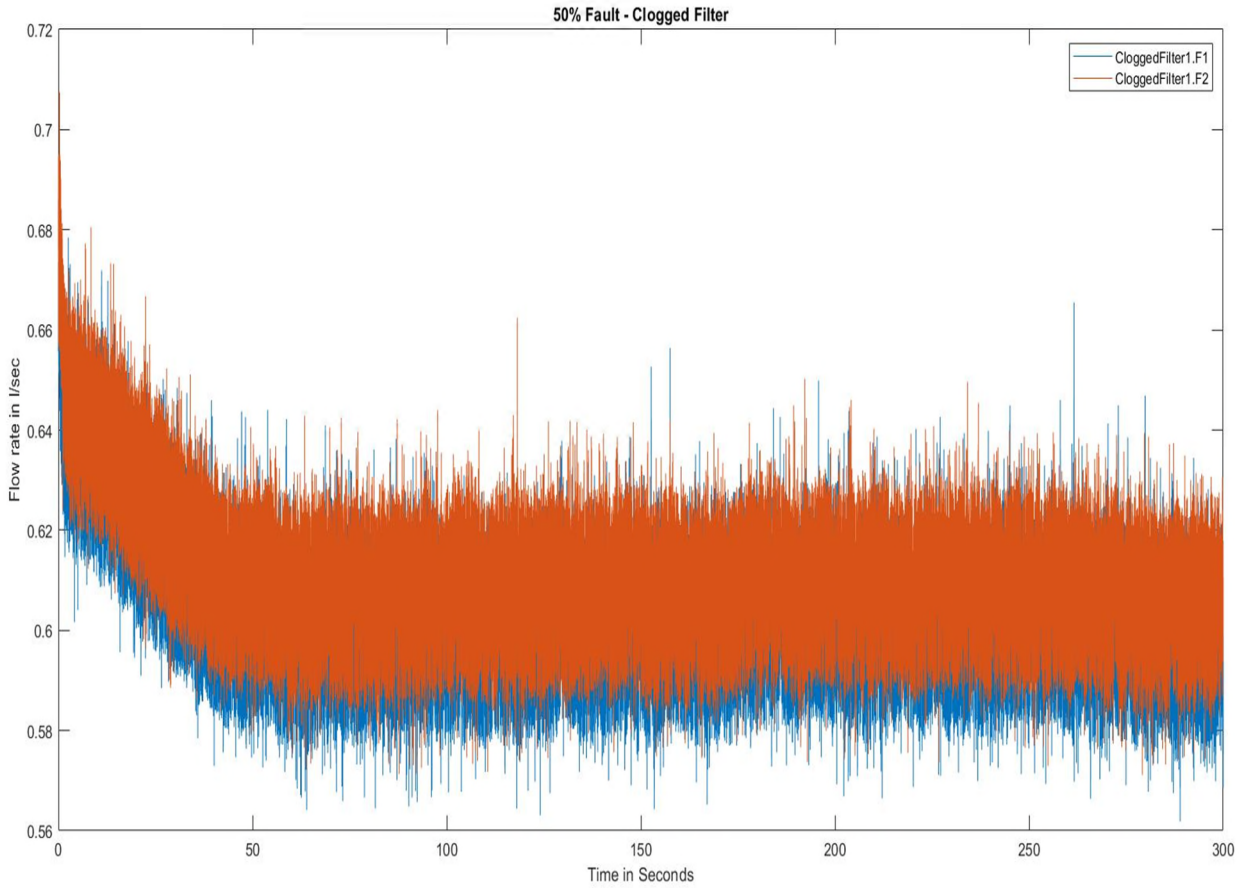

Figure 29 Clogged Filter (Flowrate) – 50% Severity

3.2.1.5 Blocked Flowmeter

For the sticking valve scenario, the DPV 4 valve is open at 75% and 50% to imitate the blocked flowmeter at 25% and 50% and the valve not opening to its maximum has pressure and flow rate difference across the fuel system.

3.2.1.5.1 Pressure

In the case of a leaking pipe fault, the valve DPV4 is positioned between the two-gear pump which is operating at a variable speed to maintain the flow rate. The pressure sensor that is placed before the DPV4 valve is P5 and the one after is P6, the pressure drops at P6 due to the leaking pipe simulation. The pressure sensor reading of P1 & P2 is constant for 25% severity and they follow a slightly different pattern for the first 10sec of the experiment.

As shown in Figure 30 & Figure 31 initial pressure differed all the following pressure reading follows the same pattern except for the pressure reading of P3 and P7 which are placed after the gear pump (1&2), all the other pressure sensor reading follow the same pattern. The pressure rate drops at the P5 sensor which is placed before gear pump 2.

The pressure P6 reading follows the same pattern for Figure 30 Blocked Flowmeter (Pressure Sensor) – 25% Severity & Figure 31 Blocked Flowmeter (Pressure Sensor) – 50% Severity. There is a massive drop in the pressure drop at P6 is noted.

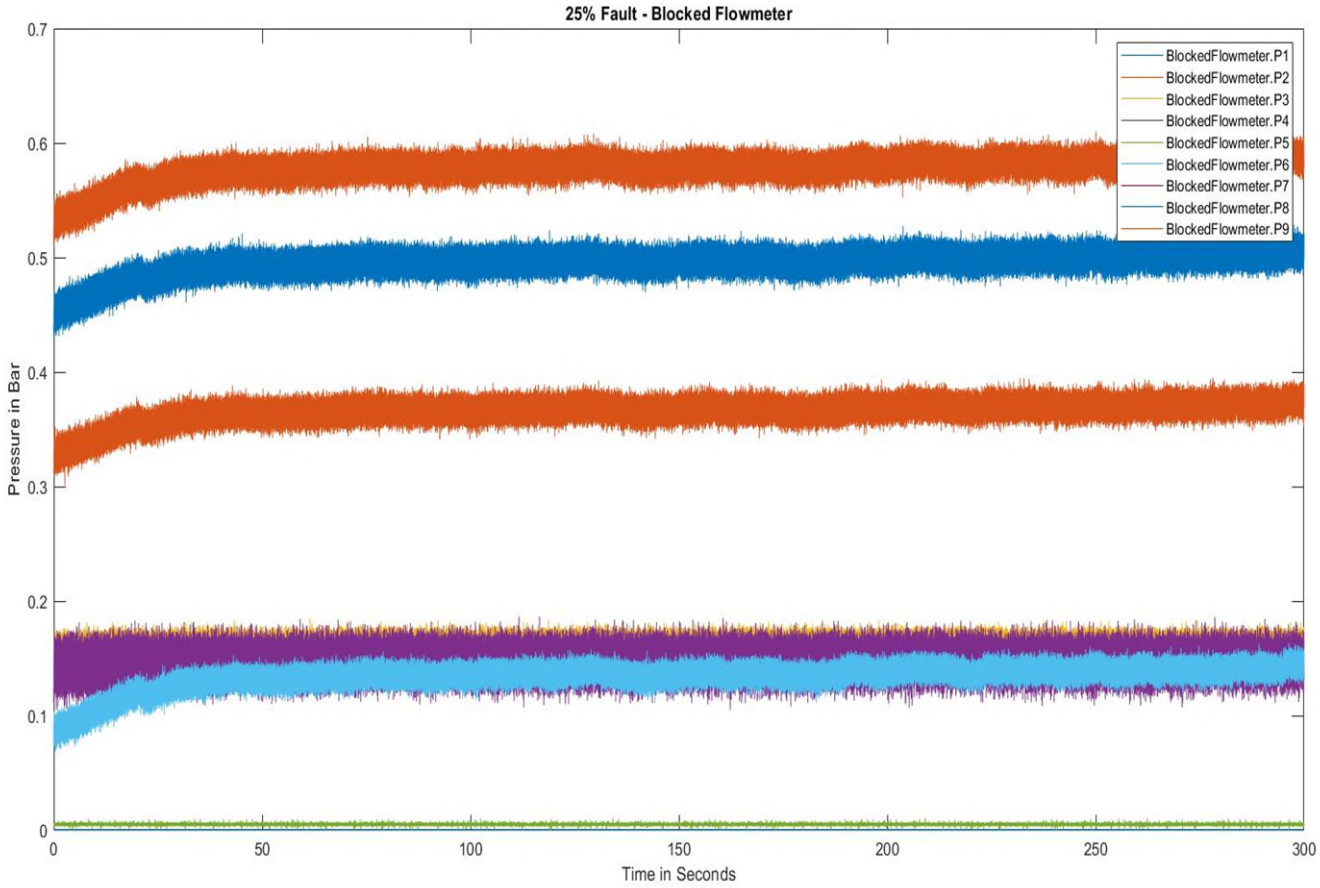

Figure 30 Blocked Flowmeter (Pressure Sensor) – 25% Severity

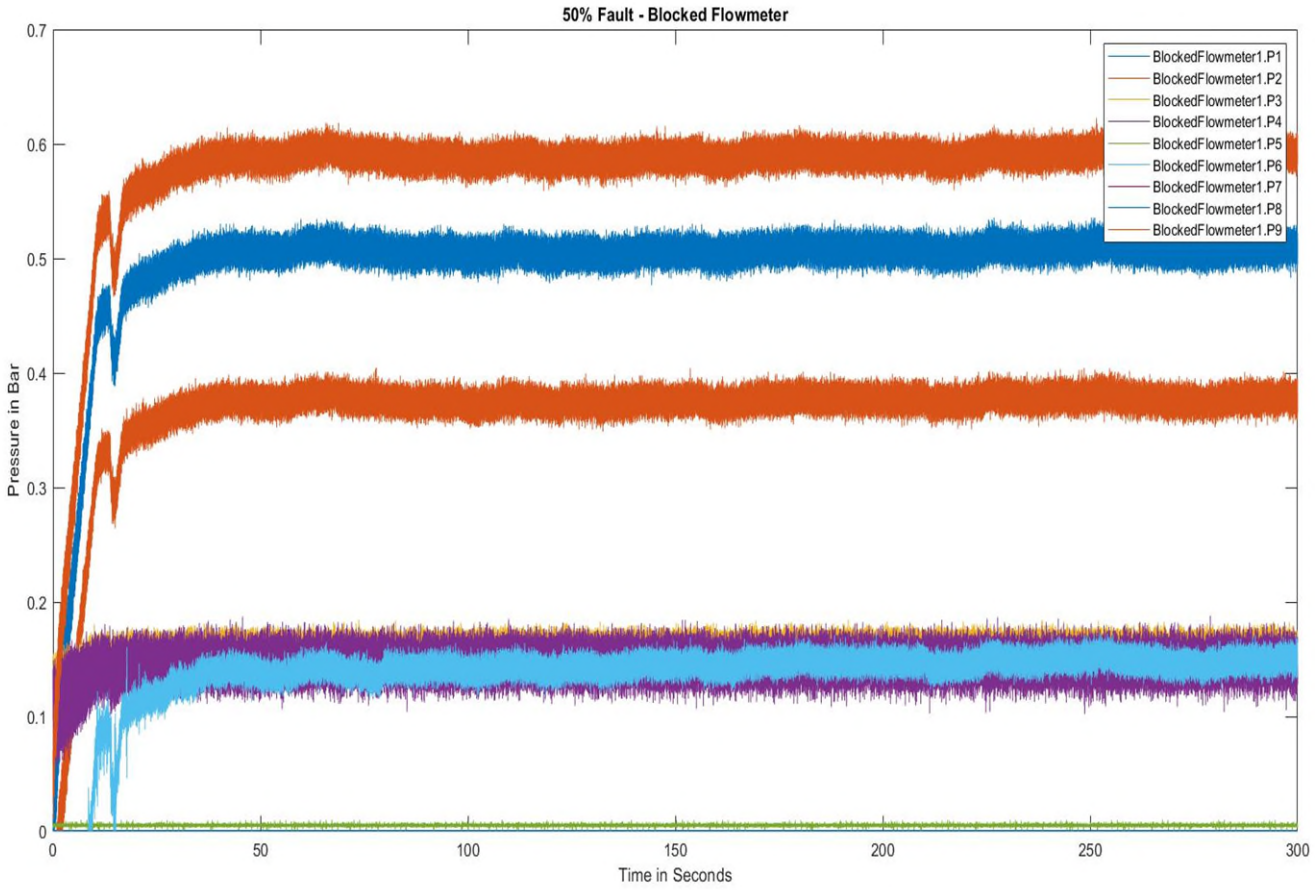

Figure 31 Blocked Flowmeter (Pressure Sensor) – 50% Severity

3.2.1.5.2 Flowrate

The flow rate for the healthy scenario was approximately 0.65l/sec at F2 and 0.6 l/sec at F1. For the 25%, severity scenario blocked flow meter fault the flow rate was dropped before the flow reaches the fault DPV. 50% severity the flow at F1 has stayed constant, but as observed for the pressure sensor Figure 31 the first 10 sec reading for the sensor has dropped.

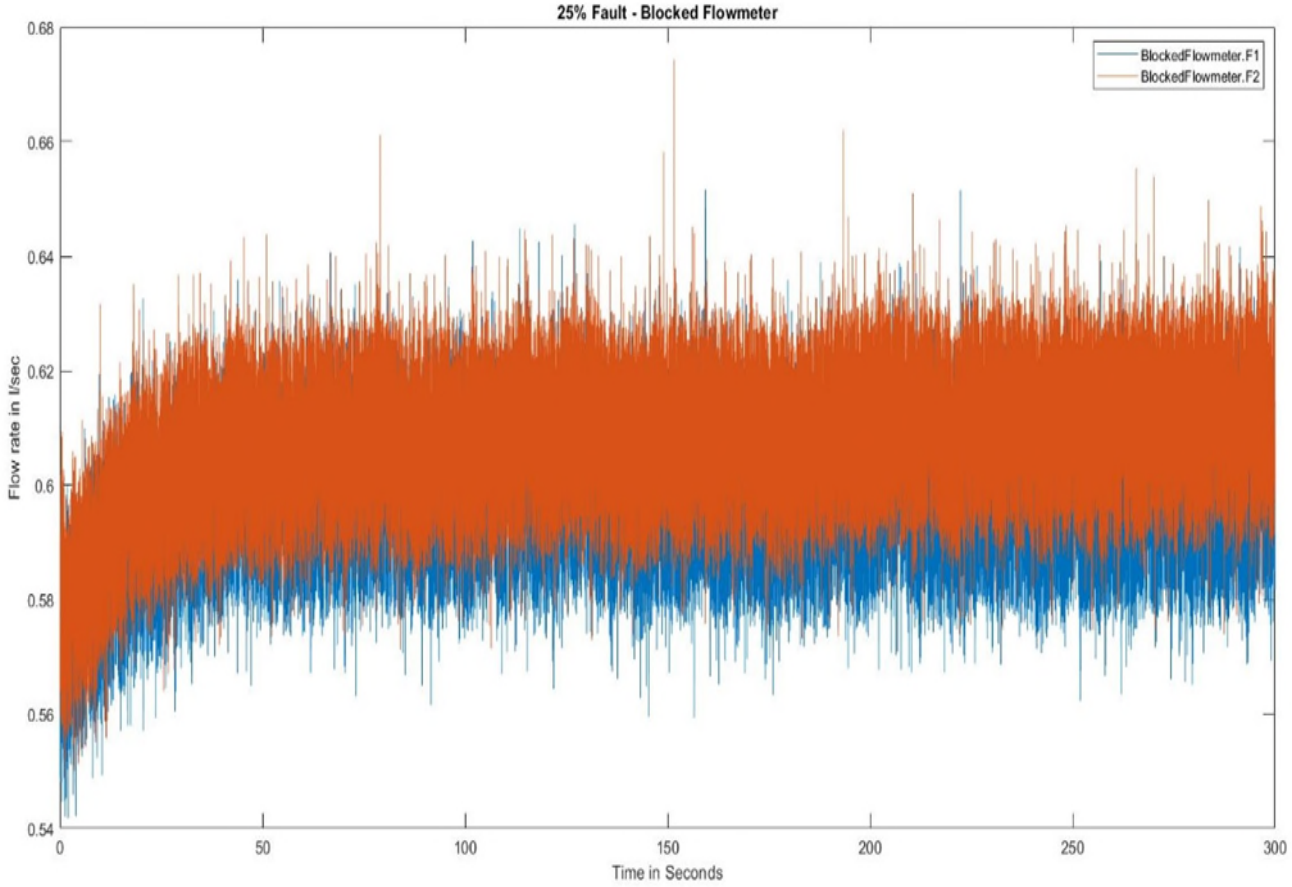

Figure 32 Blocked Flowmeter (Flowrate) – 25% Severity

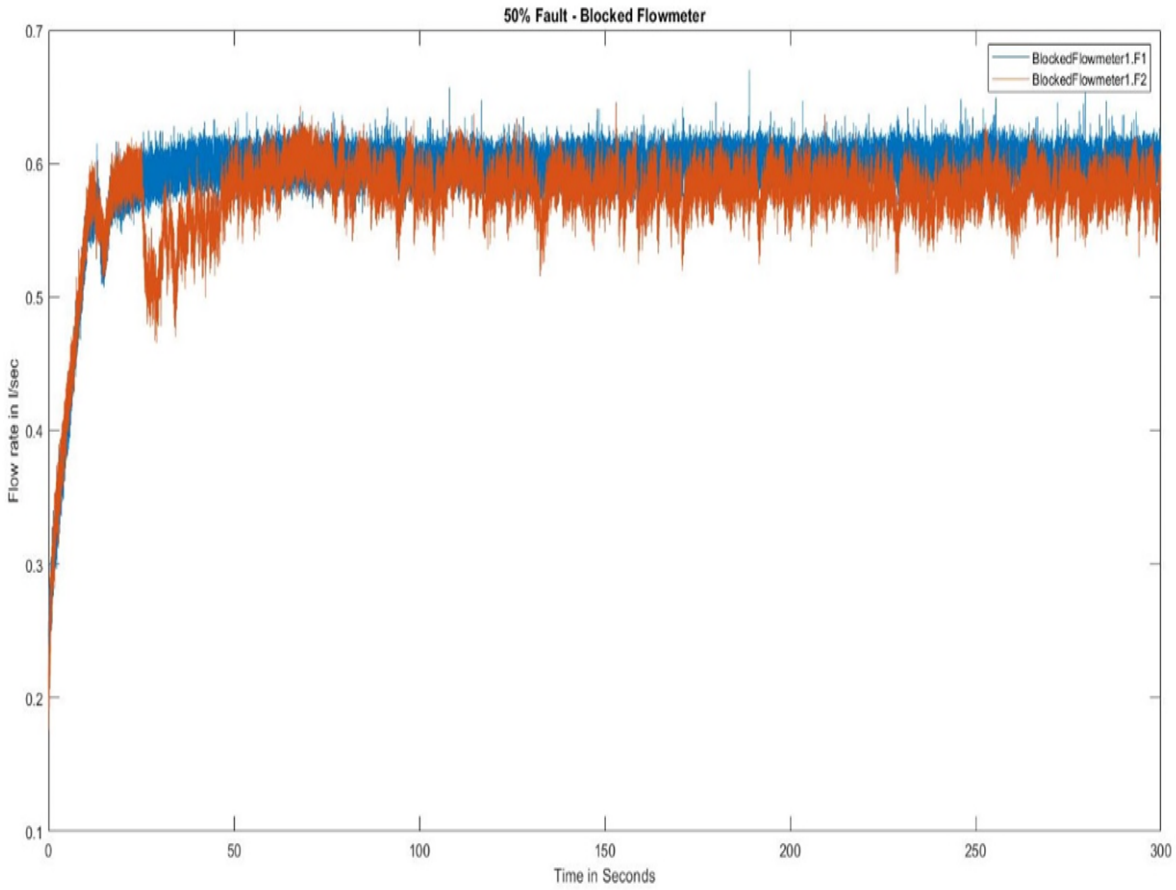

Figure 33 Blocked Flowmeter (Flowrate) –50% Severity

3.2.1.6 Clogged Nozzle

For the sticking valve scenario, the DPV 5 valve is open at 75% and 50% to imitate the clogged nozzle at 25% and 50% and the valve not opening to its maximum has pressure and flow rate difference across the fuel system.

3.2.1.6.1 Pressure

In the case of a Clogged nozzle fault, the valve DPV 5 is positioned between the two-gear pump which is operating at variable speed. The pressure sensor that is placed before DPV 5 valve is P6 and the one after is P7, the pressure increases at P6 due to the clogged nozzle simulation. The pressure sensor reading of P1 & P2 will not change.

As shown in Figure 34 & Figure 23 initial pressure differed all the following pressure reading follows the same pattern except for the pressure reading of P3 and P7 which are placed after the gear pump (1&2), all the other pressure sensor reading follow the same pattern. The pressure rate drops at the P5 sensor which is placed before gear pump 2.

The Pressure sensor observed is placed after the pump2 due to this reason the pressure increases to compensate for the flow reduction. Even though the pressure reading follows the same pattern in Figure 34. Figure 21 Sticking Valve (Flow Rate) –50% Severity Figure 35 shows a massive increase in pressure P6.

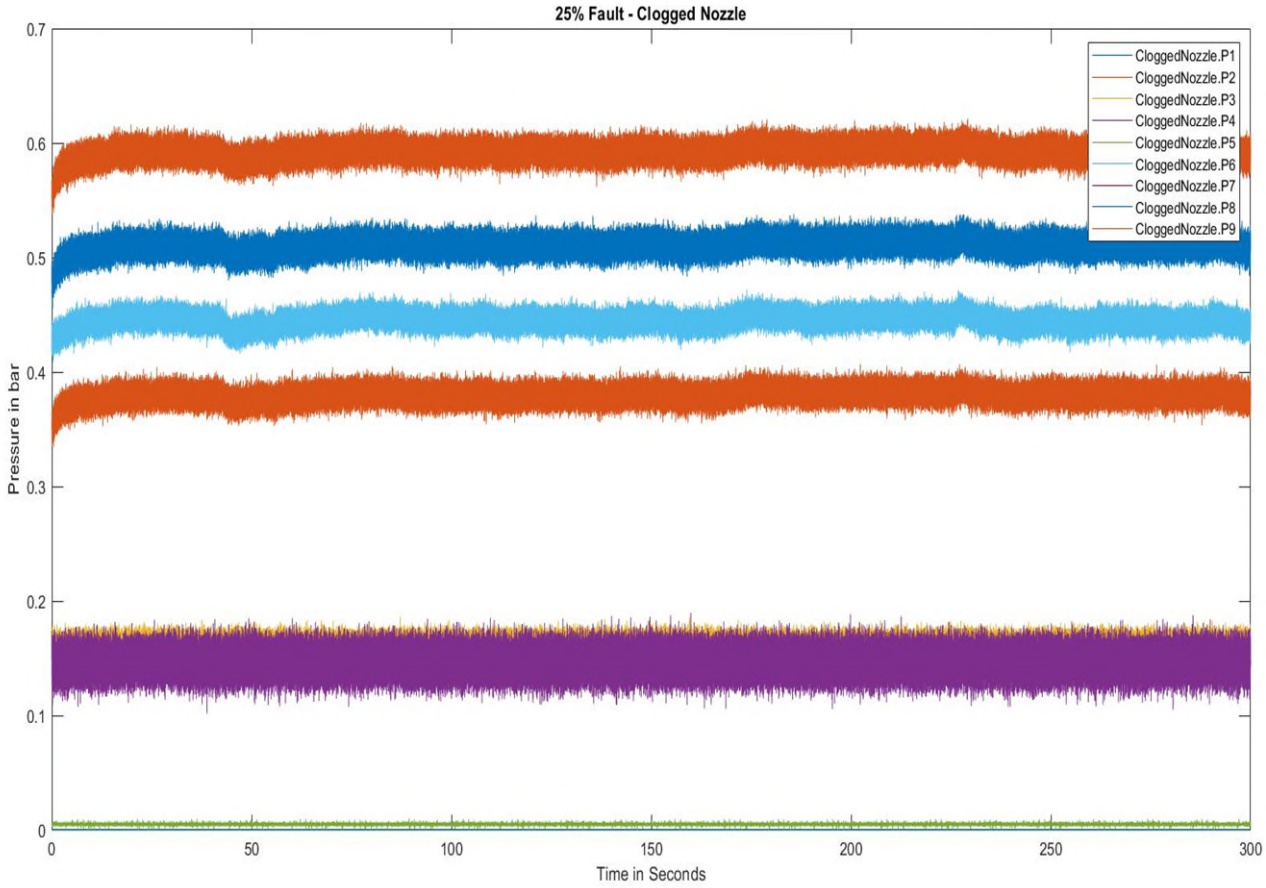

Figure 34 Clogged Nozzle (Pressure Sensor) – 25% Severity

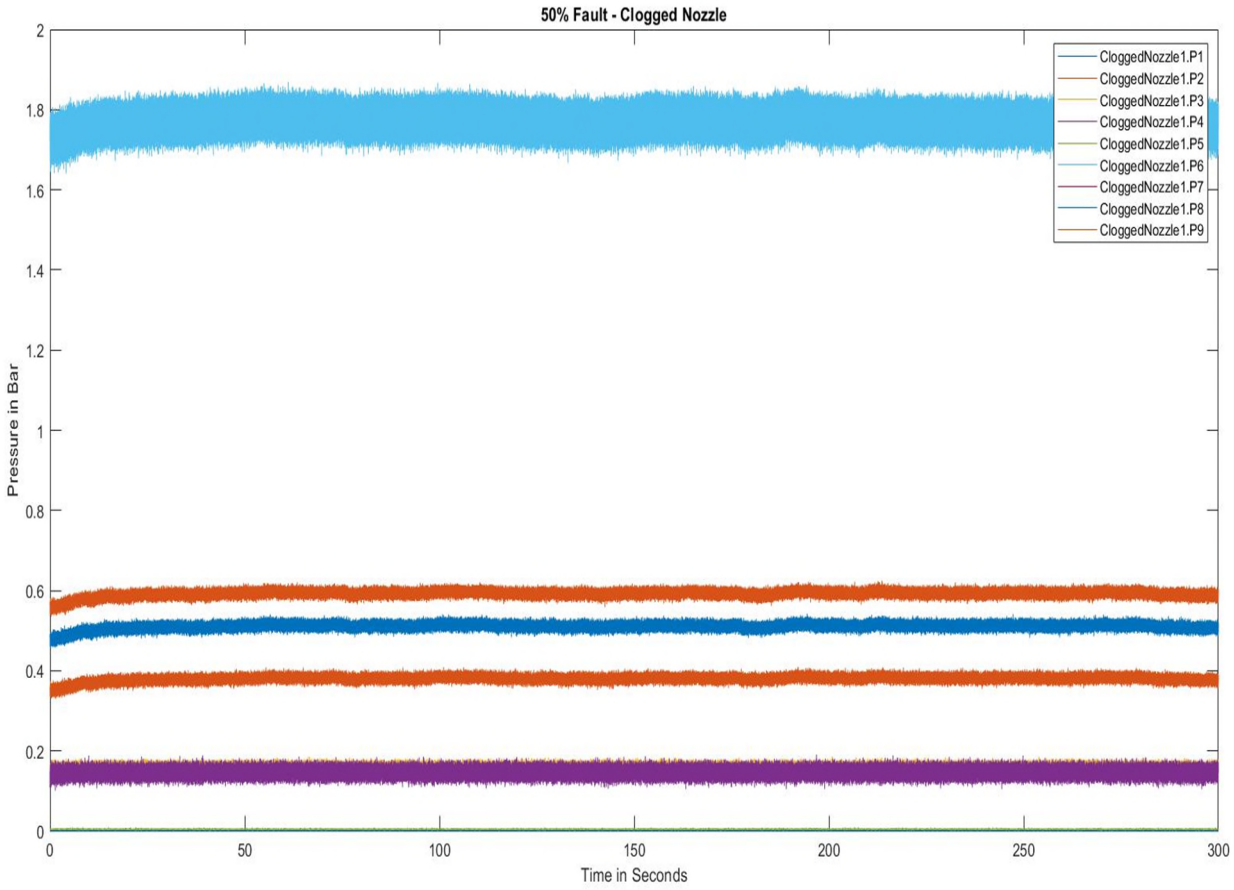

Figure 35 Clogged Nozzle (Pressure Sensor) – 50% Severity

3.2.1.6.2 Flowrate

The flow rate F1 is almost stable as the healthy case and the flow rate measured at flow meter F2 has a drop-in flow rate comparatively. The Flow rate represented in Figure 36 Clogged Nozzle (Flowrate) – 25% Severity is less impacted compared to Figure 37 Clogged Nozzle (Flowrate) – 50% Severity

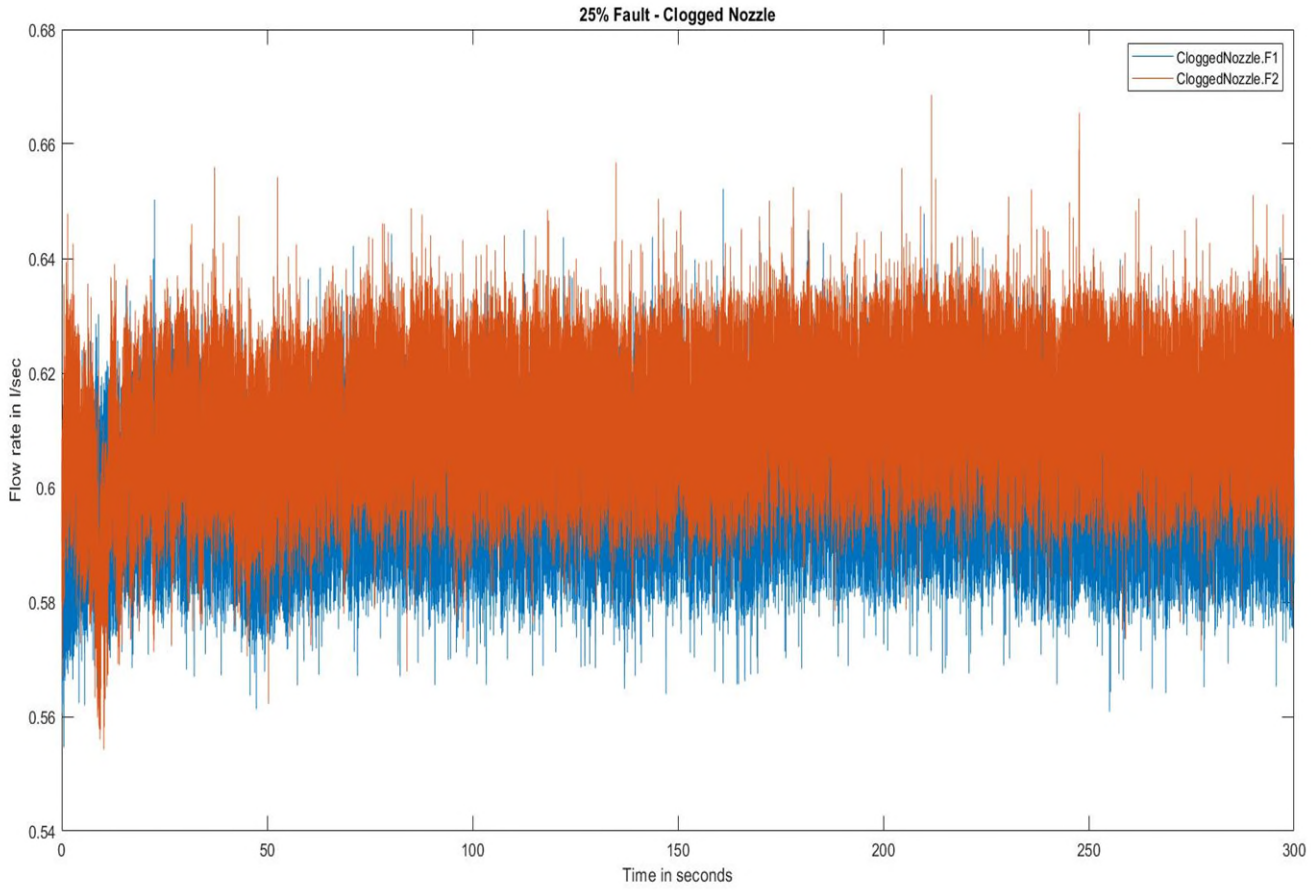

Figure 36 Clogged Nozzle (Flowrate) – 25% Severity

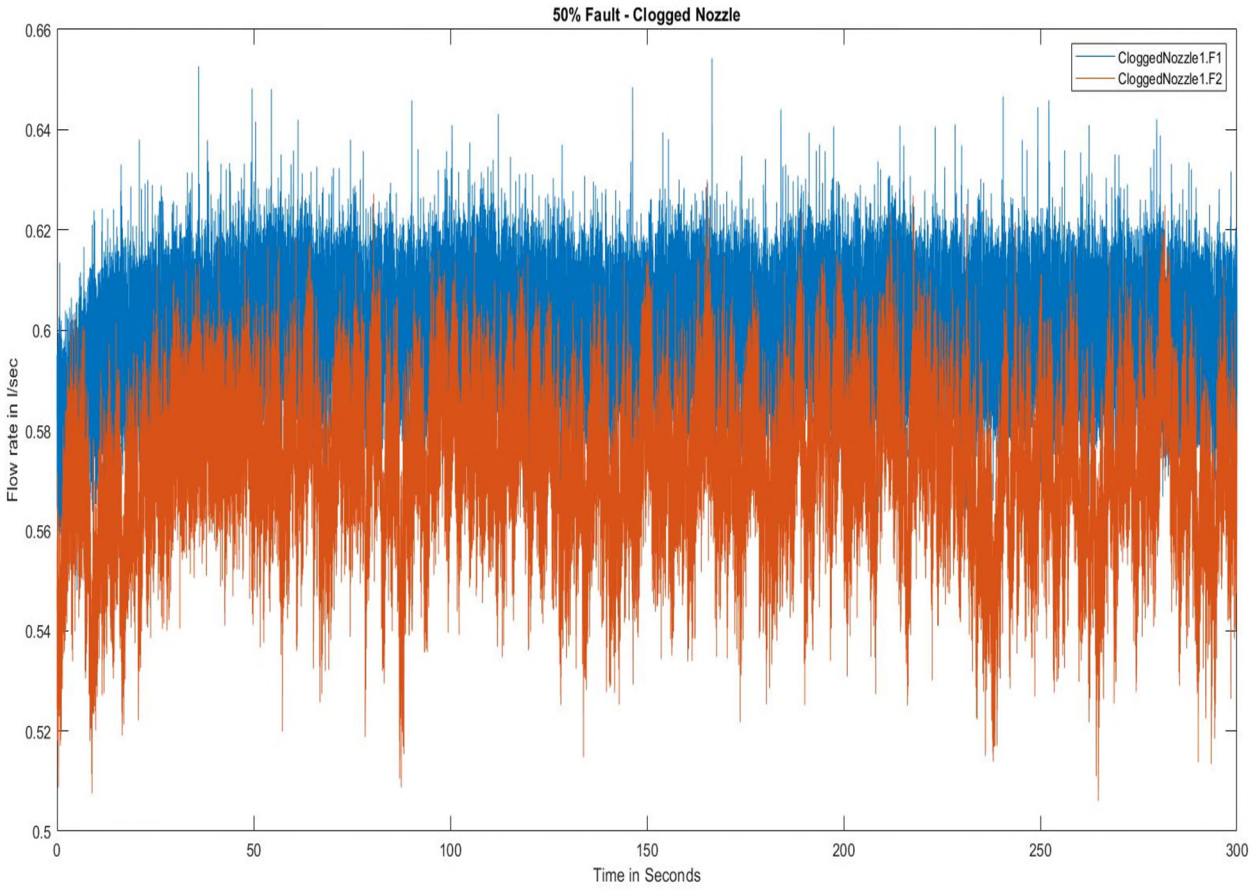

Figure 37 Clogged Nozzle (Flowrate) – 50% Severity

3.2.2 Data Interpretation

3.2.2.1 Pressure sensor P1

Even though theoretically as there are no faults emulated near the pressure P1 should be constant and close to atmospheric pressure. The minimum pressure for a healthy case was noted as 0.44 bar and a max of 0.68 bar. In the fault simulation minimum of 0 is observed for 25% leaking pipe and 50% blocked flowmeter. And the maximum 0.93 bar is noted for the 25% sticking valve which is close to the P1.

Fault type	Min	Max	Mean	Median	Mode	Std	Range
Healthy	0.4429	0.681	0.5215	0.5255	0.5324	0.02597	0.1652
25% Sticking Valve	0.5327	0.9301	0.5816	0.5748	0.5771	0.3010	0.3974
50% Sticking Valve	0.6697	0.8536	0.7346	0.7370	0.7373	0.0263	0.1839
25% Leaking pipe	0	0.5564	0.4748	0.4713	0.4693	0.0239	0.5564
50% Leaking pipe	0.454	0.5514	0.4835	0.4825	0.4825	0.0099	0.0974
25% Clogged Filter	0.3847	0.6137	0.5404	0.5394	0.5403	0.00979	0.2289
50% Clogged Filter	0.736	0.885	0.7685	0.7639	0.761	0.01762	0.149
25% Blocked Flowmeter	0.4294	0.528	0.4954	0.4969	0.4982	0.01106	0.0990
50% Blocked Flowmeter	0	0.5365	0.4949	0.5059	0.5087	0.05621	0.5365
25% Clogged Nozzle	0.455	0.5378	0.5105	0.5107	0.5114	0.00751	0.8228
50% Clogged Nozzle	0.4554	0.5424	0.5107	0.5112	0.5114	0.00882	0.0870

Table 5 Pressure sensor P1

3.2.2.2 Pressure sensor P2

The Pressure sensor placed after the DPV1 Sticking valve decreases pressure compared to P1. However, the healthy minimum P1 is noted as 0.3bar and the maximum is 0.47bar. It is expected that P2 follow the same pattern as P1 as they are next to each other, but they differ.

Fault type	Min	Max	Mean	Median	Mode	Std	Range
Healthy	0.3191	0.472	0.3902	0.3934	0.3787	0.0235	0.1529
25% Sticking Valve	0.328	0.6317	0.3729	0.3672	0.3695	0.0250	0.3037
50% Sticking Valve	0.1762	0.325	0.2246	0.2246	0.251	0.0188	0.1488
25% Leaking pipe	0	0.4197	0.3442	0.3417	0.3406	0.0206	0.4197
50% Leaking pipe	0.3242	0.4115	0.353	0.3519	0.3511	0.0090	0.08728
25% Clogged Filter	0.2755	0.484	0.4171	0.4162	0.4167	0.0090	0.2085
50% Clogged Filter	0.6435	0.7883	0.6719	0.6677	0.6661	0.01661	0.1449
50% Clogged Filter	0.3011	0.3949	0.3659	0.3672	0.3669	0.00997	0.09385
25% Blocked Flowmeter	0.5102	0.6101	0.5777	0.5793	0.5816	0.01137	0.09993
50% Blocked Flowmeter	0.3011	0.3949	0.3659	0.3672	0.3669	0.00997	0.09385
25% Clogged Nozzle	0.3345	0.4067	0.3797	0.3798	0.3787	0.00694	0.07219
50% Clogged Nozzle	0.3298	0.4093	0.3803	0.3906	0.3787	0.0082	0.07957

Table 6 Pressure sensor P2

3.2.2.3 Pressure Sensor P3

The Pressure sensor P3 is placed after the DPV2 (Leaking pipe) and the gear pump1 (that represents the low-pressure pump) gradually lowers the pressure reading compared to P1 & P2.

Fault type	Min	Max	Mean	Median	Mode	Std	Range
Healthy	0.1338	0.1937	0.1651	0.165	0.1656	0.00753	0.05993
25% Sticking Valve	0.1218	0.212	0.1527	0.1523	0.1498	0.0081	0.09017
50% Sticking Valve	0.09695	0.1566	0.1303	0.1302	0.1288	0.00681	0.5967
25% Leaking pipe	0.05818	0.1803	0.152	0.1523	0.154	0.00800	0.1221
50% Leaking pipe	0.1239	0.1813	0.1529	0.1532	0.154	0.00736	0.05744
25% Clogged Filter	0.2145	0.2832	0.2476	0.2477	0.2486	0.00755	0.06874
50% Clogged Filter	0.6032	0.7136	0.6377	0.6372	0.6335	0.0114	0.1104
25% Blocked Flowmeter	0.127	0.1845	0.1587	0.1589	0.1624	0.0075	0.05744
50% Blocked Flowmeter	0.06725	0.1847	0.1578	0.1587	0.1603	0.00975	0.1175
25% Clogged Nozzle	0.1305	0.1859	0.1591	0.1594	0.1624	0.00728	0.05547
50% Clogged Nozzle	0.127	0.1863	0.1585	0.1587	0.1603	0.00773	0.05928

Table 7 Pressure sensor P3

The Pressure drop increases in time corresponding to increasing fault level. Except for the clogged filter faults, the mean, median and mode of the P3 data remained almost the same.

3.2.2.4 Pressure Sensor P4

The Pressure sensor P4 is placed after the pressure relief valve. The pressure during this experiment didn't go over 1 bar the pressure relief valve didn't get activated. The P4 Sensor doesn't indicate any faults, it helps to maintain the pressure of the rig, to avoid any accidents during the data collection.

Fault type	Min	Max	Mean	Median	Mode	Std	Range
Healthy	0.1037	0.1964	0.1512	0.151	0.1503	0.00959	0.9264
25% Sticking Valve	0.09796	0.2114	0.1382	0.1379	0.1334	0.01006	0.1134
50% Sticking Valve	0.05946	0.1563	0.1182	0.1182	0.1166	0.00911	0.09685
25% Leaking pipe	0.03252	0.1835	0.1389	0.139	0.1355	0.01113	0.151
50% Leaking pipe	0.09586	0.1823	0.1397	0.1396	0.1376	0.01069	0.08647
25% Clogged Filter	0.1884	0.2881	0.2356	0.2355	0.2323	0.01103	0.09974
50% Clogged Filter	0.5797	0.7191	0.6291	0.6286	0.6212	0.01466	0.1394
25% Blocked Flowmeter	0.1051	0.1865	0.1463	0.1462	0.1461	0.01099	0.08147
50% Blocked Flowmeter	0.05275	0.1881	0.1456	0.1459	0.144	0.01246	0.1354

25% Clogged Nozzle	0.1016	0.1897	0.1466	0.1464	0.1482	0.01083	0.08804
50% Clogged Nozzle	0.101	0.191	0.1465	0.1463	0.144	0.1125	0.09002

Table 8 Pressure sensor P4

3.2.2.5 Pressure Sensor P5

The Pressure sensor P5 that is placed after the DPV3 gradually lowers the pressure as this DPV represents a Clogged Filter. The Pressure drop increases in time corresponding to increasing fault level. Except for the clogged filter faults, the mean, median and mode of the P5 data remained almost the same. The pressure reading is at the minimum for the leaking pipe for severity compared to other readings of P5.

Fault type	Min	Max	Mean	Median	Mode	Std	Range
Healthy	0	0.01199	0.004913	0.004903	0.004772	0.00056	0.01199
25% Sticking Valve	0	0.01107	0.004895	0.004903	0.004772	0.000535	0.01107
50% Sticking Valve	0	0.01068	0.0049	0.004903	0.004772	0.000507	0.01068
25% Leaking pipe	0	0.00976	0.00491	0.004903	0.004772	0.00046	0.00976
50% Leaking pipe	0	0.01172	0.004911	0.004903	0.004772	0.000459	0.01172
25% Clogged Filter	0	0.01041	0.04912	0.004903	0.004772	0.000457	0.01041

50% Clogged Filter	0	0.01068	0.004921	0.004903	0.004903	0.000448	0.01068
25% Blocked Flowmeter	0	0.01068	0.004914	0.004903	0.004772	0.000448	0.01068
50% Blocked Flowmeter	0	0.00989	0.004914	0.004903	0.004772	0.000450	0.00989
25% Clogged Nozzle	0	0.01002	0.004911	0.004903	0.004772	0.000451	0.01002
50% Clogged Nozzle	0	0.00976	0.004897	0.004903	0.004772	0.000446	0.00976

Table 9 Pressure sensor P5

3.2.2.6 Pressure Sensor P6

The Pressure sensor P6 is placed after the DPV4 (Blocked Flowmeter) and gear pump 2(that represents the high-pressure pump) gradually increases the pressure reading compared to P5.

Fault type	Min	Max	Mean	Median	Mode	Std	Range
Healthy	0.1533	0.3361	0.2367	0.240	0.25	0.03018	0.1828
25% Sticking Valve	0.1644	0.4775	0.2201	0.2111	0.2122	0.03283	0.3132
50% Sticking Valve	0.1969	0.3672	0.2542	0.2563	0.2563	0.02532	0.1703
25% Leaking pipe	0	0.2086	0.1197	0.1157	0.1134	0.01818	0.2086
50% Leaking pipe	0.1048	0.2048	0.1305	0.1289	0.1302	0.01009	0.1001

25% Clogged Filter	0.04528	0.2383	0.1481	0.1461	0.1449	0.01106	0.193
50% Clogged Filter	0.2052	0.3545	0.2305	0.2257	0.2248	0.01731	0.1493
25% Blocked Flowmeter	0.06799	0.1632	0.1339	0.1359	0.1365	0.01111	0.0952
50% Blocked Flowmeter	0	0.1737	0.1369	0.1438	0	0.02905	0.1737
25% Clogged Nozzle	0.4087	0.4723	0.445	0.4451	0.4454	0.06608	0.06355
50% Clogged Nozzle	1.641	1.869	1.77	1.77	1.74	0.03451	0.2274

Table 10 Pressure sensor P6

3.2.2.7 Pressure Sensor P7

The Pressure sensor P7 is placed after the DPV5 and gear pump 2(that represents the high-pressure pump) gradually increases the pressure reading compared to P5. Except for the clogged filter faults, the mean, median and mode of the P3 data remained almost the same.

Fault type	Min	Max	Mean	Median	Mode	Std	Range
Healthy	0	0.121	0.03614	0.03758	0	0.02265	0.121
25% Sticking Valve	0.000306	0.3069	0.04552	0.03836	0.03841	0.03038	0.3066
50% Sticking Valve	0.05122	0.214	0.1079	0.1095	0.1066	0.02366	0.1627

25% Leaking pipe	0	0.02577	0.00012	0	0	0.00101	0.0577
50% Leaking pipe	0	0.01842	0	0	0	0.00356	0.0184
25% Clogged Filter	0	0.05674	0.00054	0	0	0.00372	0.0567
50% Clogged Filter	0.06907	0.2071	0.09607	0.09191	0.08991	0.01568	0.1381
25% Blocked Flowmeter	0	0	0	0	0	0	0
50% Blocked Flowmeter	0	0	0	0	0	0	0
25% Clogged Nozzle	0	0	0	0	0	0	0
50% Clogged Nozzle	0	0	0	0	0	0	0

Table 11 Pressure sensor P7

3.2.2.8 Pressure Sensor P8

The Pressure sensor P6 is placed after the DPV5 and gear pump 2(that represents the high-pressure pump) gradually increases the pressure reading compared to P5. Except for the clogged filter faults, the mean, median and mode of the P3 data remained almost the same.

Fault type	Min	Max	Mean	Median	Mode	Std	Range
Healthy	0	0.0685	0.0025	0	0	0.0073	0.0685
25% Sticking Valve	0	0.2607	0.008	0	0	0.0239	0.2607

50% Sticking Valve	0.0087	0.1623	0.065	0.0667	0.0664	0.0233	0.1536
25% Leaking pipe	0	0	0	0	0	0	0
50% Leaking pipe	0	0	0	0	0	0	0
25% Clogged Filter	0	0.0092	0	0	0	0	0.0092
50% Clogged Filter	0.0334	0.1673	0.058	0.0538	0.0538	0.0155	0.1339
25% Blocked Flowmeter	0	0	0	0	0	0	0
50% Blocked Flowmeter	0	0	0	0	0	0	0
25% Clogged Nozzle	0	0	0	0	0	0	0
50% Clogged Nozzle	0	0	0	0	0	0	0

Table 12 Pressure sensor P8

3.2.2.9 Flowrate F1

The flow rate F1 is measured after gear pump 2 which represents a high-pressure pump. The flow rate for this experiment is kept constant still, even though the minimum and maximum flow rate differs the mean, median and mode of the flow remained constant.

Fault type	Min	Max	Mean	Median	Mode	Std	Range
Healthy	0.4976	0.6920	0.6017	0.6025	0.609	0.0165	0.1945
25% Sticking Valve	0.5246	0.7425	0.6032	0.6032	0.6019	0.0172	0.2179
50% Sticking Valve	0.5060	0.7287	0.6037	0.6035	0.6008	0.0175	0.2228

25% Leaking pipe	0.2270	0.6828	0.6023	0.6006	0.5998	0.0170	0.4558
50% Leaking pipe	0.5616	0.6638	0.6022	0.6012	0.6008	0.007651	0.1022
25% Clogged Filter	0.5142	0.6757	0.6016	0.6004	0.5998	0.008208	0.1614
50% Clogged Filter	0.5618	0.6899	0.6036	0.601	0.6008	0.01057	0.128
25% Blocked Flowmeter	0.5418	0.6517	0.5978	0.5986	0.5987	0.00747	0.1098
50% Blocked Flowmeter	0.315	0.6704	0.5911	0.5986	0.5987	0.03886	0.4554
25% Clogged Nozzle	0.5546	0.6522	0.6004	0.6004	0.6008	0.006032	0.09756
50% Clogged Nozzle	0.567	0.6542	0.5987	0.599	0.5998	0.006618	0.1075

Table 13 Flow meter F1

3.2.2.10 Flow meter F2

The flow rate F2 is measured before the engine throttle after all the faults. Similar to F1 the flow rate of F2 for this experiment is kept constant. The minimum and maximum flow rates differ however the mean, median and mode of the flow remained constant.

Fault type	Min	Max	Mean	Median	Mode	Std	Range
Healthy	0.4311	0.7384	0.606	0.6107	0.6293	0.03683	0.3073
25% Sticking Valve	0.5073	0.7933	0.6311	0.6283	0.6293	0.03162	0.286

50% Sticking Valve	0.5777	0.7531	0.6498	0.6497	0.6519	0.6519	0.1754
25% Leaking pipe	0.2705	0.6553	0.5775	0.5776	0.5789	0.01815	0.3848
50% Leaking pipe	0.5685	0.6766	0.6069	0.6059	0.6057	0.007408	0.1081
25% Clogged Filter	0.4507	0.6998	0.6085	0.6075	0.6067	0.008572	0.2491
50% Clogged Filter	0.5712	0.7074	0.6106	0.608	0.6067	0.01071	0.1363
25% Blocked Flowmeter	0.5488	0.6744	0.6071	0.6082	0.6088	0.008175	0.1255
50% Blocked Flowmeter	0.1759	0.646	0.5748	0.583	0.5868	0.03872	0.4701
25% Clogged Nozzle	0.5542	0.6686	0.6111	0.6117	0.613	0.007029	0.1144
50% Clogged Nozzle	0.506	0.6299	0.5725	0.5738	0.5789	0.01276	0.1239

Table 14 Flow meter F2

3.3 Faults Detection and Diagnosis (FDD)

In the last decade Fault detection and diagnostics (FDD) has been used in the aerospace, process controls, automotive, manufacturing, and nuclear industries. A fuel control unit (FCU) that fails to manage the fuel supply to the engines can be observed by the flight crew, but a short duration speed increase or decrease or other components working harder to compensate the fault of another to supply fuel system cannot be observed from the cockpit. Fault in a complex fuel system is not usually apparent and the source of the problem may be hidden by the symptoms that develop as the other subsystems respond to compensate for the fault in one component.

The main objective of FDD is to detect the existence of a fault in a component (Fault Detection) and locate the fault that occurred (Fault Isolation), the size or divergence of the degradation and the time-varying performance of the fault (Fault identification).

3.3.1 Fault/Anomaly Detection

Detection is a binary system that detects anomalies indicating either a healthy or a faulty system in the component [91]. Detection is the process of identifying emerging failures and/or anomalies in the data. Fault detection is typically based on quantifying the irregularities between the current and the expected behaviour of the system in healthy conditions[92].

3.3.2 Fault Isolation

Fault isolation finds the root cause of the malfunction of the system and isolates the faulty component. Faults can be isolated manually by visual inspection of burned components or by using an external tester to diagnose the system. For a more complex system and an urgent mission, faults can also be isolated automatically by diagnosis methods[76].

3.3.3 Fault Identification

Fault identification is the method of locating the component and estimating the severity, size, or nature of that caused fault in the component[93].

3.4 Problem Solving

The classification method is also called a supervised learning method, it consists of assigning instances from a specific set of domains defined by a set of continuous or discrete attributes to a predefined discrete data class, also known as a target class[94]. Classification methods learn from specific datasets, called training sets, and create models that act as potential command class tasks. Before the actual classification phase, these models are validated against specific data commonly contained in the validation set. In fault diagnosis, the data is often labelled as healthy and faulty before employing the training model. The main problem that classification methods suffer from is imbalanced data learning.

Most real condition monitoring data is fault-free, and there is a significant discrepancy between observations that belong to the regular class and those that have faults. Due to this reason, a bias is created during the training phase allowing the resulting model to separate healthy from faulty in real-world scenarios. The time-series data poses additional challenges, as techniques such as normalization can lose the temporal structure of the observation. In addition, the classification algorithm has the disadvantage of not being able to detect undetected faults during the training phase of the model.

3.5 Machine Learning Method

Several classification methods are described in the literature, and three major methods have emerged in the last decade: the decision tree method, neural networks (NN) and Autoencoder (AE).

3.5.1 Decision Tree

Decision trees handle numeric and categorical variables by excluding feature conditions using a split method. Decision tree classification has benefits in terms of flexibility, non-parametric properties, and the ability to manage non-linear relationships between features and Targets. The inputs can be divided into possible classes by the tree structure of decision tree formation[95].

The formation of the tree structure defined in the decision rule model is based on the if / else statement. Decision trees are one of the well-known classification tools because they provide careful accuracy and cheap calculations [47]. The targeting output monitors the training set using a recursive binary split method. Subsequent questions with a "yes" or "no" result will ask you to cut the sample chamber. A node is where tests are run against an element. Then the test results are presented to another node. You can think of this node as a branch. There are three types of nodes in the decision tree: root node, leaf node, and internal node as shown in Figure 38

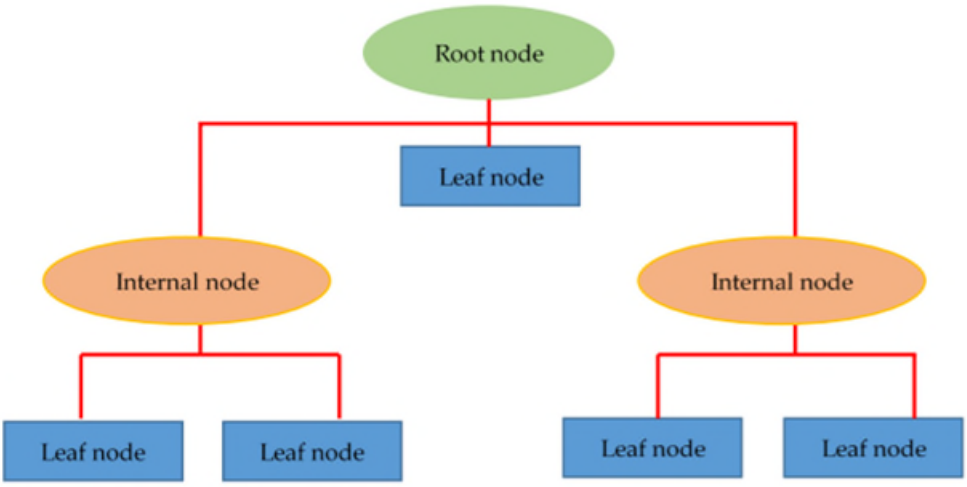

Figure 38 Decision Tree Architecture

The result of the test depends on the purity of each node. The node will stop when it reaches the optimum post level of class purity. The optimal level is defined when the node has only output types within the node. Next, the element values are always tested against the decision tree and new samples are categorized. The class prediction of the tested sample is maintained by the association path from the root node to the leaf node. The basic process of getting a decision tree is to find an attribute that is repeatedly tested on one node and then test it on another node. This entire mapping process, which identifies tests and branches, is called splitting.

3.5.2 Neural Networks

A neural network is one of the most widely used data-driven methods for data from complicated systems. The NN architecture is based on the workings of biological nervous systems, the structure of a neural network is made up of several processing units called neurons, which are often organized into layers. The input observations are weighted and summed using a transfer function. The results of this calculation and the threshold values are used as input to a deterministic activation function that decides whether neurons should be activated. The activation function typically produces values in the range [0, 1] also known as the rate of fire. Figure 39 shows the architecture of the neural network [81].

In this study, we apply a multi-layer feedforward neural network (NN) model for fault diagnosis. As mentioned above NN is an interconnected group of nodes inspired by the simplification of neurons in the human brain. The first input is x, which is passed to the first layer (h) of the neuron. The input is received by the three functions and produces the output. This output is then passed to the second layer (g). Further output is calculated based on the output of the first layer. Then combine these secondary outputs to create the final output of the model.

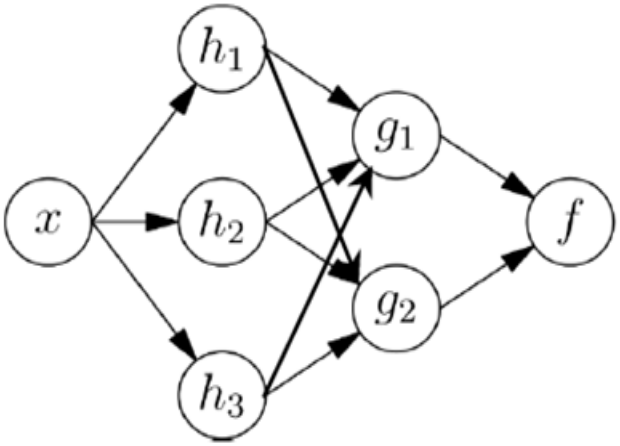

Figure 39 Neural Network Architecture

The main advantage of the neural network is that the model doesn't need historical data to train, it can be trained using the current sensor data. Furthermore, it can deal with the sophisticated correlation between inputs and outputs, also it produces better results even with noisy data. The disadvantage of this model is that it requires more operating time and data compared other two suggested machine learning methods.

The training or learning process of an Artificial Neural Network consists of adjusting the synaptic weights (weight matrix W) so that the application of a set of inputs can produce a set of desired outputs. The supervised training of the ANN used in this work is based on the backpropagation learning algorithm. The functions square error ($E(k)$) and mean square error (E_M) are used as performance criteria to stop the training process.

The squared error provides the instantaneous value of the sum of the squared errors of all neurons in the output layer of the network with the *k*th training pattern, as shown in the below equation

$$E(k) = \frac{1}{2} \sum_{j=1}^{N2} (d_j(k) - y2_j(k))^2$$ Equation 1

where $d_j(k)$ is the value of the desired output neuron *j* relative to the *k*th input pattern.

The mean square error is obtained from the sum of the squared errors for all input patterns used in the training set of the network, according to equation 2

$$E_M = \frac{1}{p} \sum_{k=1}^{p} E(k)$$ Equation 2

where the parameter *p* specifies the number of training patterns or the number of input vectors. The objective of the learning process, using the backpropagation algorithm, consists of adjusting the weights matrix of the network to minimize the function E_M.

3.5.3 Autoencoder

AE is a type of unsupervised three-layer neural network that can take input vectors and form sophisticated concepts in the next layer through nonlinear mapping. AE attempts to approximate an identical target output value, closer to the input value by minimizing the expected reconstruction error. The first layer is the input layer, the middle layer is the hidden layer, and the last layer is the output layer.

The AE network can use the activation function to perform a non-linear transformation from the previous layer to the next layer. The learning process of

the AE network consists of two stages, the encoder stage, and the decoder stage. The encoder transforms the input into a more abstract feature vector, and the decoder reconstructs the input from the feature vector[55]. Figure 40 is the basic architecture of an AE.

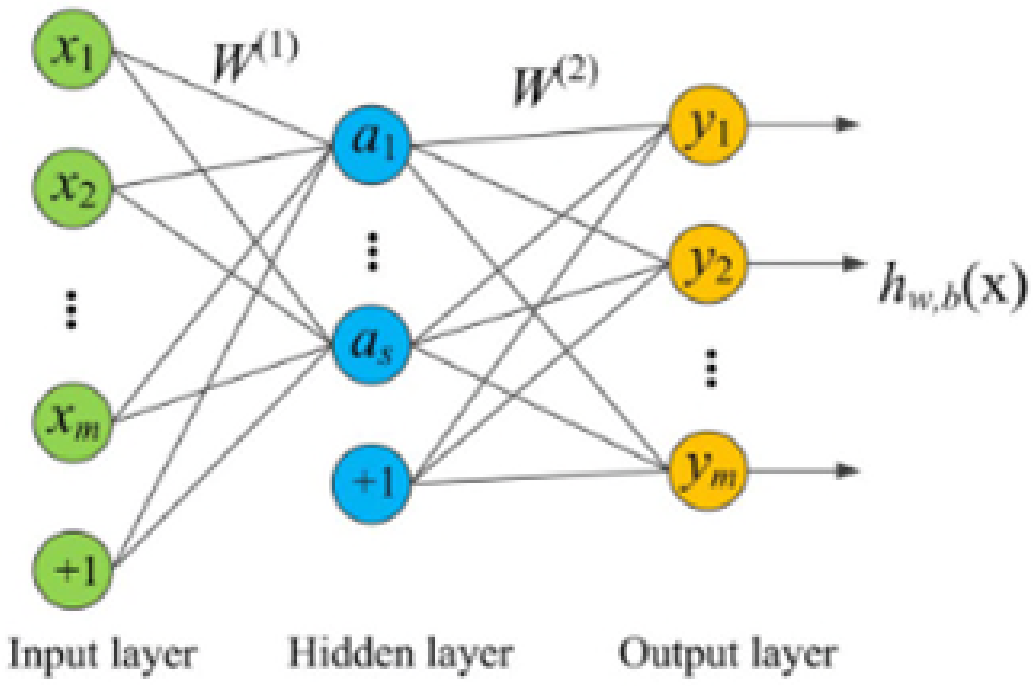

Figure 40 Autoencoder Architecture

An autoencoder is a symmetrical neural network that can learn the features in an unsupervised manner by reducing the reconstruction error. The basic structure of an autoencoder is shown in Figure 40 in which the neural network learns to approximate the hidden layer so that the input data can be reconstructed with fewer errors in the output layer. Initially, the input passes through the encoder, which is a fully connected Artificial Neural Network (ANN), to produce the code. The decoder, which has a similar ANN structure, produces the output only using the code.

3.5.3.1 Forward Propagation

In order to calculate the output of the network the values of the neurons in the hidden layer are calculated first.

Equation 3

$$V_i = g^{(h)}(\sum_j W_{i,j}^{(h)} x_j + b_i^{(h)})$$

where V_i is the value of hidden neuron i, $W(h)_{i,j}$ is the weight between neuron i in the hidden layer and neuron j in the input layer, x_j is the value of input neuron j, $b^{(h)}$ i is a bias for neuron i in the hidden layer and g (h) (. . .) is the activation function for the hidden layer. The superscript (h) specifies that the weights, biases, and activation functions are specific to the hidden layer. Similarly, the output of the network is then calculated using,

Equation 4

$$y_i = g^{(o)}(\sum_j W_{i,j}^{(o)} V_j + b_i^{(o)})$$

where yi is the value of output neuron i and the superscript (o) specifies that the weights, biases and activation function are specific to the output layer. If there is more than one hidden layer, the procedure is the same; the values of the neurons in the layers are calculated layer by layer until reaching the output layer.

3.5.3.2 Backpropagation

Backpropagation is used to train the network by altering the weights of the network to reach optimal results. The optimal result is reached by trying to minimize a function called the loss function. The loss function measures how close the output of the network is to the wanted output of the network (called the target values, t_i). In this thesis, the mean squared error, Equation (3), is used as a loss function.

Equation 5

$$L = \frac{1}{n}\sum_{i=1}^{n}(t_i - y_i)^2$$

3.5.3.3 Activation function

There are many types of activation functions, but for networks that are trained using backpropagation, the activation function must be differentiable.

Here three types of activation functions are presented: linear, sigmoid and ReLU. The simplest activation function is linear, see Equation (4).

Equation 6

$$g(x) = x$$

The sigmoid activation function is usually implemented as the logistic function, as in Equation (5), the goal is to calculate probabilities since it outputs a value between 1 and 0.

Equation 7

$$g(x) = \frac{1}{1 + e^{-x}}$$

3.6 Comparing the results from different algorithms

The confusion matrix comprises data on the predicted and actual classifications. Confusion matrices are usually tabular and are used to evaluate the performance of a classifier on a test dataset where the true value is established. Figure 18 illustrates the basic terms in the confusion matrix formed in the table.

Terms are usually in integer form:

• True positives (TP) are when the model correctly predicts the positive class

• True negatives (TN) are when the outcome from the model corrects and predicts the negative class

• False positives (FP) are when the results from the model are falsely predicted as the positive class

• False Negative (FN) is when the results from the model are unexpectedly predicted as negative class

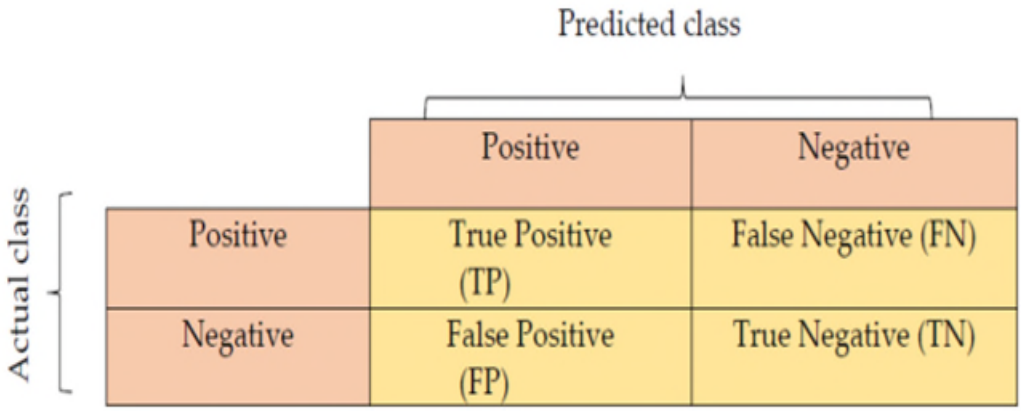

Figure 41 Confusion Matrix Table

Based on the basic concept of the confusion matrix, a list of rates that perform classifier performance is simulated. Table 4 shows a list of rates and their formulas. Five scoring methods were used. That is accuracy, precision, recall, F1 scoring, and misclassification.

Matrix	Equation	
Accuracy	$\frac{TP+TN}{TP+TN+FP+FN}$	**Equation 8**
Precision	$\frac{TP}{TP+FN}$	**Equation 9**
Recall	$\frac{TP}{TP+FP}$	**Equation 10**
F1 score	$2 * \frac{Precision*Recall}{Precision+Recall}$	**Equation 11**

Error Rate 1- Accuracy **Equation 12**

4 Results

4.1 Machine Learning for Diagnosis

Machine learning algorithms can be implemented as a “black-box” approach for classification and all the user needs to do is adjust a few parameters, depending on the machine learning algorithm used. The data was split into a training set, for fitting the diagnostic models, and a testing set for evaluating the performance of the resulting model. 70% of the data remaining is used for training, leaving 20% for testing and 10% for validation. The split into training and test data was done using Python coding. This allowed for splitting the data into partitions based on the class frequency of the target variable, where the class of an observation is either Healthy or Faulty. Thus, the proportion of Heathy to Faulty Datasets in both the training and test data was the same as in the original data.

The classifiers were built using Scikit-learn: a machine-learning library in python. Training and testing time for the classifiers were within a few seconds/ Minutes. The experiment was carried out on a machine with 8GB RAM, an intel i7 processor and 1TB memory.

4.1.1 Decision Tree

The decision tree targets the output by monitoring the training set using a recursive binary split method. Subsequent questions with a "yes" or "no" result will ask you to cut the sample chamber. A node is where tests are run against an element. Then the test results are presented to another node.

4.1.2 Neural Network

The networks are trained in the same way as a neuron; inputs are fed to the first layer, the information propagates through the network, and the output is given. This output is compared to the labelled faulty or healthy conditions, and the error is often called the cost function. Training means that weights and biases are adjusted to minimize the cost function. The most used tool to make these adjustments is Gradient Descent, meaning that all weights are adjusted along the gradient of the cost function. To map the features to the measured capacity,

stated as a SOH, a simple neural network was used. It had two fully connected layers, and all neurons had a Relu activation function. It was trained by gradient descent, without any drop-out applied or another preprocessing unit.

4.1.3 Autoencoder

Autoencoder is trained by using backpropagation with Mean Squared Error (MSE) as a loss function. This meant that the output of the autoencoder was calculated using the training data, and then the MSE between the reconstructed and the training data was used to update the weights. The MSE for the validation data was also calculated, but this error was never used to update weights. Instead, it was used as a criterion for early stopping, meaning that the training would stop if the autoencoder started to overfit the training data and thereby worsen the reconstruction of the validation data. The training was done using batch training, with batch size 256, which combined with the optimizer ADAM is a preferred way of training deep neural networks since it lowers the risk of getting stuck in a local minimum.

4.2 Fault Detection

4.2.1 Data

After pre-processing, the final dataset contains 10 signals and 1 labelled column of target variables, with 404002 homogenous time steps, including 204001 healthy and 200001 faulty samples. The fault detection problem is either a decision problem or a binary classification problem. The data is divided into three parts: 70% for training, 20% for testing data, and 10% for validation. Validation data is used during training to avoid overfitting problems by monitoring the performance of the trained model on the training and validation data until the model's performance trained on the validation dataset starts to decrease while the performance of the model training model on the training dataset continues to increase. As represented in Table 15 & Figure 42 the data healthy data is labelled as 0 and the Faulty data is represented as 1.

Data type	Fault no
Healthy data	0
Faulty data	1

Table 15 Data labelling - Detection

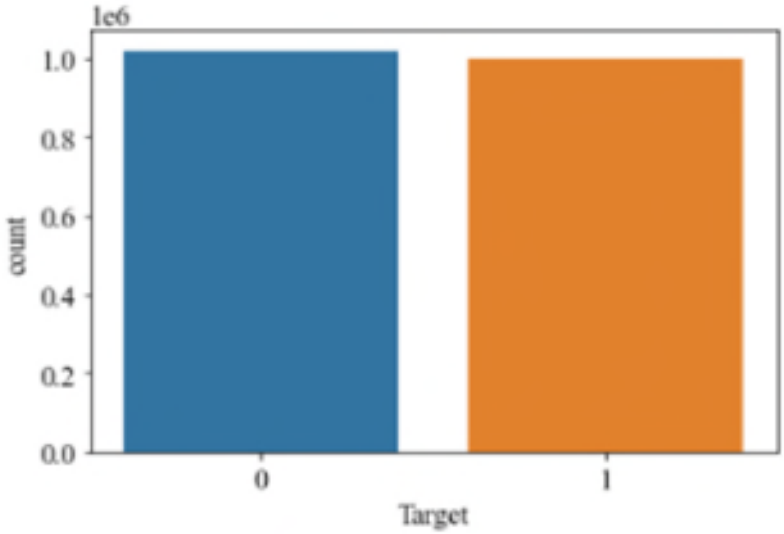

Figure 42 Data for Detection

4.2.2 Decision Tree – Confusion Matrix

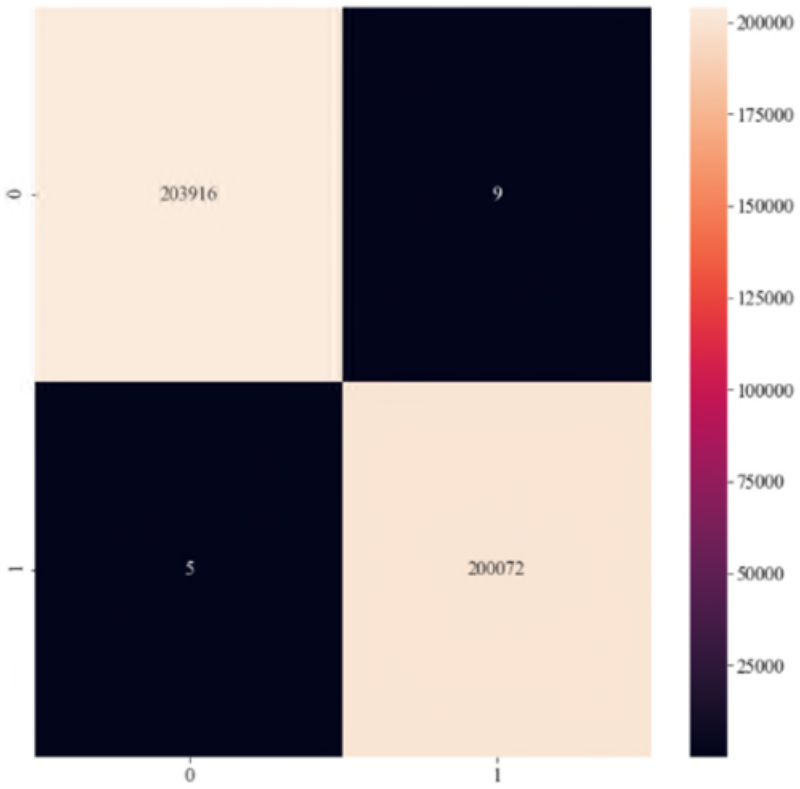

Figure 43 Decision Tree-detection - Confusion Matrix

Misclassification rate - 0.0034653293795575274%

4.2.3 Decision Tree – Classification Report

Average Accuracy	0.9999653467062044
Weighted Precision	0.9999653469088022
Weighted Recall	0.9999653467062044
F1 score	0.9999653467094692
Time taken	125.98188424110413 seconds

Table 16 Decision Tree – Classification Report

4.2.4 Fault Classification

Fault State	Precision	Recall	F1-score	Support
0	1.00	1.00	1.00	203925
1	1.00	1.00	1.00	200077

Table 17 Decision Tree fault classification - Detection

4.2.5 Neural Network – confusion matrix

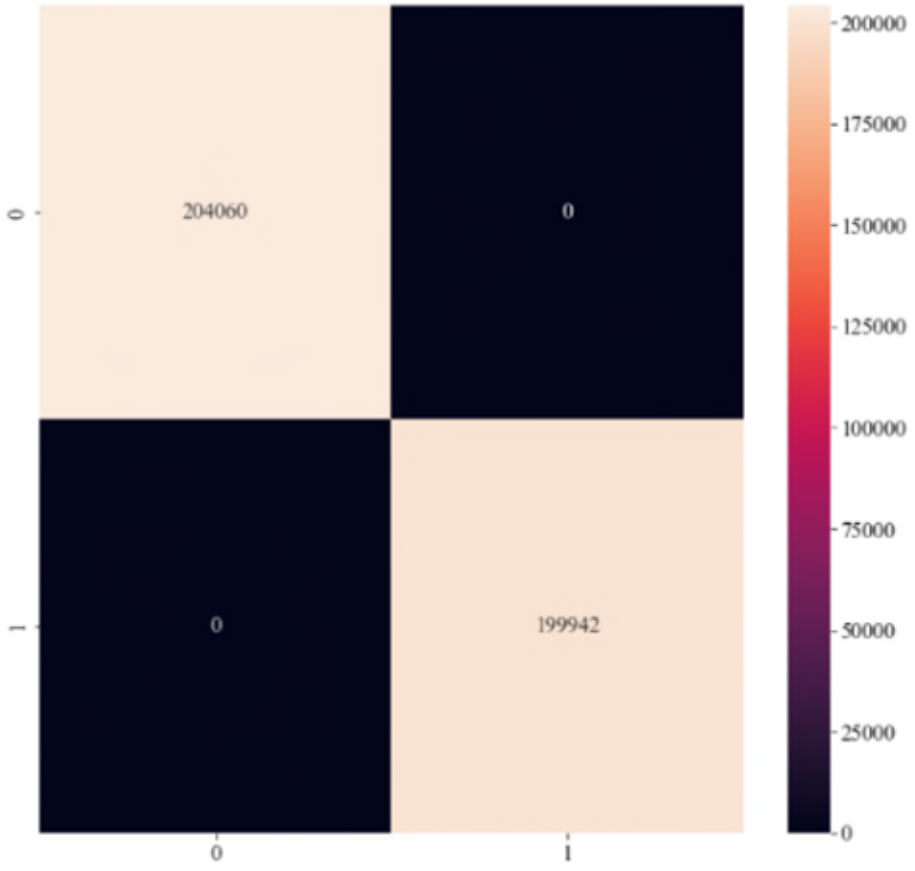

Figure 44 Neural Network-Detection - Confusion Matrix

The misclassification rate is 0.0%

4.2.6 Neural Network – Classification report

Average Accuracy	1.0
Weighted Precision	1.0
Weighted Recall	1.0
F1 score	1.0
Time taken	2811.112918138504 seconds

Table 18 Neural Network – Classification report

4.2.7 Fault classification

Fault State	Precision	Recall	F1-score	Support
0	1.00	1.00	1.00	204060
1	1.00	1.00	1.00	199942

Table 19 Neural Network fault classification – Detection

4.2.8 Autoencoder – Confusion matrix

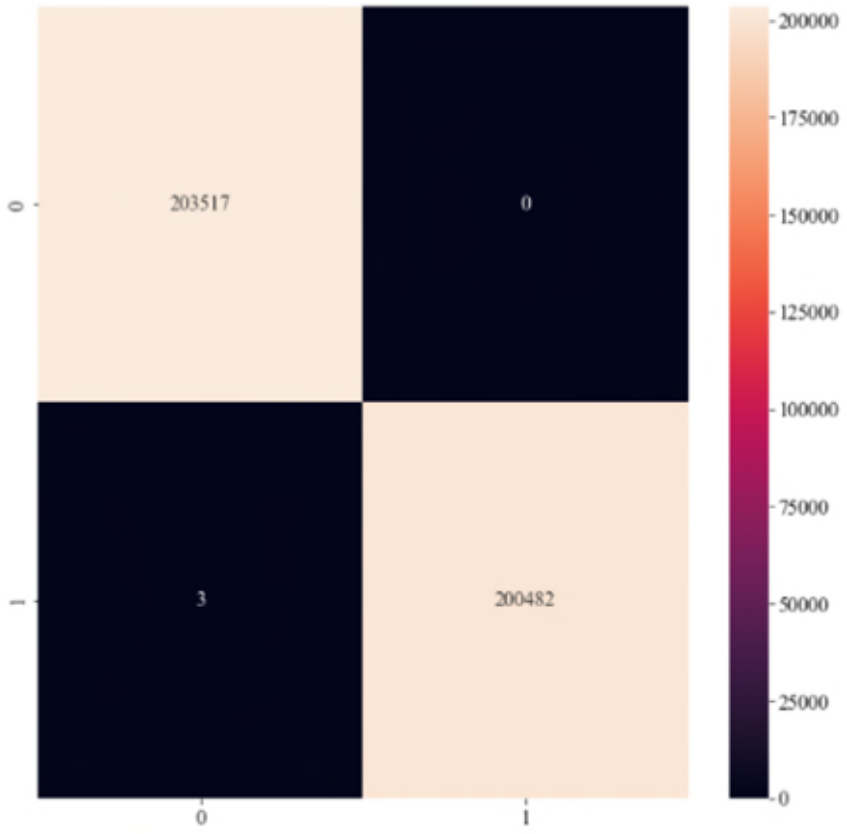

Figure 45 Autoencoder- detection - Confusion Matrix

The misclassification rate is 0.000742570581333755 8%

4.2.9 Autoencoder – Classification report

Average Accuracy	0.9999925742941866
Weighted Precision	0.9999925744036458
Weighted Recall	0.9999925742941866
F1 score	0.9999925742937723
Time taken	794.2934033870697 seconds

Table 20 Autoencoder – Classification report

4.2.10 Fault Classification

Fault State	Precision	Recall	F1-score	Support
0	1.00	1.00	1.00	203517
1	1.00	1.00	1.00	200485

Table 21 Autoencoder fault classification - Detection

4.3 Fault Isolation

4.3.1 Data

After pre-processing, the final dataset contains 10 signals and 1 labelled column of target variables, with 4,04,002 homogenous time steps, including 2,04,001 healthy and 40,000 in each category of faulty samples making it a total of 2,00,001 faulty samples. The fault detection problem is either a decision problem or a binary classification problem. The data is divided into three parts: 70% for training, 20% for testing data, and 10% for validation. Validation data is used during training to avoid overfitting problems by monitoring the performance of the trained model on the training and validation data until the model's performance trained on the validation dataset starts to decrease while the performance of the model training model on the training dataset continues to increase.

Data type	Fault no
Healthy data	0
Sticking valve	1
Pipe leakage	3
Clogged filter	5
Blocked flowmeter	7
Clogged nozzle	9

Table 22 Data labelling - Isolation

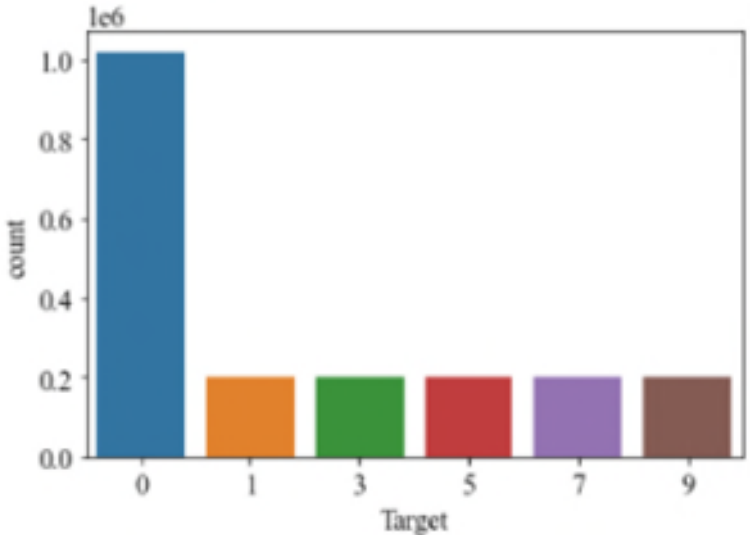

Figure 46 Data for Isolation

4.3.2 Decision Tree – Confusion Matrix

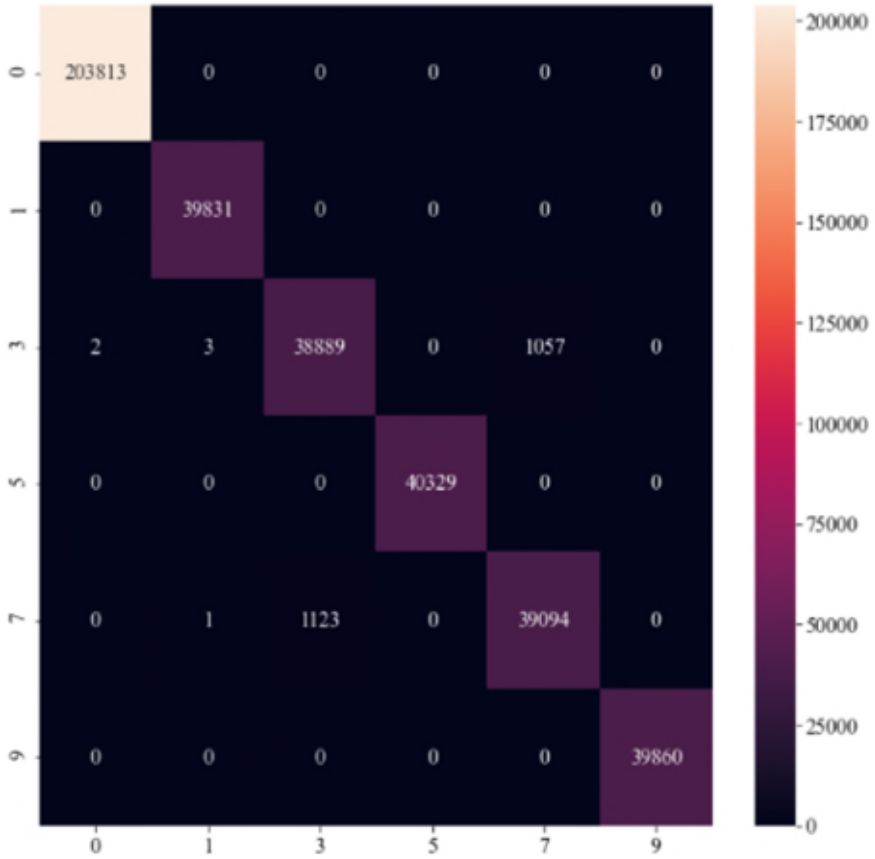

Figure 47 Decision Tree-Isolation - Confusion Matrix

The misclassification rate is 0.5410864302651968%

4.3.3 Decision Tree Classification Report

Average Accuracy	0.9945891356973481
Weighted Precision	0.9945890086337982
Weighted Recall	0.9945891356973481
F1 score	0.9945889486227966
Time taken	113.82081747055054 seconds

Table 23 Decision Tree- Classification Report

4.3.4 Fault Classification

Fault State	Precision	Recall	F1-score	Support
0	1.00	1.00	1.00	203813
1	1.00	1.00	1.00	39831
3	0.97	0.97	0.97	39951
5	1.00	1.00	1.00	40329
7	0.97	0.97	0.97	40218
9	1.00	1.00	1.00	39860

Table 24 Decision Tree fault classification - Isolation

4.3.5 Neural Network – confusion matrix

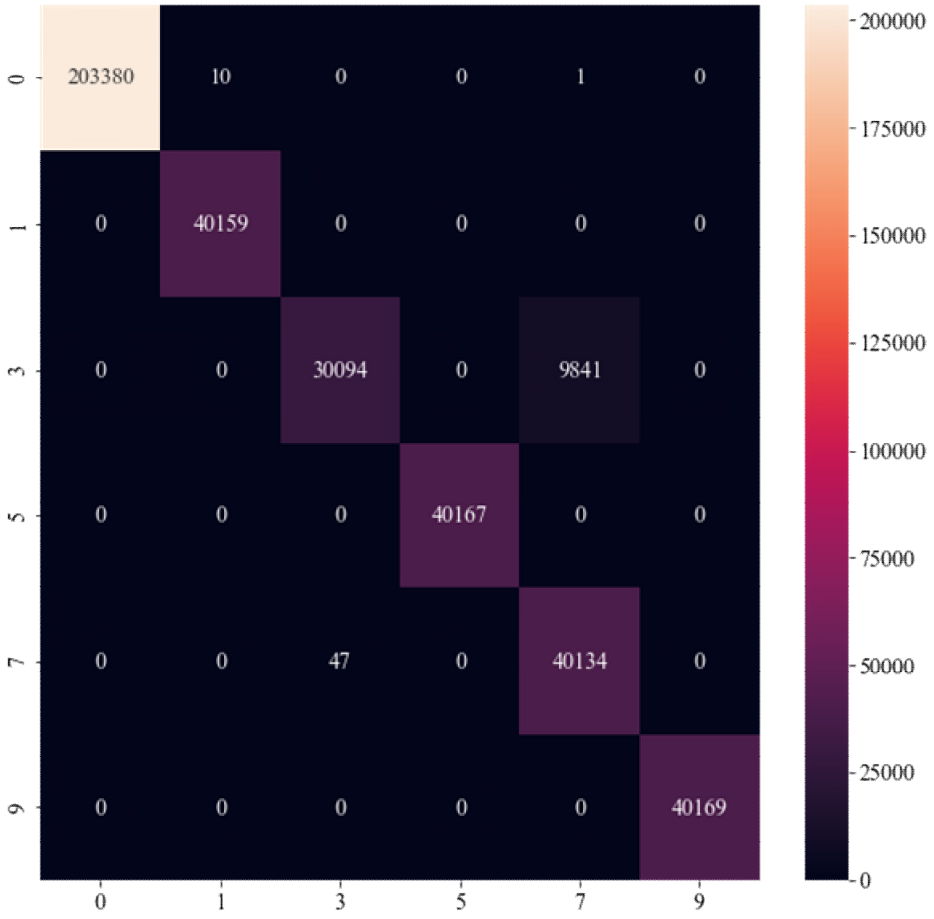

Figure 48 Neural Network- Isolation - Confusion Matrix

The misclassification rate is 2.4502353948742828%

4.3.6 Neural Network – Classification report

Average Accuracy	0.9754976460512572
Weighted Precision	0.9802345137961023
Weighted Recall	0.9754976460512572
F1 score	0.975116964218678
Time taken	6784.163096189499 seconds

Table 25 Neural Network – Classification report

4.3.7 Fault classification

Fault State	Precision	Recall	F1-score	Support
0	1.00	1.00	1.00	203391
1	1.00	1.00	1.00	40159
3	1.00	0.75	0.86	39935
5	1.00	1.00	1.00	40167
7	0.80	1.00	0.89	40181
9	1.00	1.00	1.00	40169

Table 26 Neural Network fault classification - Isolation

4.3.8 Autoencoder – Confusion matrix

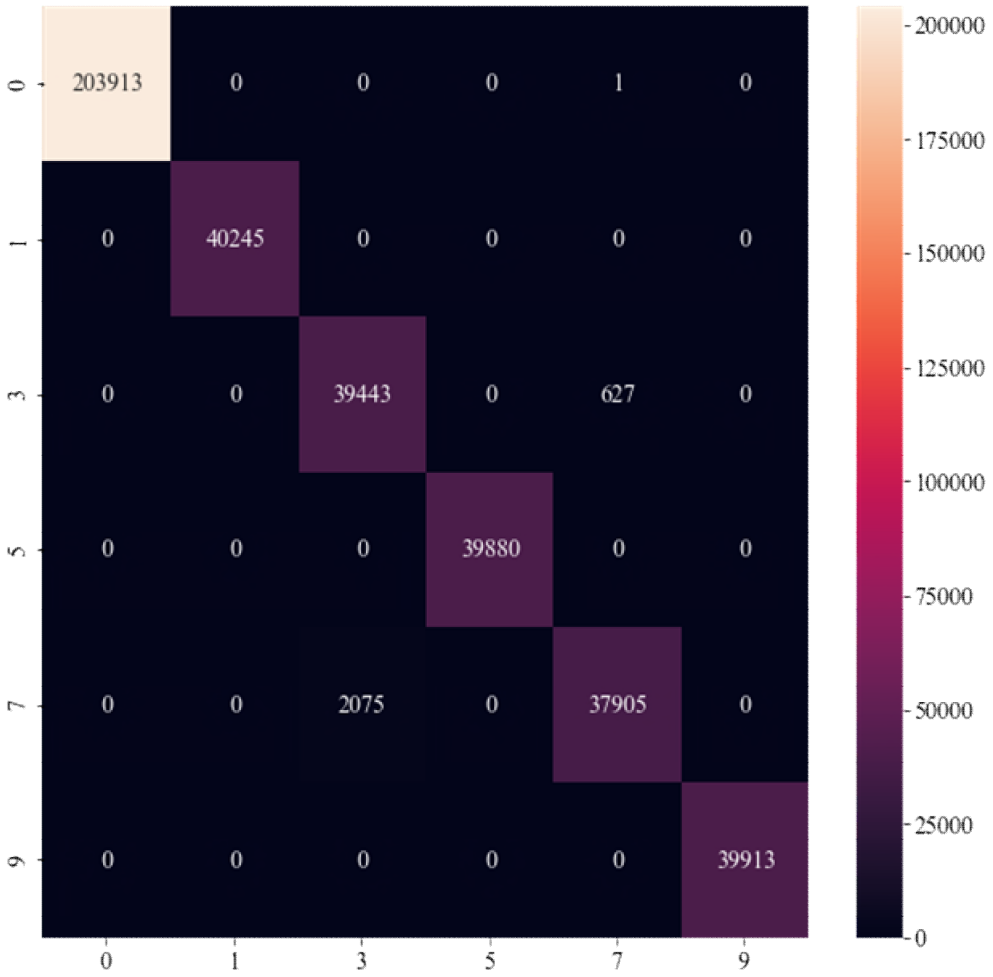

Figure 49 Autoencoder- Isolation - Confusion Matrix

The misclassification rate is 0.6690560937817139%

4.3.9 Autoencoder – Classification report

Average Accuracy	0.9933094390621828
Weighted Precision	0.9934301954248881
Weighted Recall	0.9933094390621828
F1 score	0.9933071344056486
Time taken	2468.599531888962 seconds

Table 27 Autoencoder – Classification report

4.3.10 Fault Classification

Fault State	Precision	Recall	F1-score	Support
0	1.00	1.00	1.00	203914
1	1.00	1.00	1.00	40245
3	0.95	0.98	0.97	40070
5	1.00	1.00	1.00	39880
7	0.98	0.95	0.97	39980
9	1.00	1.00	1.00	39913

Table 28 Autoencoder fault classification - Isolation

4.4 Fault Identification

4.4.1 Data

After pre-processing, the final dataset contains 10 signals and 1 labelled column of target variables, with 4,04,002 homogenous time steps, including 2,04,001 healthy and 20,000 in each category of faulty samples making it a total of 2,00,001 faulty samples. The fault detection problem is either a decision problem or a binary classification problem. The data is divided into three parts: 70% for training, 20% for testing data, and 10% for validation.

Data type	Fault no
Healthy data	0
25% sticking valve	1
50% sticking valve	2
25 % pipe leakage	3
50% pipe leakage	4
25% clogged filter	5
50% clogged filter	6
25% blocked flowmeter	7
50% blocked flowmeter	8
25% clogged nozzle	9
50% clogged nozzle	10

Table 29 Data labelling - Identification

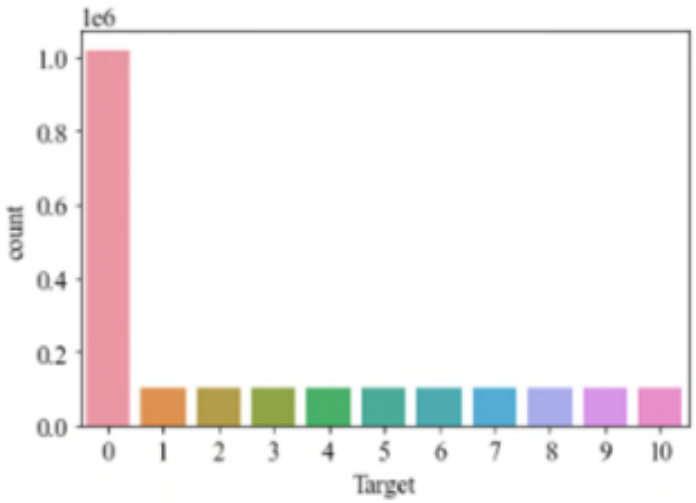

Figure 50 Data for identification

4.4.2 Decision Tree – Confusion Matrix

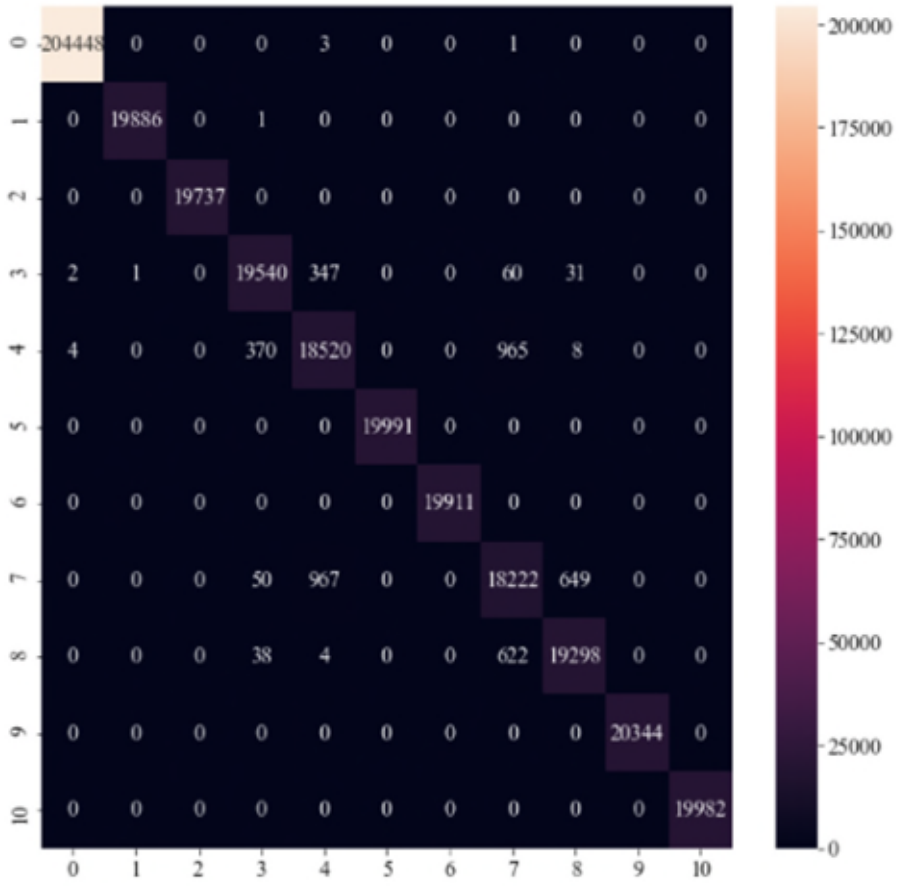

Figure 51 Decision Tree-identification - Confusion Matrix

The misclassification rate is 1.0205395022796917%

4.4.3 Decision Tree - Classification Report

Average Accuracy	0.9897946049772031
Weighted Precision	0.9897896926051261
Weighted Recall	0.9897946049772031
F1 score	0.9897920928329654
Time taken	118.94167399406433 seconds

Table 30 Decision Tree - Classification Report

4.4.4 Fault Classification

Fault State	Precision	Recall	F1-score	Support
0	1.00	1.00	1.00	204452
1	1.00	1.00	1.00	19887
2	1.00	1.00	1.00	19737
3	0.98	0.98	0.98	19981
4	0.93	0.93	0.93	19867
5	1.00	1.00	1.00	19991
6	1.00	1.00	1.00	19911
7	0.92	0.92	0.92	19888
8	0.97	0.97	0.97	19962
9	1.00	1.00	1.00	20344
10	1.00	1.00	1.00	19982

Table 31 Decision Tree fault classification - Identification

4.4.5 Neural Network – confusion matrix

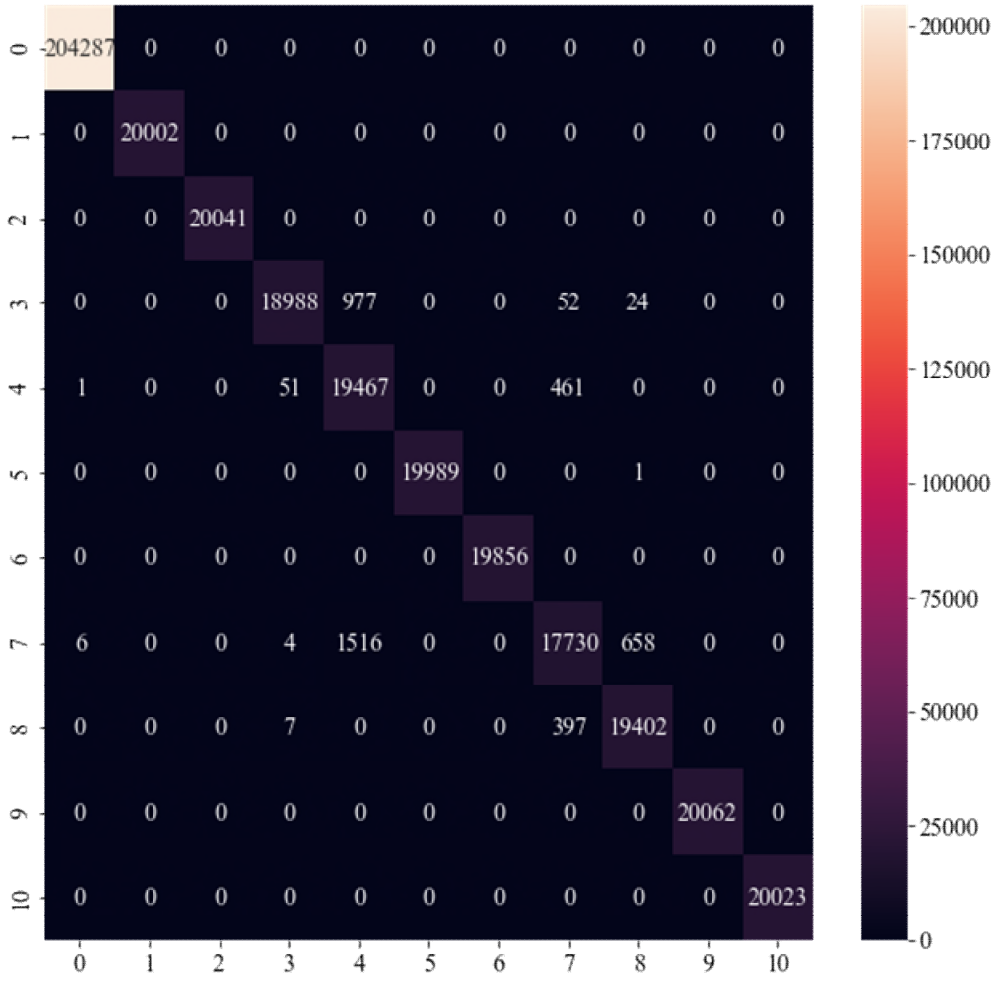

Figure 52 Neural Network-Identification - Confusion Matrix

The misclassification rate is 1.0284602551472517%

4.4.6 Neural Network – Classification report

Average Accuracy	0.9897153974485274
Weighted Precision	0.9901333280592975
Weighted Recall	0.9897153974485274
F1 score	0.9897389251139921
Time taken	7574.180066347122 seconds

Table 32 Neural Network – Classification report

4.4.7 Fault Classification

Fault State	Precision	Recall	F1-score	Support
0	1.00	1.00	1.00	204287
1	1.00	1.00	1.00	20002
2	1.00	1.00	1.00	20041
3	1.00	0.95	0.97	20041
4	0.89	0.97	0.93	19980
5	1.00	1.00	1.00	19990
6	1.00	1.00	1.00	19856
7	0.95	0.89	0.92	19914
8	0.97	0.98	0.97	19806
9	1.00	1.00	1.00	20062
10	1.00	1.00	1.00	20023

Table 33 Neural Network fault classification - Identification

4.4.8 Autoencoder – Confusion matrix

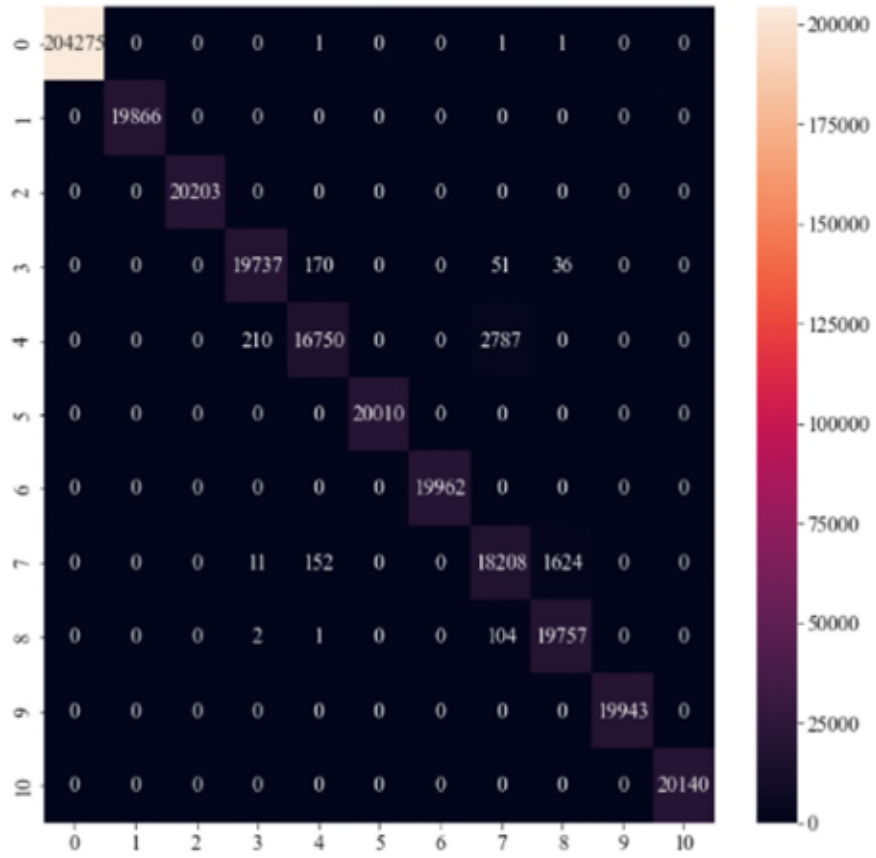

Figure 53 Autoencoder- Identification - Confusion Matrix

The misclassification rate is 1.2749936881500585%

4.4.9 Autoencoder – Classification report

Average Accuracy	0.9872500631184994
Weighted Precision	0.987820011882034
Weighted Recall	0.9872500631184994
F1 score	0.9871980198412297
Time taken	2270.288529396057 seconds

Table 34 Autoencoder – Classification report

4.4.10 Classification

Fault State	Precision	Recall	F1-score	Support
0	1.00	1.00	1.00	204287
1	1.00	1.00	1.00	19866
2	1.00	1.00	1.00	20203
3	0.99	0.99	0.99	19994
4	0.98	0.85	0.91	19747
5	1.00	1.00	1.00	20010
6	1.00	1.00	1.00	19962
7	0.86	0.91	0.89	19995
8	0.92	0.99	0.96	19864
9	1.00	1.00	1.00	19943
10	1.00	1.00	1.00	20140

Table 35 Autoencoder fault classification – Identification

4.5 Conclusion

Validation data is used during training to avoid overfitting problems by monitoring the performance of the trained model on the training and validation data until the model's performance trained on the validation dataset starts to decrease while the performance of the model training model on the training dataset continues to increase.

5 Discussion

Aircraft maintenance is a very crucial operation to increase the life span of the aircraft taking into consideration the environmental impacts and costs of processes. One of the main issues to estimate the effect of part change in the maintenance phase is to calculate the frequency of the failure rate of the components using the probability of the failure. In the MRO the whole system is replaced during the scheduled maintenance but to optimise the un-scheduled maintenance, the parts or components should be categorised as repairable and non-repairable before they are replaced. To attain this knowledge, more research on component failures must be carried out.

Fault in a complex fuel system is not usually apparent and the source of the problem may be hidden by the symptoms that develop as the other subsystems respond to compensate for the fault in one component. The data collected for this research is with a constant flow rate of 0.65 l/min, showing that in every case the fault detection is done on the physical characteristics of system efficiency. In this thesis, the machine learning method is utilized and compared to find the solution for fault detection, isolation, and identification in aircraft fuel systems.

The research uses data from several sensors located next to the crucial components to estimate the health of each component and the entire system. Moreover, for the fault to be detected the individual sensor should identify the anomalies and the readings will monitor the faulty behaviour. As the data shows the data from the flow meter determines the speed of the pump speed and acts as the fault indicator.

5.1 Benefits and Limitations of using PHM for Aircraft Fuel Systems

5.1.1 Benefits

- The Diagnostic process can improve with the development of sensor technology and the accessibility of improved machine learning methods.

- The Diagnostics of the Aircraft Fuel System can be predicted under the present state of the components.
- The diagnostics results can act as an encouragement for the MROs or the operators to actively monitor the data from the sensors to optimise the mission and make changes to the maintenance planning to avoid any severe accidents.

5.1.2 Drawbacks

- The data obtained for this research is laboratory-based, and it will be expensive to implement the PHM in practice. To encourage the MROs and decision-makers in the maintenance field to use PHM more reliable study on the return on investment (ROI) must be conducted.
- Even though the Machine learning techniques are highly developed, to explain and validate the results from PHM models a Human expert with domain knowledge in the Aircraft fuel system is required.

6 Conclusion

1 Identify the research gap through a literature review

2 Collecting data using the aircraft fuel system to provide historical records for the diagnosis model

3 Creating a machine learning fault detection model (Decision Tree, Neural network and Autoencoder method) based on the collected data and comparing it to other methods

4 Creating a machine learning fault isolation model (Decision Tree, Neural network and Autoencoder method) based on the collected data

5 Creating a machine learning fault identification model (Decision Tree, Neural network and Autoencoder method) based on the collected data

6 Comparing and validating the proposed method with the Machine learning-based and deep learning models.

6.1 Contribution

From the moment of manufacturing, all the components start the degradation process. However previous research considered that only the component is faulty and has not considered the effect on the other components in the system. This research considers the component faults and their effects in speeding up the degradation of other components.

As the data for the fuel rig is not readily available, an experimental fuel rig setup previous for other studies is altered to obtain reproducible data on multicomponent failures with different severity.

Machine learning has been used in fault detection of other parts of the aircraft's mainly gas-turbine engines, but no research was previously conducted to analyse the faults or degradation in the fuel system. For this reason, the present research contributes to the knowledge by developing a deep learning (Autoencoder) analysis for the degree of degradation in aircraft fuel systems to improve the robustness in fault recognition and isolation.

With a focus on utilizing machine learning and deep learning-based fault classification techniques, the contributions of this thesis - The thesis provides improved fault detection and classification methodology using sequential models, especially with Autoencoder. The comparative study indicates the better performance of the classification task by the proposed classifier in comparison to recent deep-learning techniques for this task.

All the new engineering system runs for the first time, and all of their components start to degrade. However, previous research done on working fuel systems assumes that apart from the faulty component, all other components in the system are operating in a healthy state, which could lead to a wrong diagnostic result. Considering this problem, the data collected from the Aircraft fuel system Rig can be used for any other further analysis.

6.2 Future Work

- Comparative study of component-level and system-level fault detection can be useful to improve the environmental factor the aircraft maintenance
- The fuel rig can be used to generate more complex data like the unbalanced weights of fuel tanks in the wings but simulating spillage.
- Improvement to the fuel rig
    - The fuel rig setup doesn’t have any disturbances, so the data collected is clean from noise. This does not represent the real case scenario.
    - The data collected for this thesis has provided only the pressure and flow rate difference to monitor the state of the equipment Including additional sensors that can capture other significant input measurements in the future will enable a more efficient diagnosis.

- This research considers only single independent faults and their effects, future work can be carried out on multiple faults and their effects on other components and the entire system.
- The data obtained for this research is laboratory-based, and it will be expensive to implement the PHM in practice. To encourage the MROs and decision-makers in the maintenance field to use PHM more reliable study on the return on investment (ROI) must be conducted.

REFERENCES

1. Kampurath V., Chaitanya M. Aircraft Servicing, Maintenance, Repair & Overhaul-The Changed Scenarios Through Outsourcing. 2017. Available at: http://www.euroasiapub.org

2. Cros G. Preliminary Analysis of MCTG FY2018 Data. 14th Maintenance Cost Conference. International Air Transport Assoication; 2018. Available at: Available at: https://www.iata.org/whatwedo/workgroups/Documents/MCC-2018-ATL/Day1/1000-1030-prelim-analysis-of-mctf-data-iata.pdf (Accessed: 2 December 2021)

3. Bousdekis A., Magoutas B., Apostolou D., Mentzas G. A proactive decision making framework for condition-based maintenance. Industrial Management and Data Systems. Emerald Group Holdings Ltd.; 10 August 2015; 115(7): 1225–1250. Available at: DOI:10.1108/IMDS-03-2015-0071

4. Xie J., Pecht M. Applications Of In-Situ Health-Monitoring And Prognostic Sensors. The 9th Pan Pacific microelectronics Symposium Exhibits and Conference. 2004.

5. Tiddens WW., Braaksma AJJ., Tinga T. The Adoption of Prognostic Technologies in Maintenance Decision Making: A Multiple Case Study. Procedia CIRP. Elsevier B.V.; 2015. pp. 171–176. Available at: DOI:10.1016/j.procir.2015.08.028

6. Dai X., Gao Z. From model, signal to knowledge: A data-driven perspective of fault detection and diagnosis. IEEE Transactions on Industrial Informatics. IEEE; 2013; 9(4): 2226–2238. Available at: DOI:10.1109/TII.2013.2243743

7. Hoang DT., Kang HJ. A survey on Deep Learning based bearing fault diagnosis. Neurocomputing. Elsevier B.V.; 2019; 335: 327–335. Available at: DOI:10.1016/j.neucom.2018.06.078

8. He H., Gray J., Cangelosi A., Meng Q., McGinnity TM., Mehnen J. The Challenges and Opportunities of Artificial Intelligence for Trustworthy Robots and Autonomous Systems. IRCE 2020 - 2020 3rd International Conference on Intelligent Robotics and Control Engineering. Institute of Electrical and Electronics Engineers Inc.; 2020. pp. 68–74. Available at: DOI:10.1109/IRCE50905.2020.9199244

9. Miao Y., Wang S. Health management system based on airworthiness of the aircraft fuel system. Procedia Engineering. Elsevier Ltd; 2014. pp. 34–43. Available at: DOI:10.1016/j.proeng.2014.09.057

10. Aircraft Fuel Systems | SKYbrary Aviation Safety. Available at: https://skybrary.aero/articles/aircraft-fuel-systems (Accessed: 2 December 2021)

11. Aubin BR., Society of Automotive Engineers. Aircraft maintenance : the art and science of keeping aircraft safe. Society of Automotive Engineers; 2004. 166 p.

12. Aubin BR., Society of Automotive Engineers. Aircraft maintenance : the art and science of keeping aircraft safe. Society of Automotive Engineers; 2004. 166 p.

13. Bousdekis A., Magoutas B., Apostolou D., Mentzas G. A proactive decision making framework for condition-based maintenance. Industrial Management and Data Systems. Emerald Group Holdings Ltd.; 10 August 2015; 115(7): 1225–1250. Available at: DOI:10.1108/IMDS-03-2015-0071

14. Bousdekis A., Magoutas B., Apostolou D., Mentzas G. A proactive decision making framework for condition-based maintenance. Industrial Management & Data Systems. 2015; 115(7): 1225–1250. Available at: DOI:10.1108/IMDS-03-2015-0071

15. Tinga T., Loendersloot R. Aligning PHM, SHM and CBM by understanding the physical system failure behaviour. European Conferene of the Prognostics and Health Management Society; 2014. Available at: https://www.researchgate.net/publication/268982172

16. Vichare N., Pecht MG. Prognostics and Health Management of Electronics. Prognostics and Health Management of Electronics. 2008; 29(1): 1–315. Available at: DOI:10.1002/9780470385845

17. ISO - ISO 13374-4:2015 - Condition monitoring and diagnostics of machine systems — Data processing, communication and presentation. Available at: https://www.iso.org/standard/54933.html (Accessed: 3 January 2022)

18. Engel SJ., Gilmartin BJ., Bongort K., Hess A. Prognostics, the real issues involved with predicting life remaining. IEEE Aerospace Conference Proceedings. 2000; 6: 457–470. Available at: DOI:10.1109/AERO.2000.877920

19. Atamuradov V., Medjaher K., Dersin P., Lamoureux B., Zerhouni N. Prognostics and Health Management for Maintenance Practitioners-Review, Implementation and Tools Evaluation. International Journal of Prognostics and Health Management. 2017.

20. Benedettini O., Baines TS., Lightfoot HW., Greenough RM. State-of-the-art in integrated vehicle health management. Proceedings of the Institution of Mechanical Engineers, Part G: Journal of Aerospace Engineering. 1 March 2009; 223(2): 157–170. Available at: DOI:10.1243/09544100JAERO446

21. Subramanian N., He H., Jennions I. Fault Detection for Aircraft Fuel System with Neural Network. 9th International Conference on Through-life Engineering Service. 2020.

22. Skliros C., Esperon Miguez M., Fakhre A., Jennions IK. A review of model based and data driven methods targeting hardware systems diagnostics. Diagnostyka. Polish Society of Technical Diagnostics; 2019. pp. 3–21. Available at: DOI:10.29354/diag/99603

23. Lane R. Sensors and Sensing Technologies for Integrated Vehicle Health Monitoring Systems. AMPTIAC Quaterly. 2014. pp. 11–15.

24. Zhang B., Khawaja T., Patrick R., Vachtsevanos G., Orchard ME., Saxena A. Application of blind deconvolution denoising in failure prognosis. IEEE Transactions on Instrumentation and Measurement. 2009; 58(2): 303–310. Available at: DOI:10.1109/TIM.2008.2005963

25. Ogaji SOT., Sampath S., Singh R., Probert SD. Parameter selection for diagnosing a gas-turbine's performance-deterioration. Available at: www.elsevier.com/locate/apenergy

26. Wang C., Lu N., Cheng Y., Jiang B. A telemetry data based diagnostic health monitoring strategy for in-orbit spacecrafts with component degradation. Advances in Mechanical Engineering. 2019; 11(4): 1–14. Available at: DOI:10.1177/1687814019839599

27. Lucas P., Abu-Hanna Ameen. Prognostic Methods in Medicine. Aritificial Intelligence in Medicine. 1990; : 105–119.

28. Si X., Li T., Zhang Q., Hu X. An Optimal Condition-Based Replacement Method for Systems with Observed Degradation Signals. IEEE Transactions on Reliability. Institute of Electrical and Electronics Engineers Inc.; 1 September 2018; 67(3): 1381–1393. Available at: DOI:10.1109/TR.2018.2830188 (Accessed: 24 January 2022)

29. Vieira JP., Galvão RKH., Yoneyama T. Predictive Control for Systems with Loss of Actuator Effectiveness Resulting from Degradation Effects. Journal of Control, Automation and Electrical Systems 2015 26:6. Springer; 28 July 2015; 26(6): 589–598.

Available at: DOI:10.1007/S40313-015-0201-7 (Accessed: 24 January 2022)

30. WANG Y., GOGU C., BINAUD N., BES C., HAFTKA RT., KIM NH. A cost driven predictive maintenance policy for structural airframe maintenance. Chinese Journal of Aeronautics. Elsevier; 1 June 2017; 30(3): 1242–1257. Available at: DOI:10.1016/J.CJA.2017.02.005 (Accessed: 24 January 2022)

31. Okoh C., Roy R., Mehnen J. Predictive Maintenance Modelling for Through-Life Engineering Services. Procedia CIRP. Elsevier; 1 January 2017; 59: 196–201. Available at: DOI:10.1016/J.PROCIR.2016.09.033 (Accessed: 2 December 2021)

32. Atamuradov V., Medjaher K., Dersin P., Lamoureux B., Zerhouni N. Prognostics and Health Management for Maintenance Practitioners-Review, Implementation and Tools Evaluation. International Journal of Prognostics and Health Management. 2017.

33. Sikorska JZ., Hodkiewicz M., Ma L. Prognostic modelling options for remaining useful life estimation by industry. Mechanical Systems and Signal Processing. July 2011; 25(5): 1803–1836. Available at: DOI:10.1016/j.ymssp.2010.11.018

34. Bolander N., Qiu H., Eklund N., Hindle E., Rosenfeld T. Physics-based Remaining Useful Life Prediction for Aircraft Engine Bearing Prognosis. Conference of the Prognostics and Health Management Society. 2009.

35. Okoh C., Roy R., Mehnen J., Redding L. Overview of Remaining Useful Life prediction techniques in Through-life Engineering Services. Procedia CIRP. Elsevier; 2014. pp. 158–163. Available at: DOI:10.1016/j.procir.2014.02.006

36. Coppe A., Pais MJ., Haftka RT., Kim NH. Using a simple crack growth model in predicting remaining useful life. Journal of Aircraft.

American Institute of Aeronautics and Astronautics Inc.; 2012; 49(6): 1965–1973. Available at: DOI:10.2514/1.C031808

37. Jing C., Gao X., Zhu X., Lang S. Fault classification on Tennessee Eastman process: PCA and SVM. Proceedings - 2014 International Conference on Mechatronics and Control, ICMC 2014. Institute of Electrical and Electronics Engineers Inc.; 2015. pp. 2194–2197. Available at: DOI:10.1109/ICMC.2014.7231958

38. Kong X., Cao Z., An Q., Gao Y., Du B. Quality-related and process-related fault monitoring with online monitoring dynamic concurrent PLS. IEEE Access. Institute of Electrical and Electronics Engineers Inc.; 2018; 6: 59074–59086. Available at: DOI:10.1109/ACCESS.2018.2872790

39. Bathelt A., Ricker NL., Jelali M. Revision of the Tennessee eastman process model. IFAC-PapersOnLine. 2015. pp. 309–314. Available at: DOI:10.1016/j.ifacol.2015.08.199

40. Chiang LH., Russell EL., Braatz RD. Fault diagnosis in chemical processes using Fisher discriminant analysis, discriminant partial least squares, and principal component analysis. Chemometrics and Intelligent Laboratory Systems. 2000. Available at: www.elsevier.comrlocaterchemometrics

41. Yang Y., Suliang M., Jianwen W., Bowen J., Weixin L., Xiaowu L. Fault Diagnosis in Gas Insulated Switchgear Based on Genetic Algorithm and Density- Based Spatial Clustering of Applications with Noise. IEEE Sensors Journal. Institute of Electrical and Electronics Engineers Inc.; 15 January 2021; 21(2): 965–973. Available at: DOI:10.1109/JSEN.2019.2942618

42. F. Borges., A. Pinto., D. Ribeiro., T. Barbosa., D. Pereira., B. Barbosa., et al. An Unsupervised Method based on Support Vector Machines and Higher-Order Statistics for Mechanical Faults Detection. IEEE Latin America Transcation. 2020. pp. 1093–1102.

43. Shi J., He Q., Wang Z. GMM clustering-based decision trees considering fault rate and cluster validity for analog circuit fault diagnosis. IEEE Access. Institute of Electrical and Electronics Engineers Inc.; 2019; 7: 140637–140650. Available at: DOI:10.1109/ACCESS.2019.2943380

44. Li C., Xiong J., Zhu X., Zhang Q., Wang S. Fault diagnosis method based on encoding time series and convolutional neural network. IEEE Access. Institute of Electrical and Electronics Engineers Inc.; 2020; 8: 165232–165246. Available at: DOI:10.1109/ACCESS.2020.3021007

45. Vieira FM., Bizarria CDO., Nascimento CL., Fitzgibbon KT. Health monitoring using support vector classification on an auxiliary power unit. IEEE Aerospace Conference Proceedings. 2009. Available at: DOI:10.1109/AERO.2009.4839655

46. Zhao Q., Wang B., Zhou G., Zhang W., Guan X., Feng W. An improved fault diagnosis approach based on support vector machine. 2016 IEEE International Conference on Prognostics and Health Management, ICPHM 2016. Institute of Electrical and Electronics Engineers Inc.; 2016. Available at: DOI:10.1109/ICPHM.2016.7542827

47. Han HL., Ma HY., Yang Y. Study on the Test Data Fault Mining Technology Based on Decision Tree. Procedia Computer Science. Elsevier; 1 January 2019; 154: 232–237. Available at: DOI:10.1016/J.PROCS.2019.06.035 (Accessed: 24 January 2022)

48. Saravanan N., Ramachandran KI. Fault diagnosis of spur bevel gear box using discrete wavelet features and Decision Tree classification. Expert Systems with Applications. Pergamon; 1 July 2009; 36(5): 9564–9573. Available at: DOI:10.1016/J.ESWA.2008.07.089 (Accessed: 24 January 2022)

49. Schmidhuber J. Deep Learning in neural networks: An overview. Neural Networks. Elsevier Ltd; 2015. pp. 85–117. Available at: DOI:10.1016/j.neunet.2014.09.003

50. Kumar Jain A., Kundu P., Lad BK. Prediction of Remaining Useful Life of anAircraft Engine under Unknown Initial Wear. IIT Guwahati. 2014. Available at: http://ti.arc.nasa.gov/tech/dash/pcoe/progn

51. Zhao R., Yan R., Chen Z., Mao K., Wang P., Gao RX. Deep learning and its applications to machine health monitoring. Mechanical Systems and Signal Processing. Academic Press; 2019. pp. 213–237. Available at: DOI:10.1016/j.ymssp.2018.05.050

52. LeCun Y., Bengio Y., Hinton G. Deep learning. Nature. 28 May 2015; 521(7553): 436–444. Available at: DOI:10.1038/nature14539 (Accessed: 19 August 2018)

53. He M., He D. Deep Learning Based Approach for Bearing Fault Diagnosis. IEEE Transactions on Industry Applications. May 2017; 53(3): 3057–3065. Available at: DOI:10.1109/TIA.2017.2661250 (Accessed: 19 August 2018)

54. Junbo T., Weining L., Juneng A., Xueqian W. Fault diagnosis method study in roller bearing based on wavelet transform and stacked auto-encoder. The 27th Chinese Control and Decision Conference (2015 CCDC). IEEE; 2015. pp. 4608–4613. Available at: DOI:10.1109/CCDC.2015.7162738 (Accessed: 19 August 2018)

55. Sun W., Shao S., Zhao R., Yan R., Zhang X., Chen X. A sparse auto-encoder-based deep neural network approach for induction motor faults classification. Measurement: Journal of the International Measurement Confederation. Elsevier B.V.; 1 July 2016; 89: 171–178. Available at: DOI:10.1016/j.measurement.2016.04.007

56. Tamilselvan P., Wang P. Failure diagnosis using deep belief learning based health state classification. Reliability Engineering & System

Safety. 2013; 115: 124–135. Available at: DOI:10.1016/j.ress.2013.02.022 (Accessed: 19 August 2018)

57. Chen Z., Li W. Multisensor feature fusion for bearing fault diagnosis using sparse autoencoder and deep belief network. IEEE Transactions on Instrumentation and Measurement. Institute of Electrical and Electronics Engineers Inc.; 1 July 2017; 66(7): 1693–1702. Available at: DOI:10.1109/TIM.2017.2669947

58. Feng D., Xiao M., Liu Y., Song H., Yang Z., Hu Z. Finite-sensor fault-diagnosis simulation study of gas turbine engine using information entropy and deep belief networks. Frontiers of Information Technology & Electronic Engineering. 17 December 2016; 17(12): 1287–1304. Available at: DOI:10.1631/FITEE.1601365 (Accessed: 19 August 2018)

59. Yang R., Huang M., Lu Q., Zhong M. Rotating Machinery Fault Diagnosis Using Long-short-term Memory Recurrent Neural Network. Elsevier B.V.; 2018. pp. 228–232. Available at: DOI:10.1016/j.ifacol.2018.09.582

60. Gugulothu N., TV V., Malhotra P., Vig L., Agarwal P., Shroff G. Predicting Remaining Useful Life using Time Series Embeddings based on Recurrent Neural Networks. 4 September 2017; Available at: http://arxiv.org/abs/1709.01073 (Accessed: 19 August 2018)

61. Park D., Kim S., An Y., Jung J-Y. LiReD: A Light-Weight Real-Time Fault Detection System for Edge Computing Using LSTM Recurrent Neural Networks. Sensors. 30 June 2018; 18(7): 2110. Available at: DOI:10.3390/s18072110 (Accessed: 19 August 2018)

62. Li X., Ding Q., Sun JQ. Remaining useful life estimation in prognostics using deep convolution neural networks. Reliability Engineering and System Safety. 2018; 172. Available at: DOI:10.1016/j.ress.2017.11.021

63. Rawat W., Wang Z. Deep convolutional neural networks for image classification: A comprehensive review. Neural Computation. MIT Press Journals; 2017. pp. 2352–2449. Available at: DOI:10.1162/NECO_a_00990

64. Abdeljaber O., Avci O., Kiranyaz S., Gabbouj M., Inman DJ. Real-time vibration-based structural damage detection using one-dimensional convolutional neural networks. Journal of Sound and Vibration. 2017; 388: 154–170. Available at: DOI:10.1016/j.jsv.2016.10.043 (Accessed: 19 August 2018)

65. Lu C., Wang Z-Y., Qin W-L., Ma J. Fault diagnosis of rotary machinery components using a stacked denoising autoencoder-based health state identification. Signal Processing. 2017; 130: 377–388. Available at: DOI:10.1016/j.sigpro.2016.07.028 (Accessed: 19 August 2018)

66. Shao SY., Sun WJ., Yan RQ., Wang P., Gao RX. A Deep Learning Approach for Fault Diagnosis of Induction Motors in Manufacturing. Chinese Journal of Mechanical Engineering (English Edition). Chinese Mechanical Engineering Society; 1 November 2017; 30(6): 1347–1356. Available at: DOI:10.1007/s10033-017-0189-y

67. Sun C., Ma M., Zhao Z., Chen X. Sparse Deep Stacking Network for Fault Diagnosis of Motor. IEEE Transactions on Industrial Informatics. July 2018; 14(7): 3261–3270. Available at: DOI:10.1109/TII.2018.2819674 (Accessed: 19 August 2018)

68. Park P., di Marco P., Shin H., Bang J. Fault Detection and Diagnosis Using Combined Autoencoder and Long Short-Term Memory Network. Sensors (Basel, Switzerland). Multidisciplinary Digital Publishing Institute (MDPI); 1 November 2019; 19(21). Available at: DOI:10.3390/S19214612 (Accessed: 24 January 2022)

69. Xing-Yu Q., Peng Z., Dong-Dong F., Chengcheng X. Autoencoder-based fault diagnosis for grinding system. Proceedings of the 29th

Chinese Control and Decision Conference, CCDC 2017. Institute of Electrical and Electronics Engineers Inc.; 12 July 2017; : 3867–3872. Available at: DOI:10.1109/CCDC.2017.7979177 (Accessed: 24 January 2022)

70. ZHANG J., SUN Y., GUO L., GAO H., HONG X., SONG H. A new bearing fault diagnosis method based on modified convolutional neural networks. Chinese Journal of Aeronautics. Elsevier; 1 February 2020; 33(2): 439–447. Available at: DOI:10.1016/J.CJA.2019.07.011 (Accessed: 24 January 2022)

71. Wu Y., Yuan M., Dong S., Lin L., Liu Y. Remaining useful life estimation of engineered systems using vanilla LSTM neural networks. Neurocomputing. 2018; 275: 167–179. Available at: DOI:10.1016/j.neucom.2017.05.063 (Accessed: 19 August 2018)

72. Schmidhuber J. Deep Learning in Neural Networks: An Overview. 30 April 2014; Available at: DOI:10.1016/j.neunet.2014.09.003 (Accessed: 19 August 2018)

73. de Bruin T., Verbert K., Babuska R. Railway Track Circuit Fault Diagnosis Using Recurrent Neural Networks. IEEE Transactions on Neural Networks and Learning Systems. Institute of Electrical and Electronics Engineers Inc.; 1 March 2017; 28(3): 523–533. Available at: DOI:10.1109/TNNLS.2016.2551940

74. Zhao Z., Chen W., Wu X., Chen PCY., Liu J. LSTM network: A deep learning approach for Short-term traffic forecast. IET Intelligent Transport Systems. Institution of Engineering and Technology; 1 March 2017; 11(2): 68–75. Available at: DOI:10.1049/iet-its.2016.0208

75. Jung M., Niculita O., Skaf Z. Comparison of Different Classification Algorithms for Fault Detection and Fault Isolation in Complex Systems. Procedia Manufacturing. Elsevier B.V.; 2018; 19: 111–118.

Available at: DOI:10.1016/J.PROMFG.2018.01.016 (Accessed: 7 November 2022)

76. Safavi S., Safavi MA., Hamid H., Fallah S. Multi-sensor fault detection, identification, isolation and health forecasting for autonomous vehicles. Sensors. MDPI AG; 1 April 2021; 21(7). Available at: DOI:10.3390/s21072547

77. Sheng Y., Rovnyak SM. Decision tree-based methodology for high impedance fault detection. IEEE Transactions on Power Delivery. April 2004; 19(2): 533–536. Available at: DOI:10.1109/TPWRD.2003.820418 (Accessed: 7 November 2022)

78. Tahi M., Miloudi A., Dron JP., Bouzouane B. Decision tree and feature selection by using genetic wrapper for fault diagnosis of rotating machinery. https://doi.org/10.1080/14484846.2018.1552355. Taylor & Francis; 1 September 2018; 18(3): 496–504. Available at: DOI:10.1080/14484846.2018.1552355 (Accessed: 7 November 2022)

79. Jiarula Y., Gao J., Gao Z., Hongquan J., Rongxi W. Fault mode prediction based on decision tree. Proceedings of 2016 IEEE Advanced Information Management, Communicates, Electronic and Automation Control Conference, IMCEC 2016. Institute of Electrical and Electronics Engineers Inc.; 28 February 2017; : 1729–1733. Available at: DOI:10.1109/IMCEC.2016.7867514 (Accessed: 7 November 2022)

80. Zhang ZY., Wang KS. Wind turbine fault detection based on SCADA data analysis using ANN. Advances in Manufacturing. Shanghai University Press; 1 March 2014; 2(1): 70–78. Available at: DOI:10.1007/S40436-014-0061-6/FIGURES/7 (Accessed: 7 November 2022)

81. Zhang S., Ganesan R. Multivariable Trend Analysis Using Neural Networks for Intelligent Diagnostics of Rotating Machinery. Journal of Engineering for Gas Turbines and Power. 1997; 119(2): 378. Available at: DOI:10.1115/1.2815585 (Accessed: 19 August 2018)

82. Cunha Palácios RH., da Silva IN., Goedtel A., Godoy WF. A comprehensive evaluation of intelligent classifiers for fault identification in three-phase induction motors. Electric Power Systems Research. Elsevier Ltd; 29 June 2015; 127: 249–258. Available at: DOI:10.1016/J.EPSR.2015.06.008 (Accessed: 7 November 2022)

83. Ciaburro G., Ciaburro G. Machine fault detection methods based on machine learning algorithms: A review. Mathematical Biosciences and Engineering 2022 11:11453. American Institute of Mathematical Sciences; 2022; 19(11): 11453–11490. Available at: DOI:10.3934/MBE.2022534 (Accessed: 7 November 2022)

84. Langton R., Clark C., Hewitt M., Richards L. Fuel Storage. Aircraft Fuel Systems. John Wiley & Sons, Ltd; 29 June 2009; : 31–51. Available at: DOI:10.1002/9780470059470.CH3 (Accessed: 9 December 2021)

85. Boeing B777 System Diagrams. Available at: https://www.avsoft.com/product/boeing-b777-system-diagrams/ (Accessed: 20 January 2022)

86. Aviation Fuels with Improved Fire Safety. Aviation Fuels with Improved Fire Safety. National Academies Press; 1997. Available at: DOI:10.17226/5871

87. AERO - Engine Fuel Filter Contamination. Available at: https://www.boeing.com/commercial/aeromagazine/articles/qtr_3_08/article_03_1.html (Accessed: 9 December 2021)

88. Skaf Z., Eker OF., Jennions IK. Towards System Prognostics: Filter Clogging of a UAV Fuel System. 2017; Available at: http://www.phmap.org/data/PHM17_Proceedings_20171112.pdf (Accessed: 9 December 2021)

89. AERO - Engine Fuel Filter Contamination. Available at: https://www.boeing.com/commercial/aeromagazine/articles/qtr_3_08/article_03_1.html (Accessed: 24 January 2022)

90. Lin Y., Zakwan S., Jennions IK. A bayesian approach to fault identification in the presence of multi-component degradation. International Journal of Prognostics and Health Management. 2017; 8(1): 2153–2648.

91. Soualhi A., Clerc G., Razik H. Detection and Diagnosis of Faults in Induction Motor Using an Improved Artificial Ant Clustering Technique. IEEE Transactions on Industrial Electronics. September 2013; 60(9): 4053–4062. Available at: DOI:10.1109/TIE.2012.2230598 (Accessed: 19 August 2018)

92. Antonio Ortega Redondo René de Jesús Romero Troncoso Miguel Delgado Prieto J. ‘Fault detection and identification methodology under an incremental learning framework applied to industrial electromechanical systems’. 2017.

93. Goelles T., Schlager B., Muckenhuber S. Fault Detection, Isolation, Identification and Recovery (FDIIR) Methods for Automotive Perception Sensors Including a Detailed Literature Survey for Lidar. Available at: DOI:10.3390/s20133662

94. Munzert S., Rubba C., Meißner P., Dominic N. Automated Data Collection with R: A Practical Guide to Web Scraping and Text Mining. 2014. Available at: https://www.amazon.co.uk/Automated-Data-Collection-Practical-Scraping/dp/111883481X/ref=asc_df_111883481X/?tag=googshopuk-

21&linkCode=df0&hvadid=311000051962&hvpos=&hvnetw=g&hvrand=7313731900144794262&hvpone=&hvptwo=&hvqmt=&hvdev=c&hvdvcmdl=&hvlocint=&hvlocphy=9046205&hvtargid=pla-479618897484&psc=1&th=1&psc=1 (Accessed: 24 January 2022)

95. Vanfretti L., Arava VSN. Decision tree-based classification of multiple operating conditions for power system voltage stability assessment. International Journal of Electrical Power & Energy Systems. Elsevier; 1 December 2020; 123: 106251. Available at: DOI:10.1016/J.IJEPES.2020.106251 (Accessed: 24 January 2022)